



How to recover 3D information with SAR sensors ?

Florence Tupin, Jean Marie Nicolas



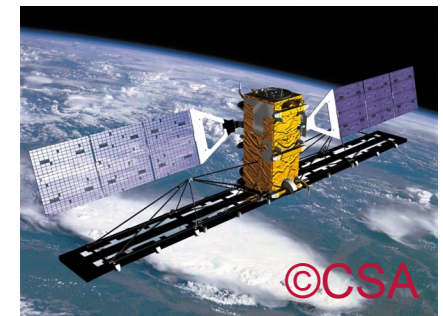
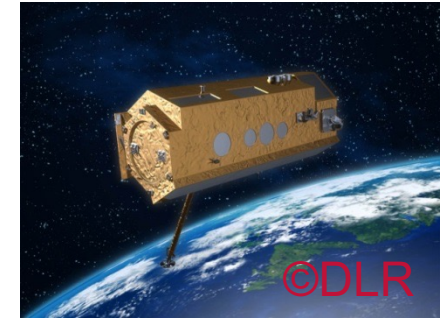
SAR systems

■ Why using SAR ?

- All time / all weather acquisition system
- Phase information !....
- Polarimetric information !...

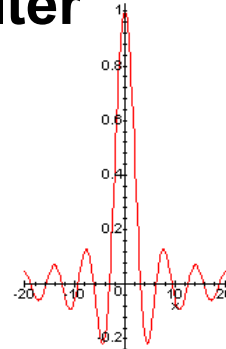
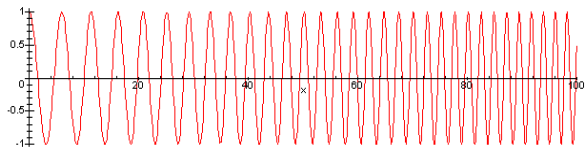
■ Applications

- Continental applications :
 - Agriculture / vegetation (forest) monitoring
 - Urban mapping, urban growth monitoring
 - Rapid mapping (disaster management, flood)
 - Digital surface model and movement monitoring
- Maritime applications :
 - Ice monitoring, ship monitoring
 - Oil spill detection

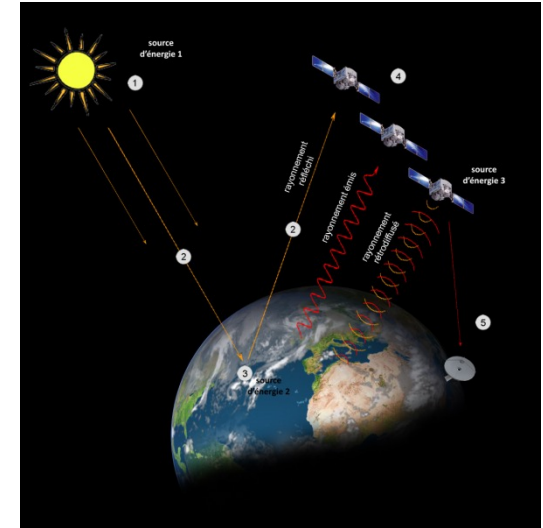
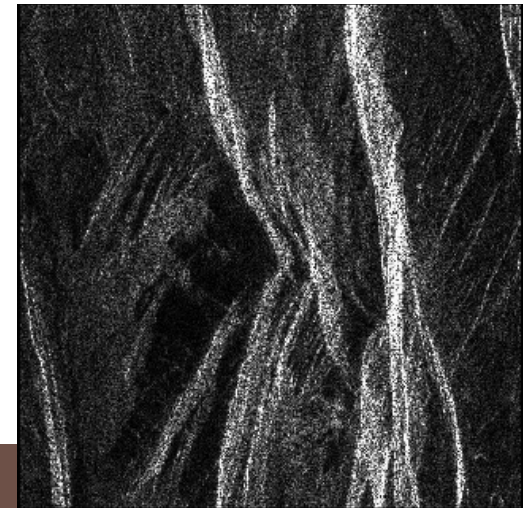
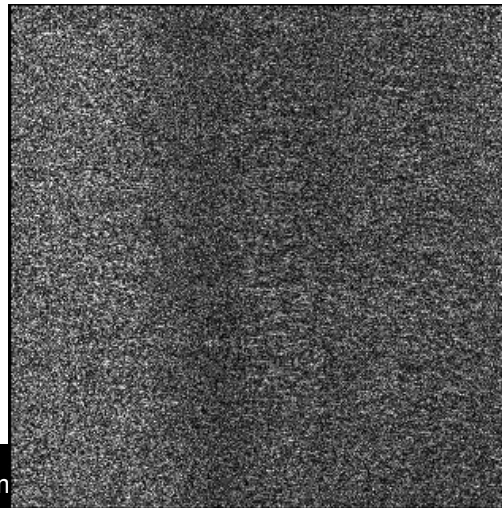
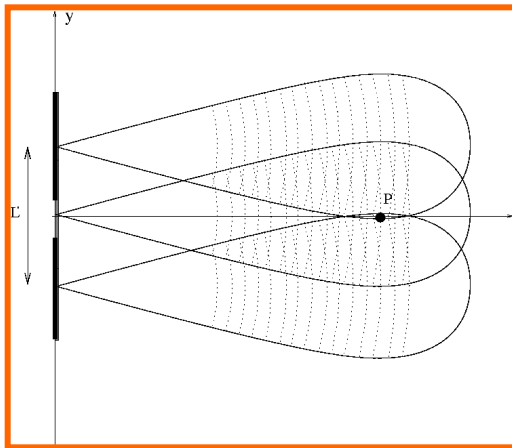


SAR acquisition

Range: chirp and matched filter



Azimuth: synthetic aperture « geometric chirp » and matched filter

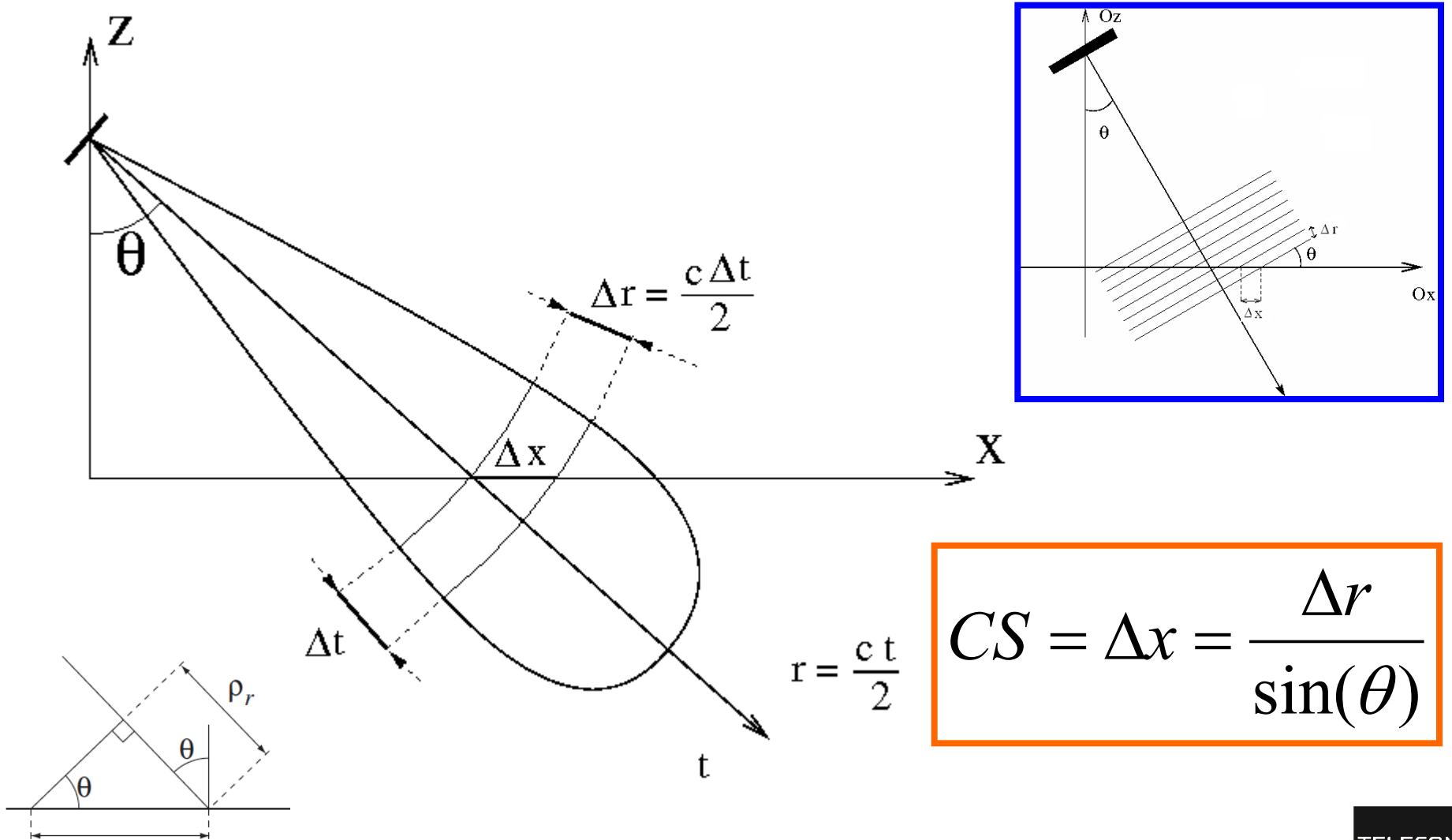




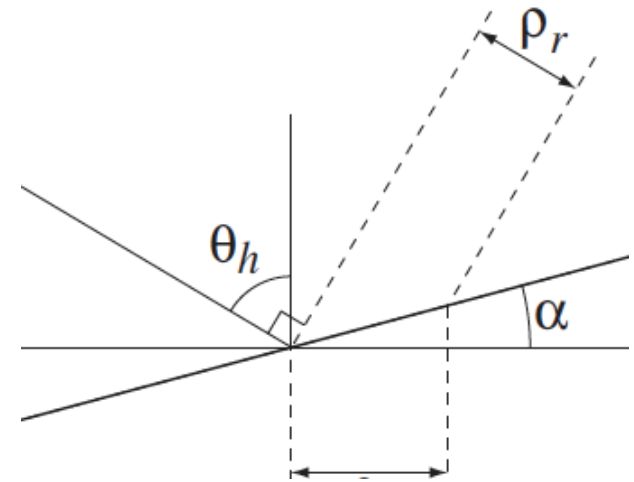
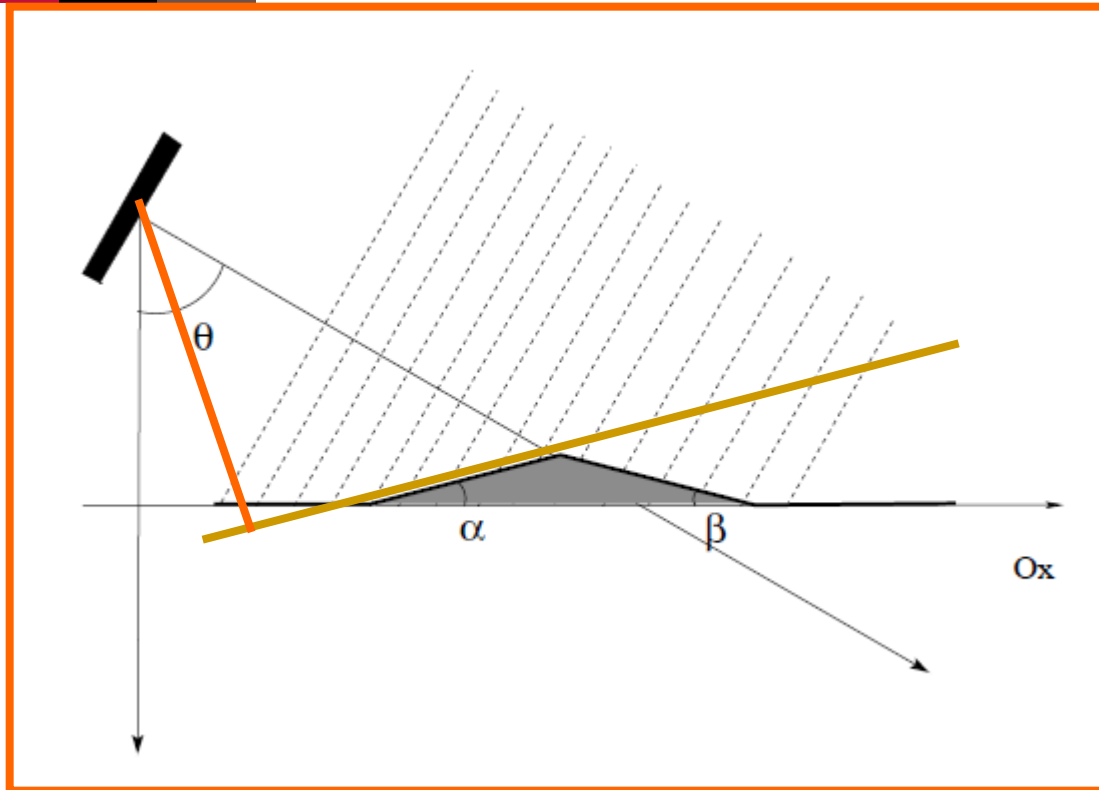
Overview of the session

- **Distance sampling and geometric distortions**
- **Mono-image elevation**
- **Radargrammetry**
- **Interferometry**

Lateral viewing and distance sampling



Influence of relief on the cell size



$$CS(\alpha) = \frac{\Delta r}{\sin(\theta - \alpha)}$$

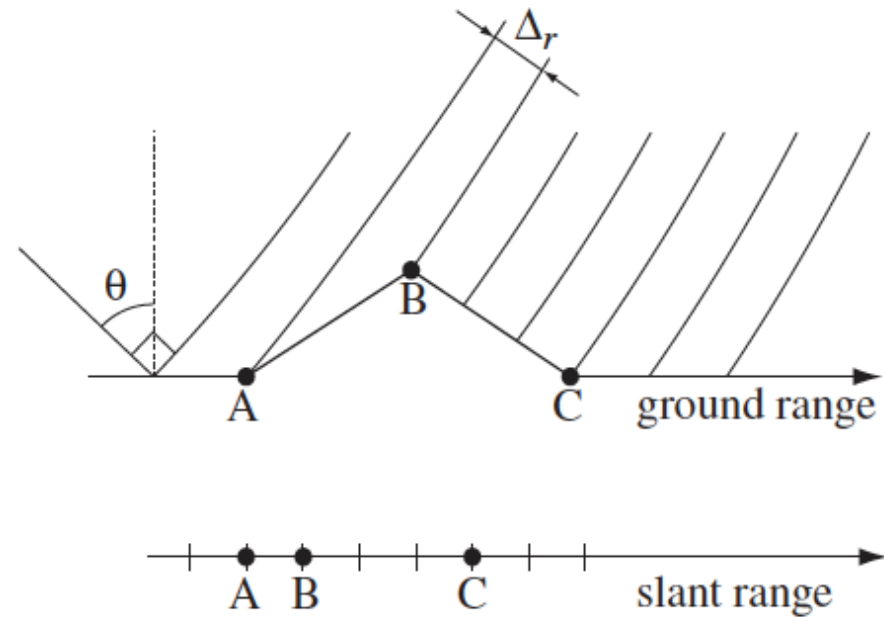
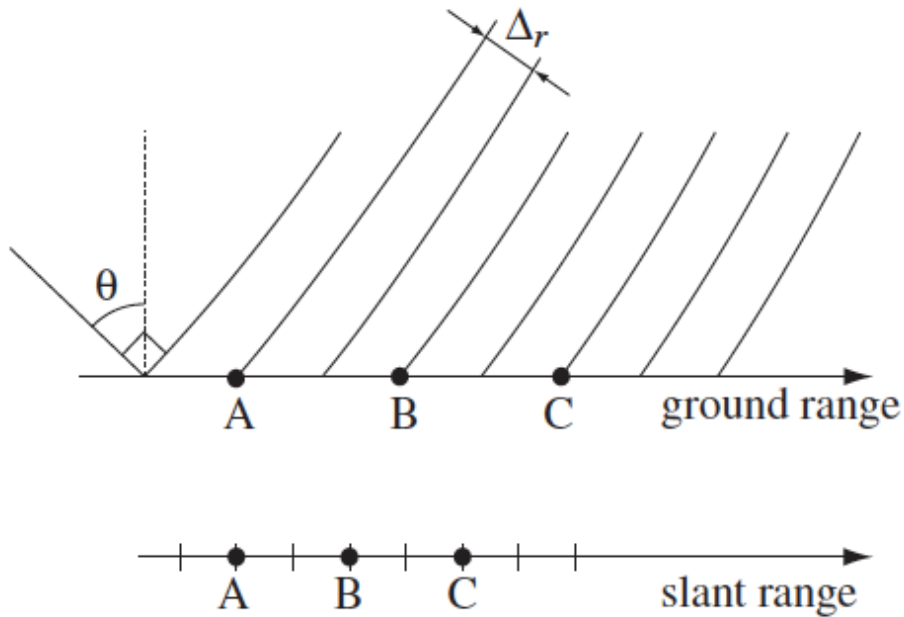
■ Slope facing the sensor :

- Forshortening in the image (a wider area of the ground is seen in the pixel)

■ Opposite side of the sensor:

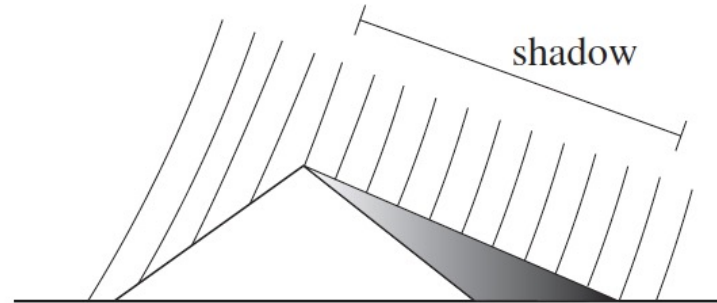
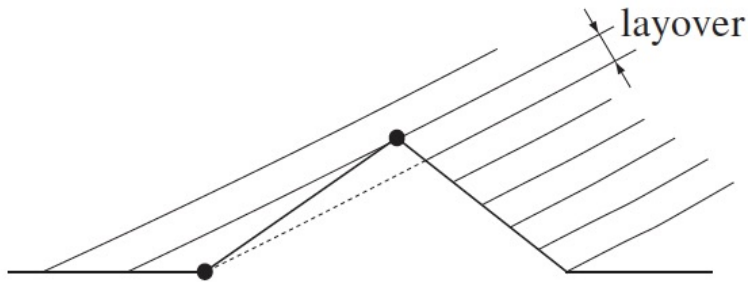
- Dilation on the image (a smaller ground area in 1 pixel)

Geometric distortions



Foreshortening / dilation

Geometric distortions



■ Overlay:

- If $\alpha > \theta$: inversion of the points and mixing of the target responses

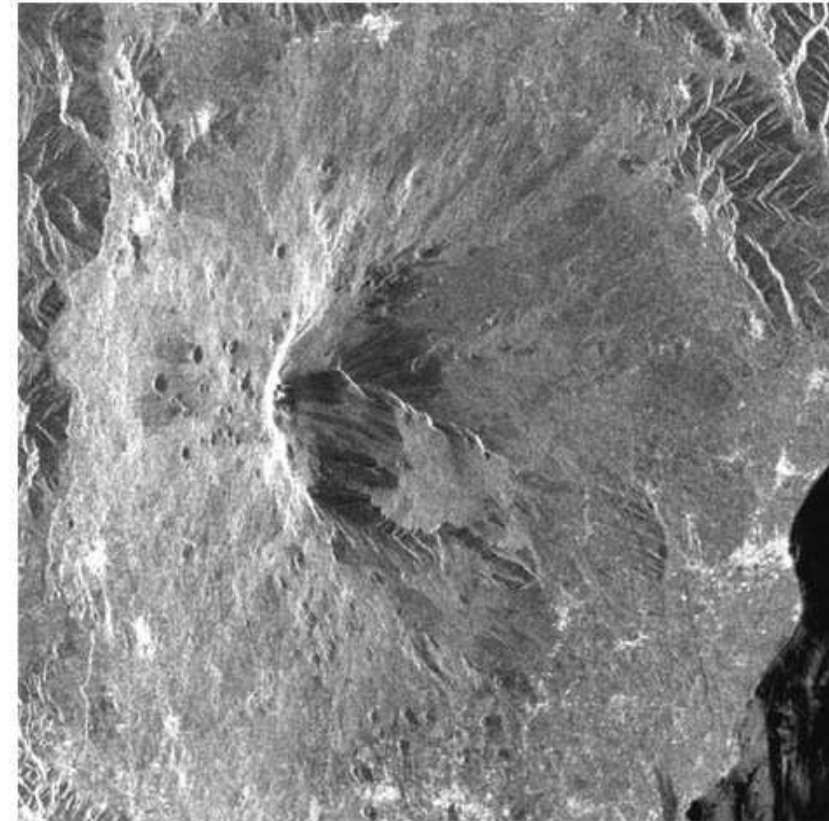
■ Shadow phenomenon:

- No illumination of the back-slope (obstacle) $\alpha' > \pi/2 - \theta$

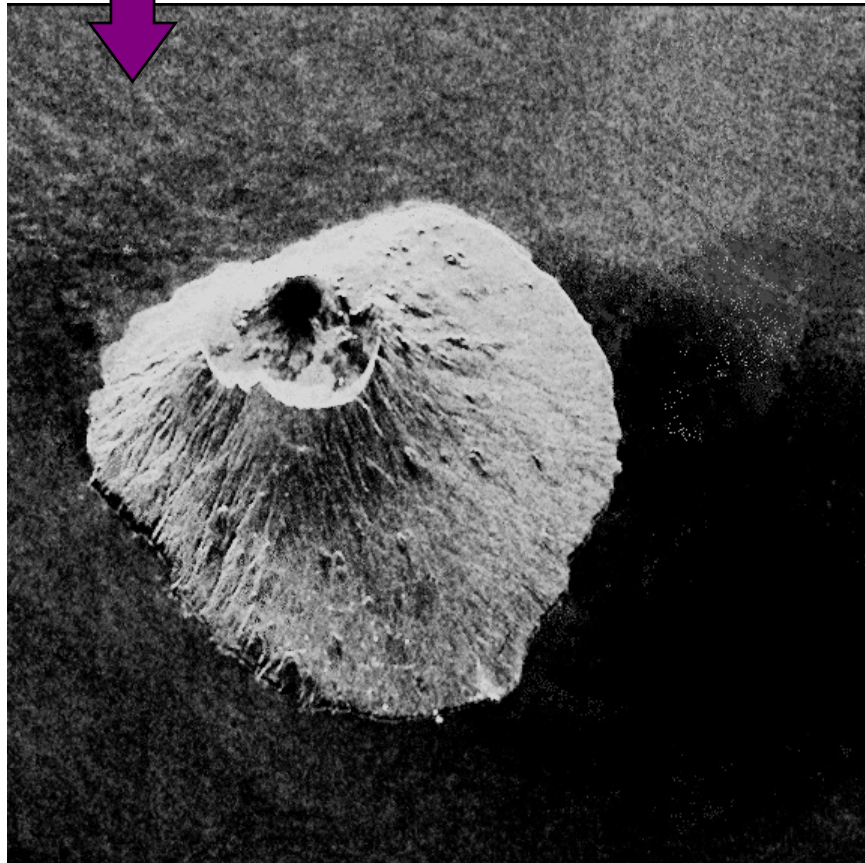
■ Influence of the incidence angle (increase in the swath) :

- Near range : lay-over ; far range : shadow

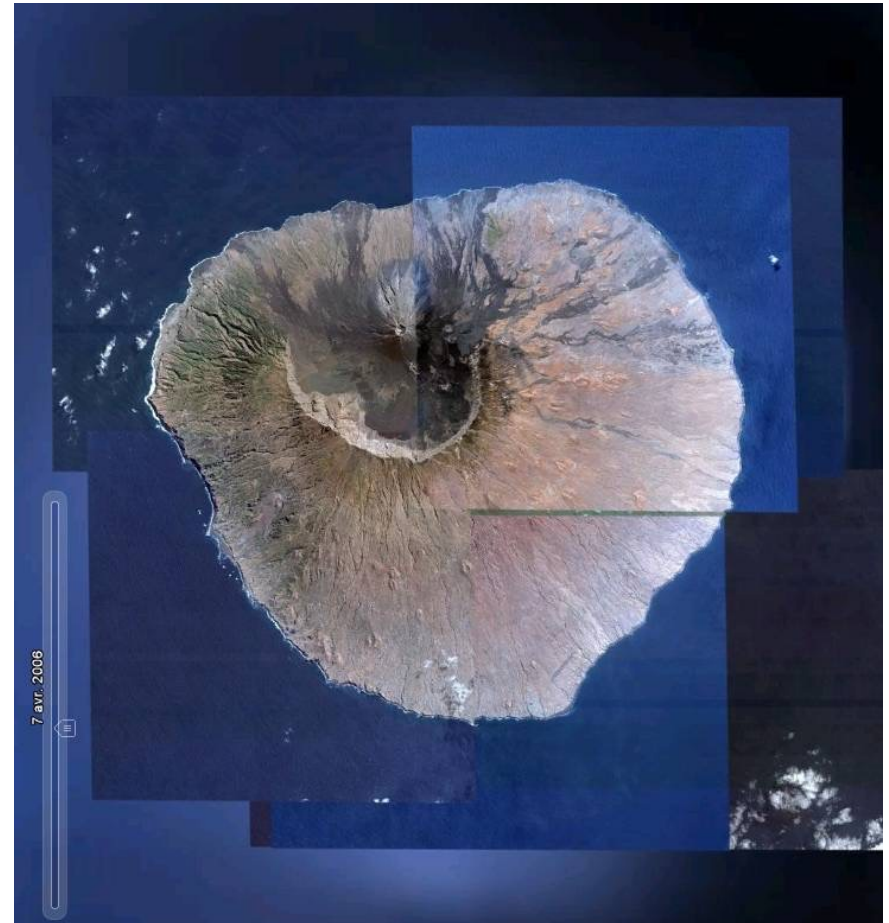
Geometric distorsion – Mount Etna



Influence of relief on the cell size

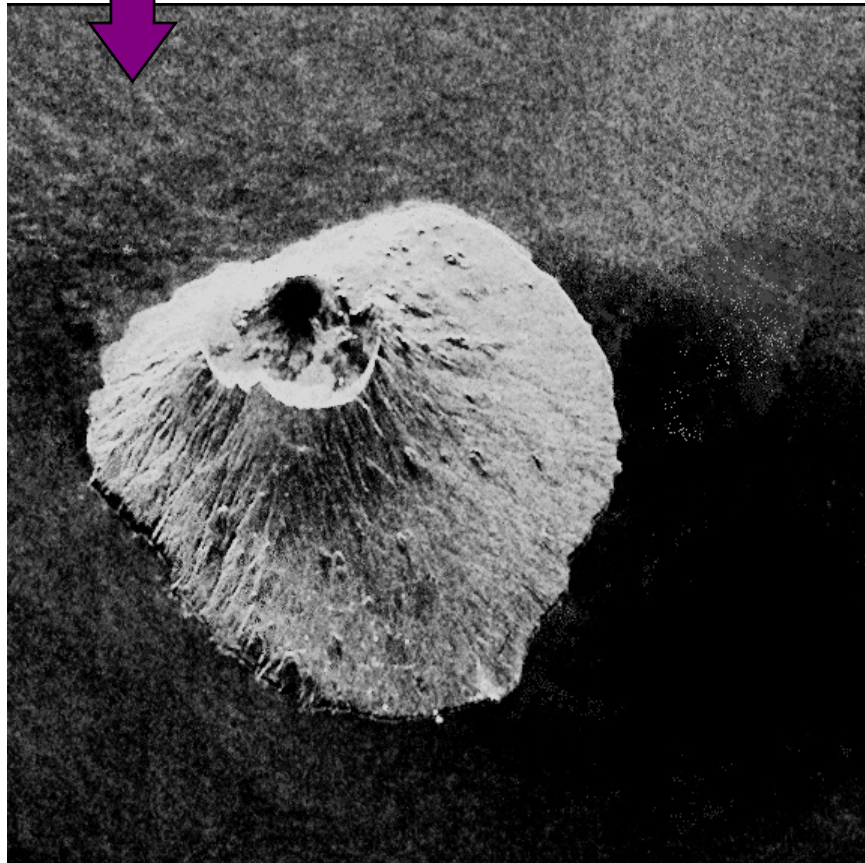


ERS image

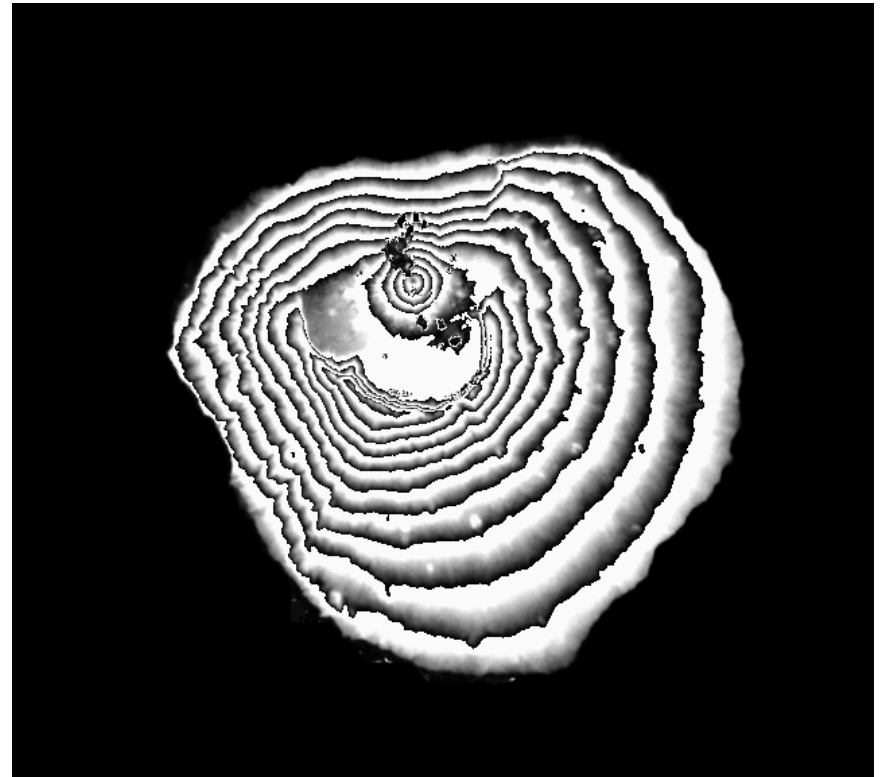


Mosaic on Google

Influence of relief on the cell size

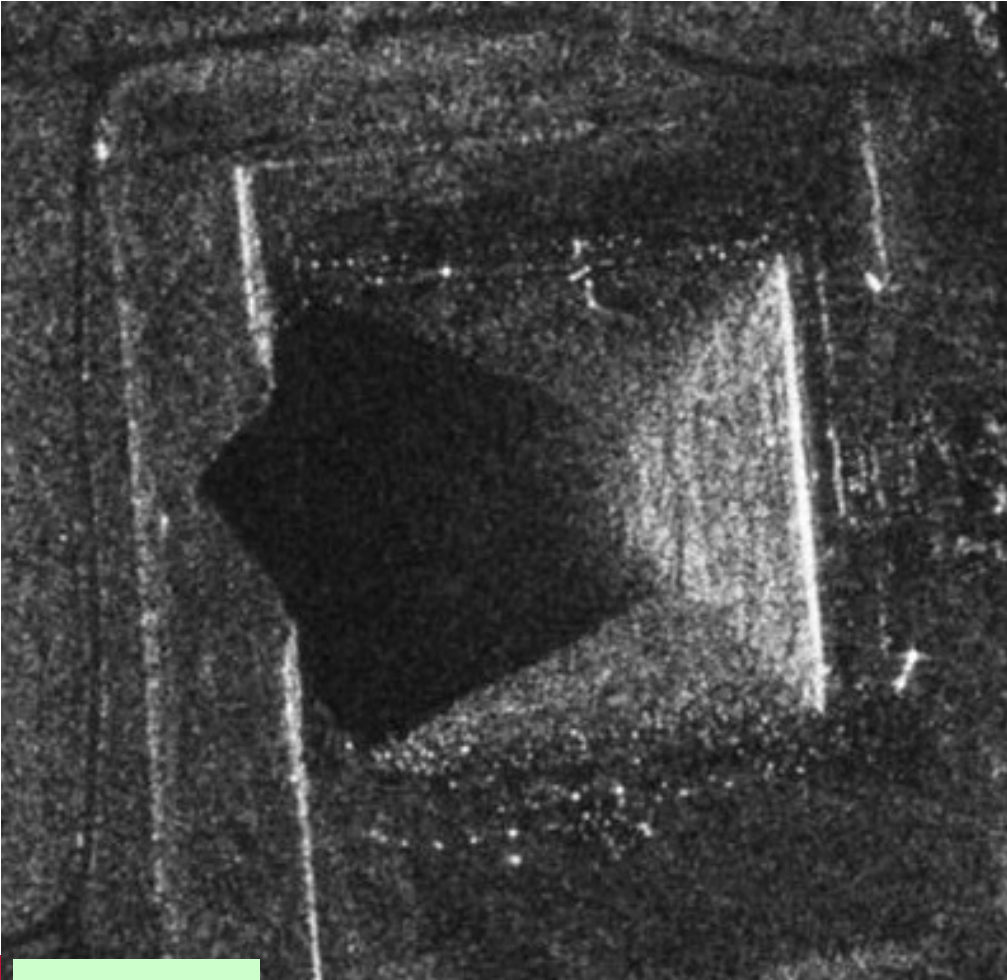


ERS image



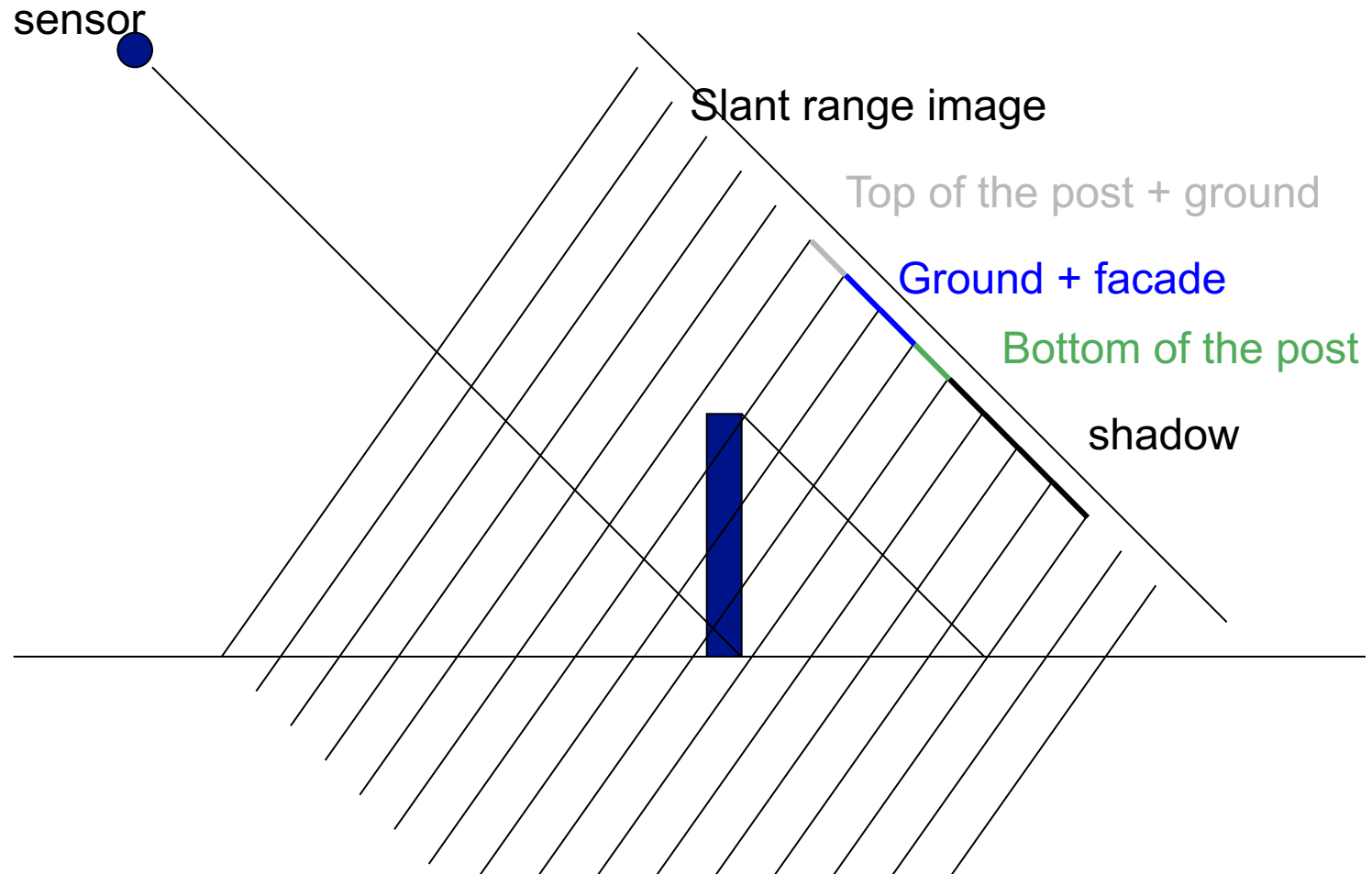
Level lines: step of 256m

Example of shadow TERRASAR-X :Gizeh

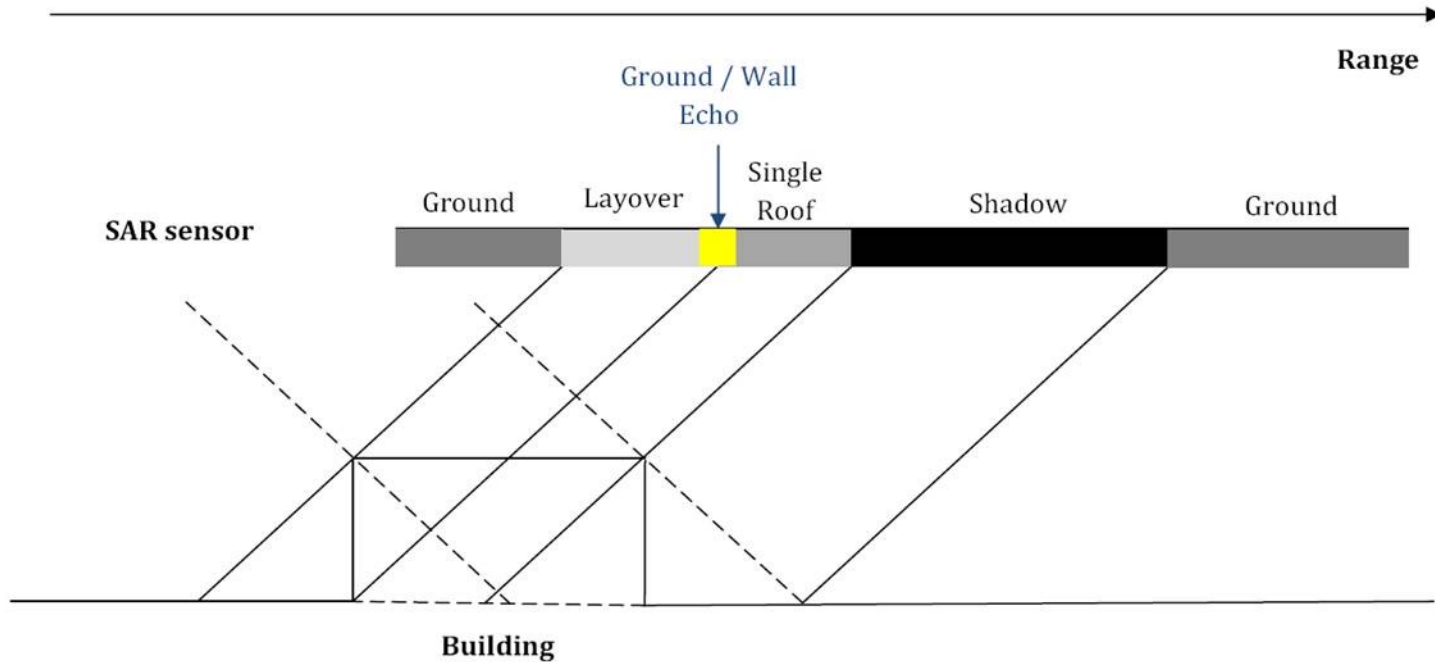


Geometric distortions

■ Example of a vertical post



Geometric distortions - building

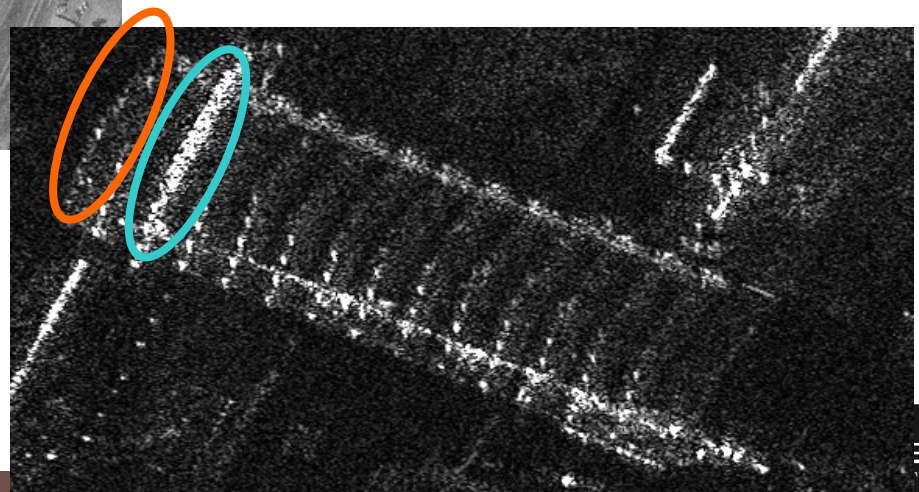


Increased effects for buildings: vertical walls

Geometric distortions - building



- Top of the roof
- Lay-over
- Ground / wall corner reflector





New-York and sky-scrapers – TerrSAR-X

Geometric distortions - summary

- **Local slope :**
 - Foreshortning / dilation
- **Slope superior than the incidence angle**
 - Lay-over
- **Slope superior than the $\frac{\pi}{2}$ – incidence angle**
 - Shadow



How recovering 3D information with SAR data ?

SAR data and 3D

- **Backscattered electro-magnetic wave:** $z = Ae^{j\phi}$
 - Amplitude: backscattering coefficient of the scene
 - Phase: geometric information + cell scatterers contribution
- **Distance sampling:**
 - Geometric distortions (lay-over, shadow)

- **3D information :**
 - Radarclinometry & shape from shading (amplitude)
 - Stereoscopy – radargrammetry (amplitude)
 - Interferometry (phase)
 - Tomography (n-D phase)



Overview of the session

- Distance sampling and geometric distortions
- **Mono-image elevation**
- Radargrammetry
- Interferometry

Elevation from amplitude « shape from shading »

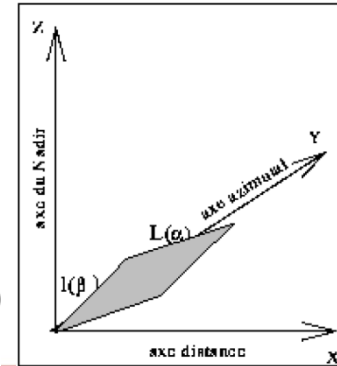
$$CS = \Delta x = \frac{\Delta r}{\sin(\theta)}$$

$$CS(\alpha) = \frac{\Delta r}{\sin(\theta - \alpha)}$$

■ Data : 1 amplitude image

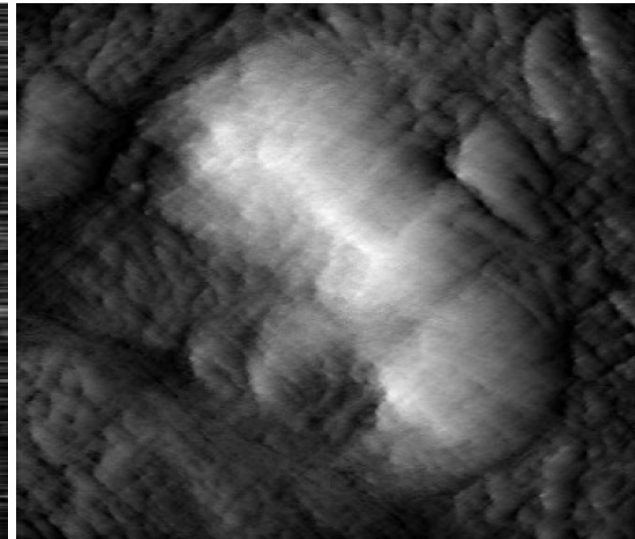
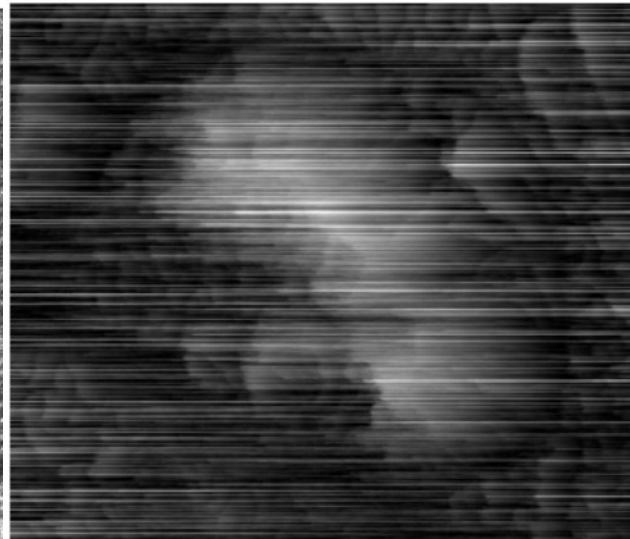
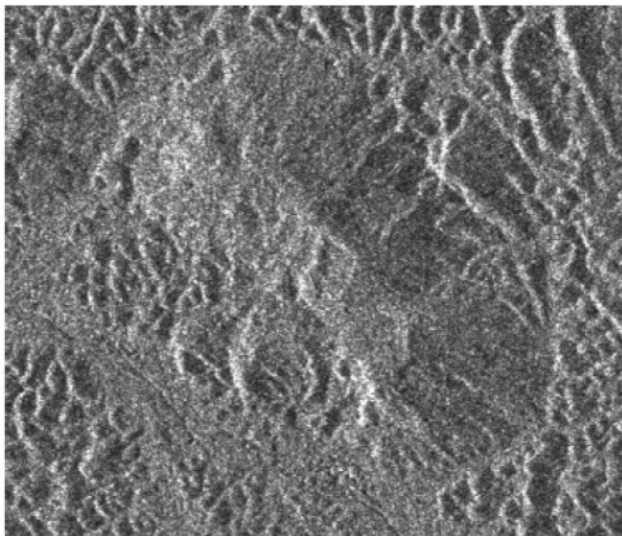
■ Radarclinometry:

- For homogeneous areas :
 - Backscattered signal = f(local slope)



$$I(\alpha) = K\sigma_0\Delta_x\Delta_yL(\alpha)$$

$$L(\alpha) = \frac{\sin(\theta)}{\sin(\theta - \alpha)}$$

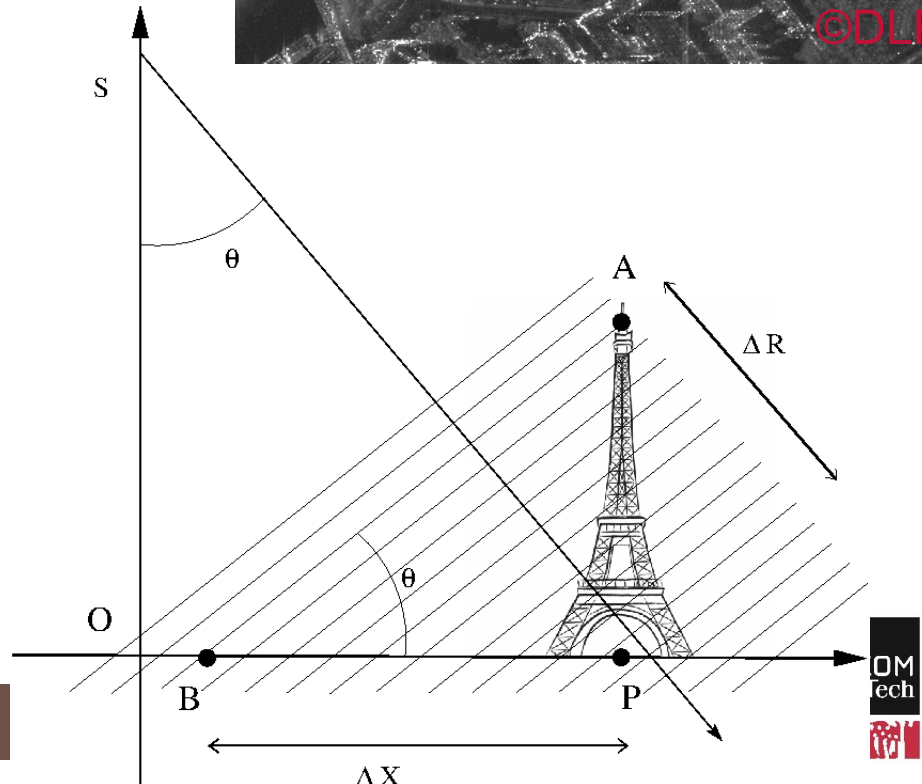


Elevation from amplitude Lay-over / shadow

- Terrasar-X, $\theta \sim 34^\circ$
- Relation between H and BP
- ΔX ground range distance between the highest point and the ground
- ΔR slant range distance

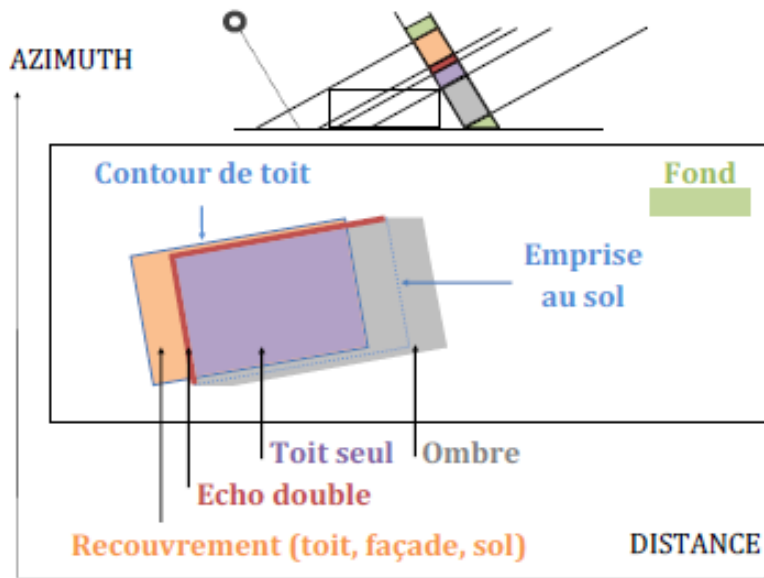
$$H = \Delta X \tan \theta$$

$$H = \frac{\Delta R}{\cos \theta}$$

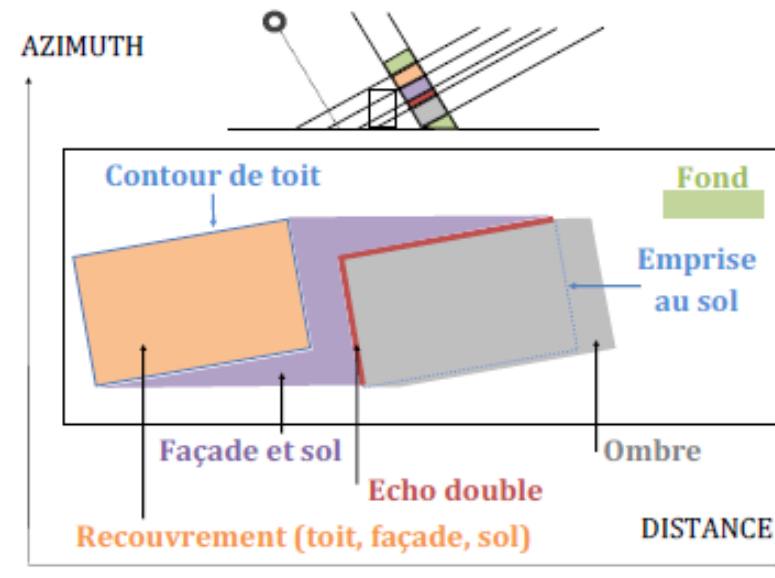


Elevation from amplitude Lay-over / shadow

- Data : 1 amplitude image
- Elevation from lay-over and shadow
 - Layover area and shadow area measurement to recover elevation information



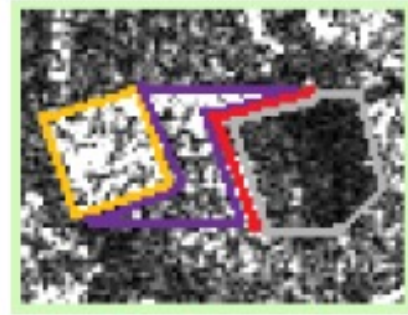
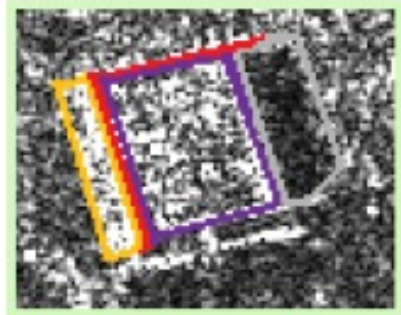
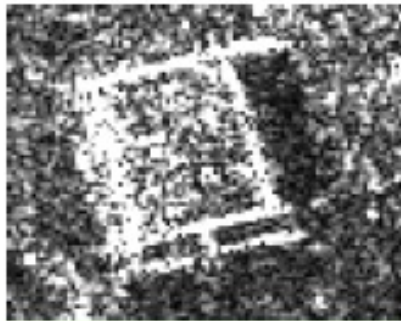
Cas 1 : $h_{b\grave{a}ti} < h_{limite}$



Cas 2 : $h_{b\grave{a}ti} > h_{limite}$

Man-made structures

Example of processing chain (1)



Cas 1 : $h_{\text{bâti}} < h_{\text{limite}}$

Cas 2 : $h_{\text{bâti}} > h_{\text{limite}}$

■ Processing chain

- Building footprint detection
- h optimization

■ Elevation extraction:

- Hypothesis of elevation h
- Computation of a radiometric signature using h , building shape and sensor parameters
- Energy minimization depending on h

■ Limits

- Rectangular shape, flat roof

Man-made structures

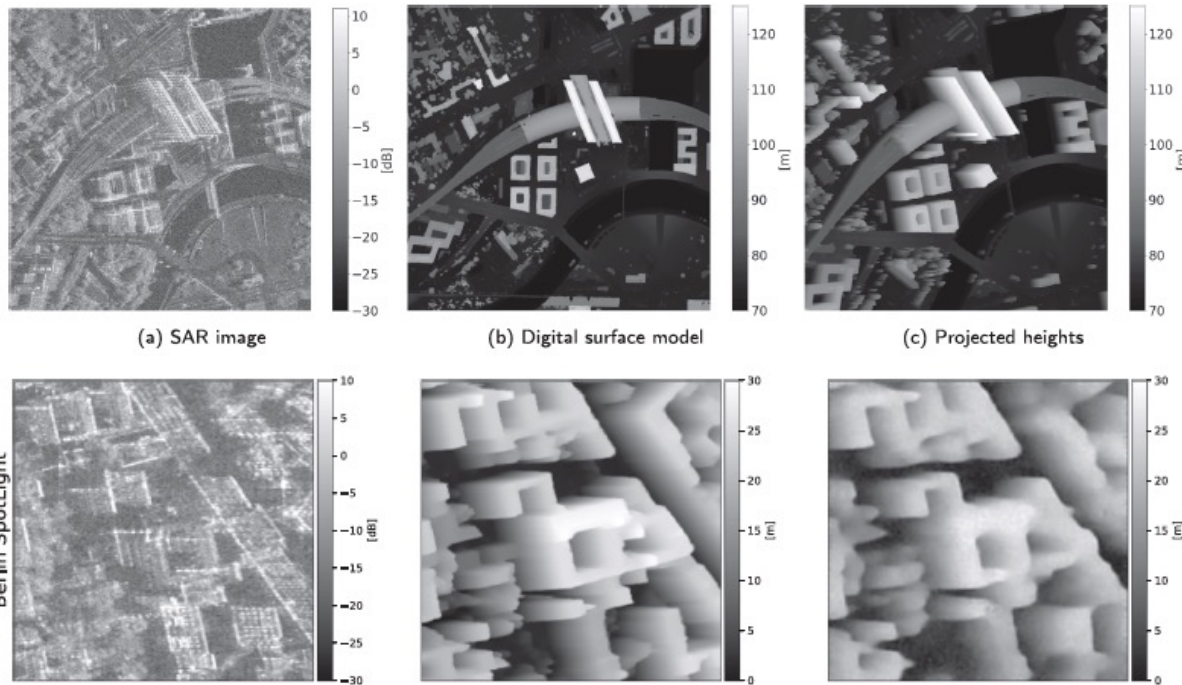
Example of processing chain (2)

■ Processing chain

- Network trained to predict height from amplitude information
- Supervised training : dataset obtained from airborne laser scanning and projected in SAR geometry

■ Test phase:

- Amplitude image
- « Similar » acquisition angle



Berlin SpotLight

Figures extracted from :
Deep learning based single-image height reconstruction from very-high-resolution SAR intensity data, M. Recla and M. Schmitt, ISPRS 2022
© ISPR Int. Journal of Photogrammetry and Remote Sensing

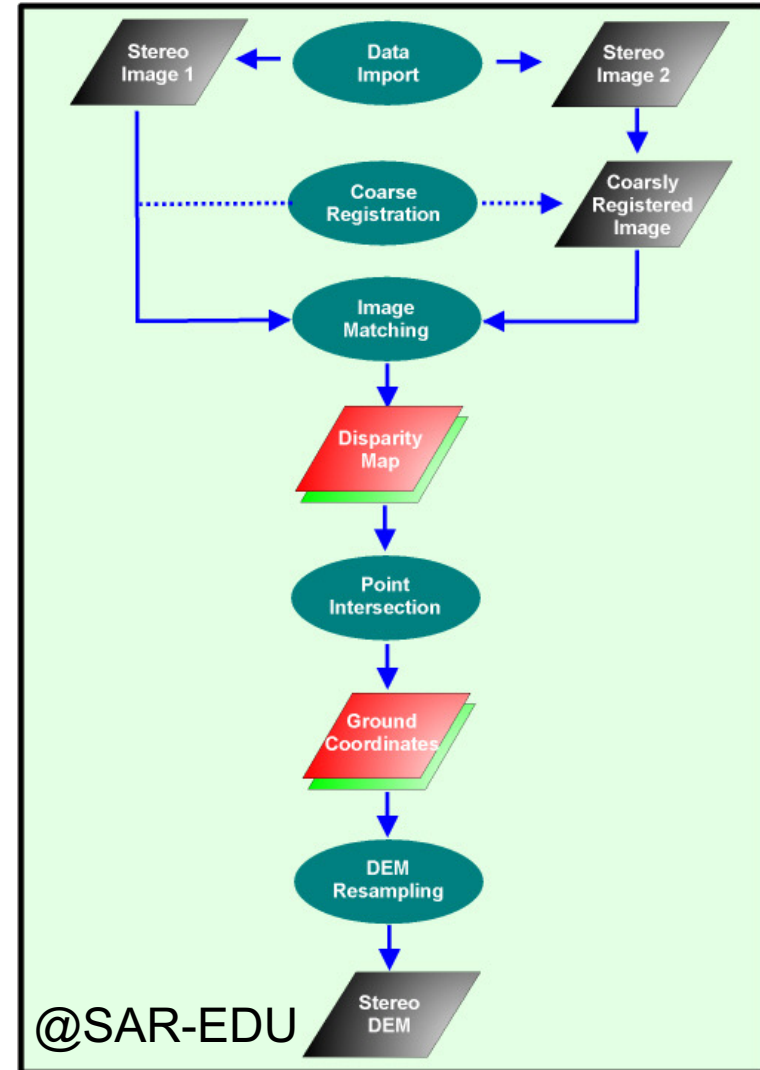


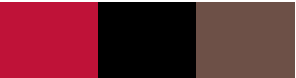
Overview of the session

- Distance sampling and geometric distortions
- Mono-image elevation
- Radargrammetry
- Interferometry

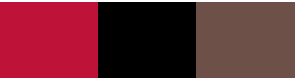
Radargrammetry / stereovision

- **Data : 2 amplitude images**
- **Principle :**
 - Point matching in Im1 and Im2
 - Geometric equations to recover 3D information



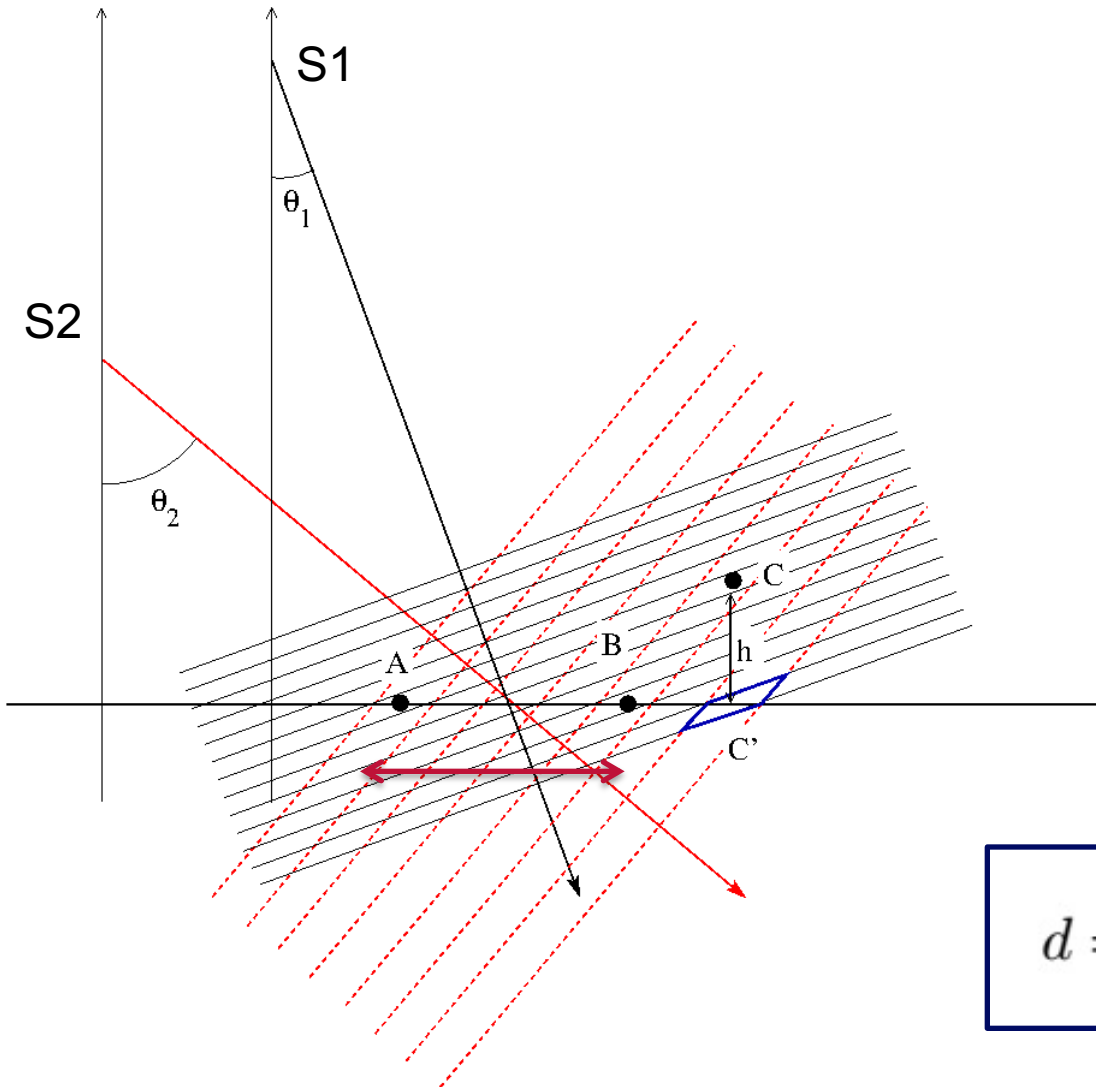


©ONERA



ONERA

Radargrammetry



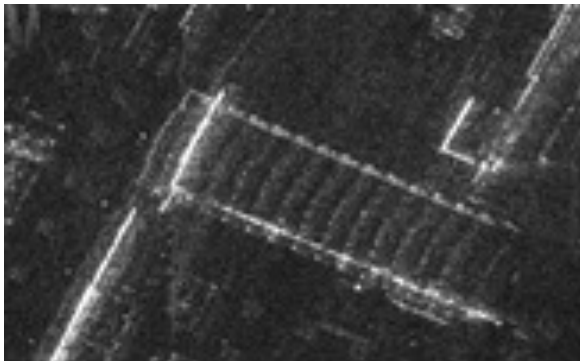
- C': point on the ground
In the same cell for both sensors
- C: point with elevation h
 - Seen in cell A for S1
 - Seen in cell B for S2
 - $d=AB$ (point matching)
 - $d=AC'-BC'$

$$AC' = h / \tan \theta_1$$

$$BC' = h / \tan \theta_2$$

$$d = h \left(\frac{1}{\tan \theta_1} - \frac{1}{\tan \theta_2} \right)$$

Radargrammetry – processing chain



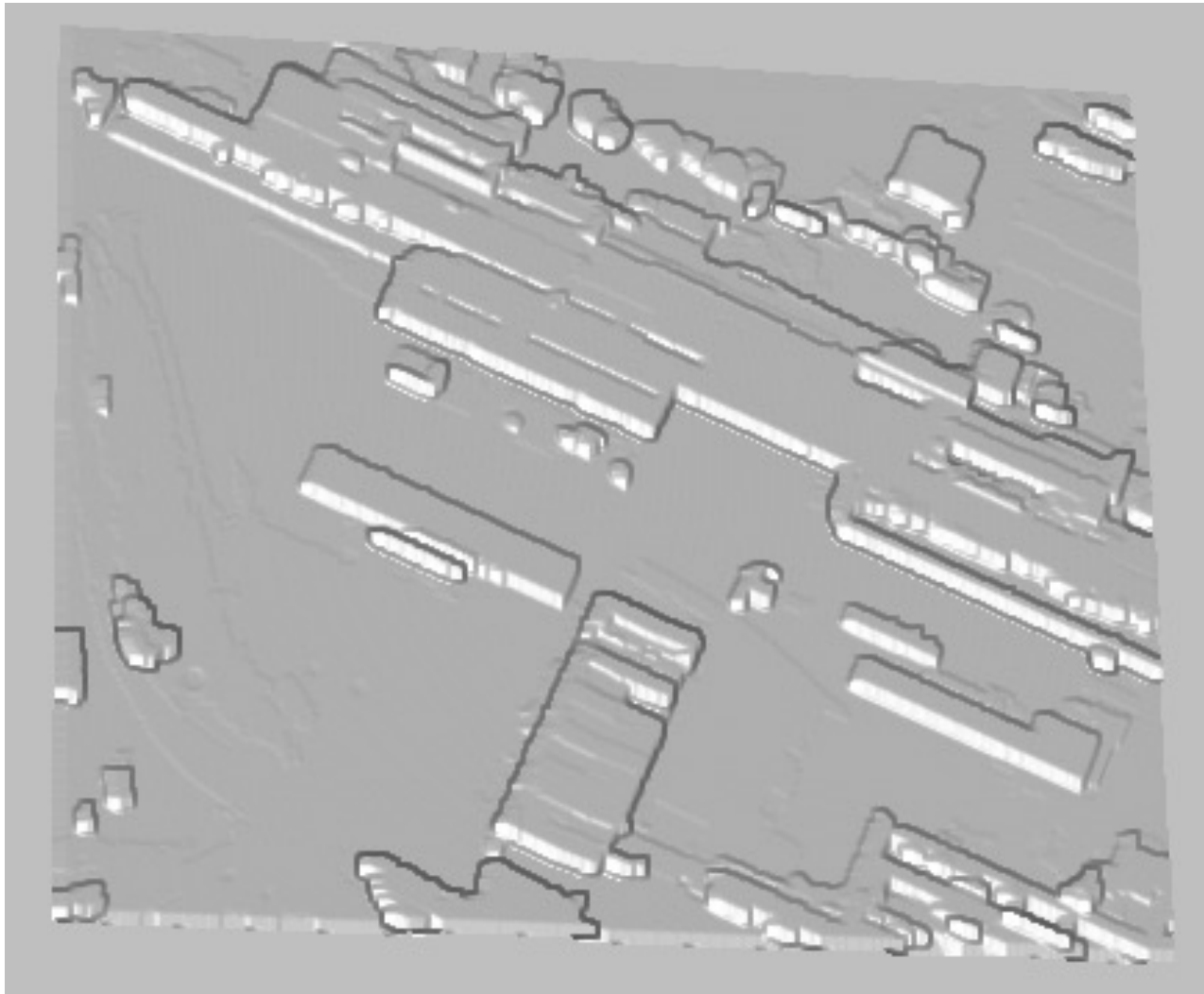
■ Steps:

- Pseudo-epipolar resampling (tie points and low-order polynomial)
- Window based matching
- Disparity map regularization
- Conversion of disparities to 3D coordinates
- Point cloud transformation into gridded DSM

■ Limits

- Sparse matching
- Corner reflectors: mostly on the ground

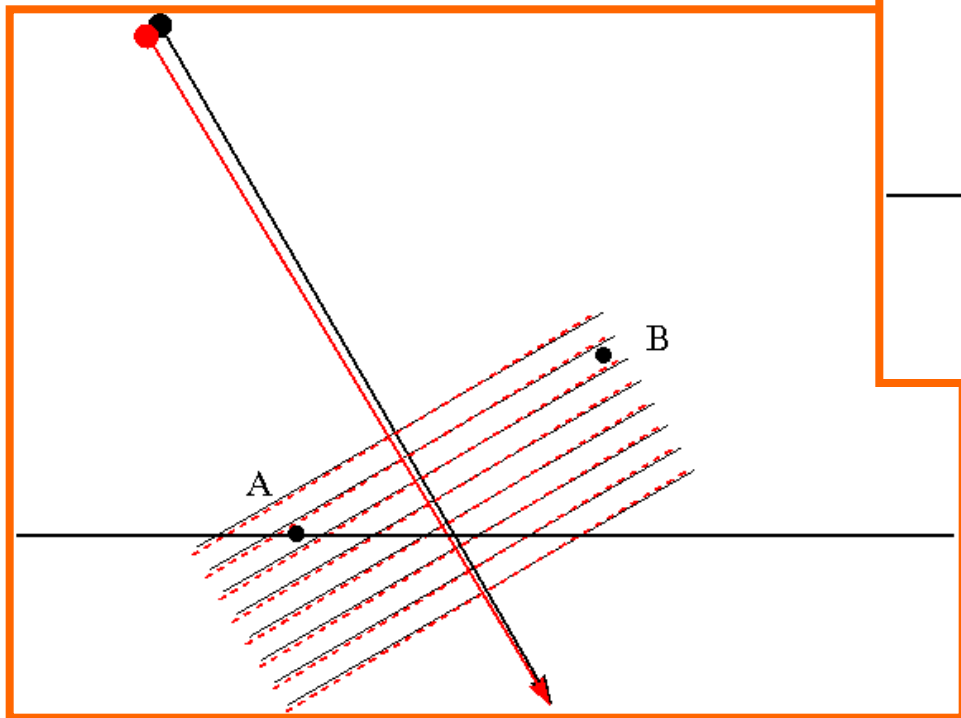
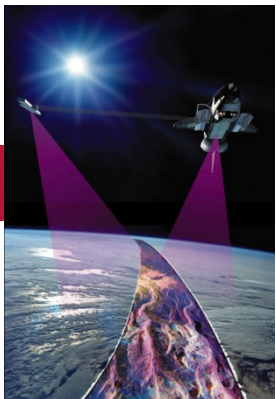
3D reconstruction – Radarg./optic



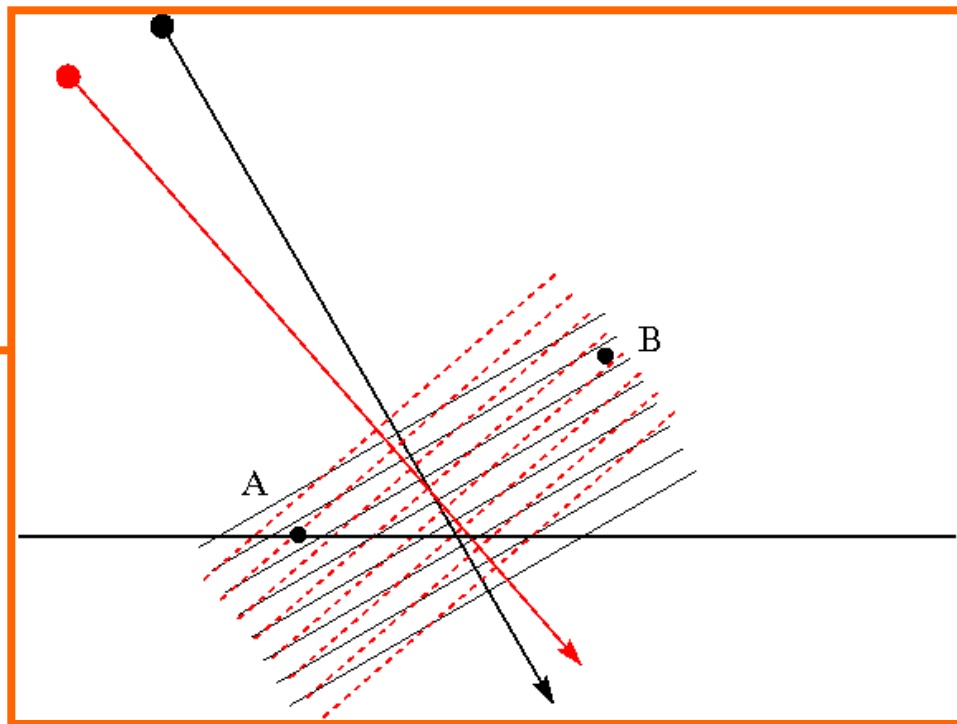


Overview of the session

- Distance sampling and geometric distortions
- Mono-image elevation
- Radargrammetry
- Interferometry



Small baseline :
interferometry



Big baseline:
radargrammetry

Phase and geometry

■ Phase of a single image (backscattered)

$$\phi(t) = 2\pi f_0 t + \phi_{pr}$$

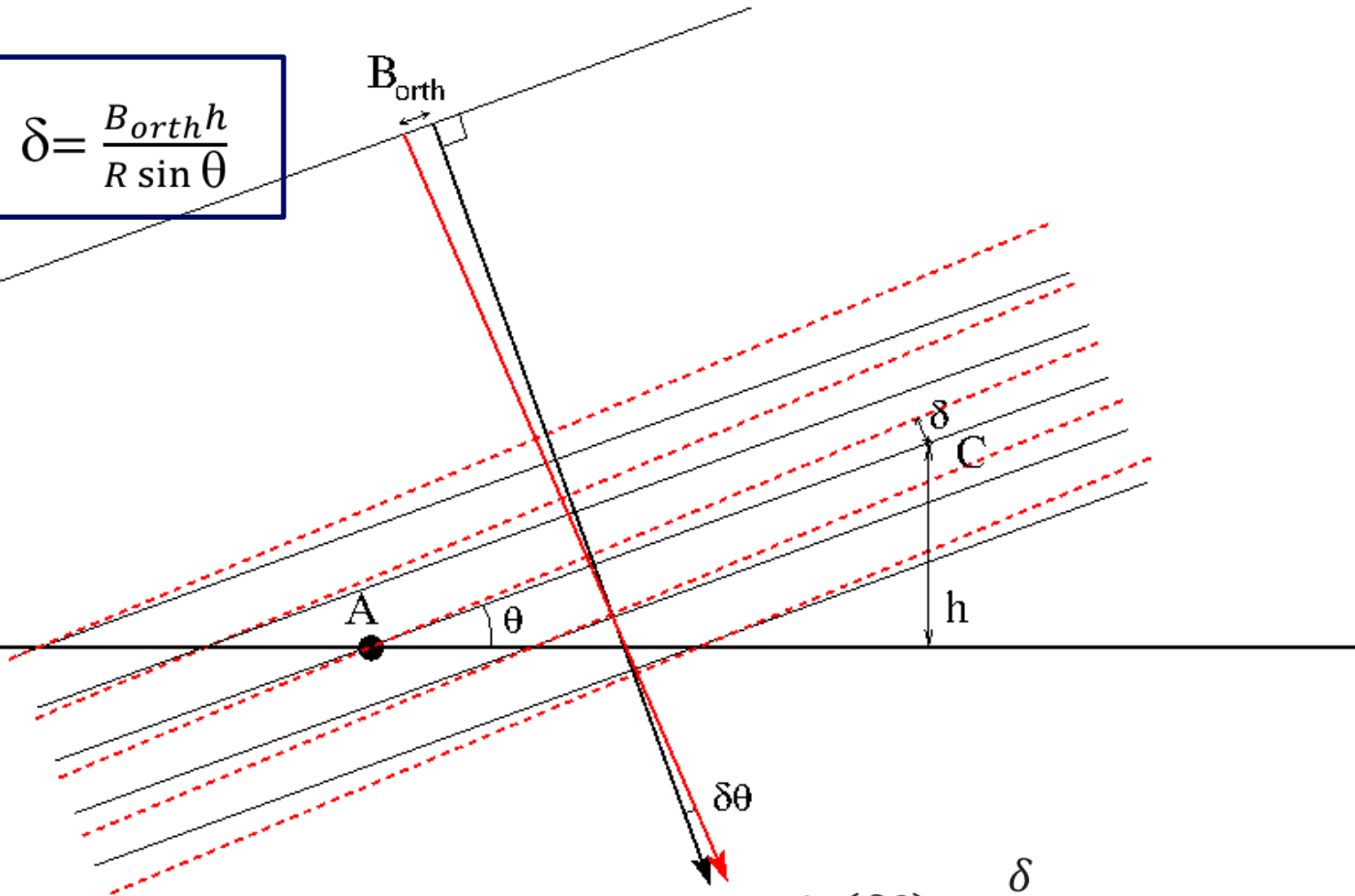
$$t = 2\frac{R}{c} = 2\frac{R}{\lambda f_0}$$

$$\phi(t) = 4\pi \frac{R}{\lambda} + \phi_{pr}$$

Combination of a geometric information (related to the range R) and the resolution cell contribution (phase shift due to cell scatterer organization)

Interferometry - principle

$$\delta = \frac{B_{orth} h}{R \sin \theta}$$

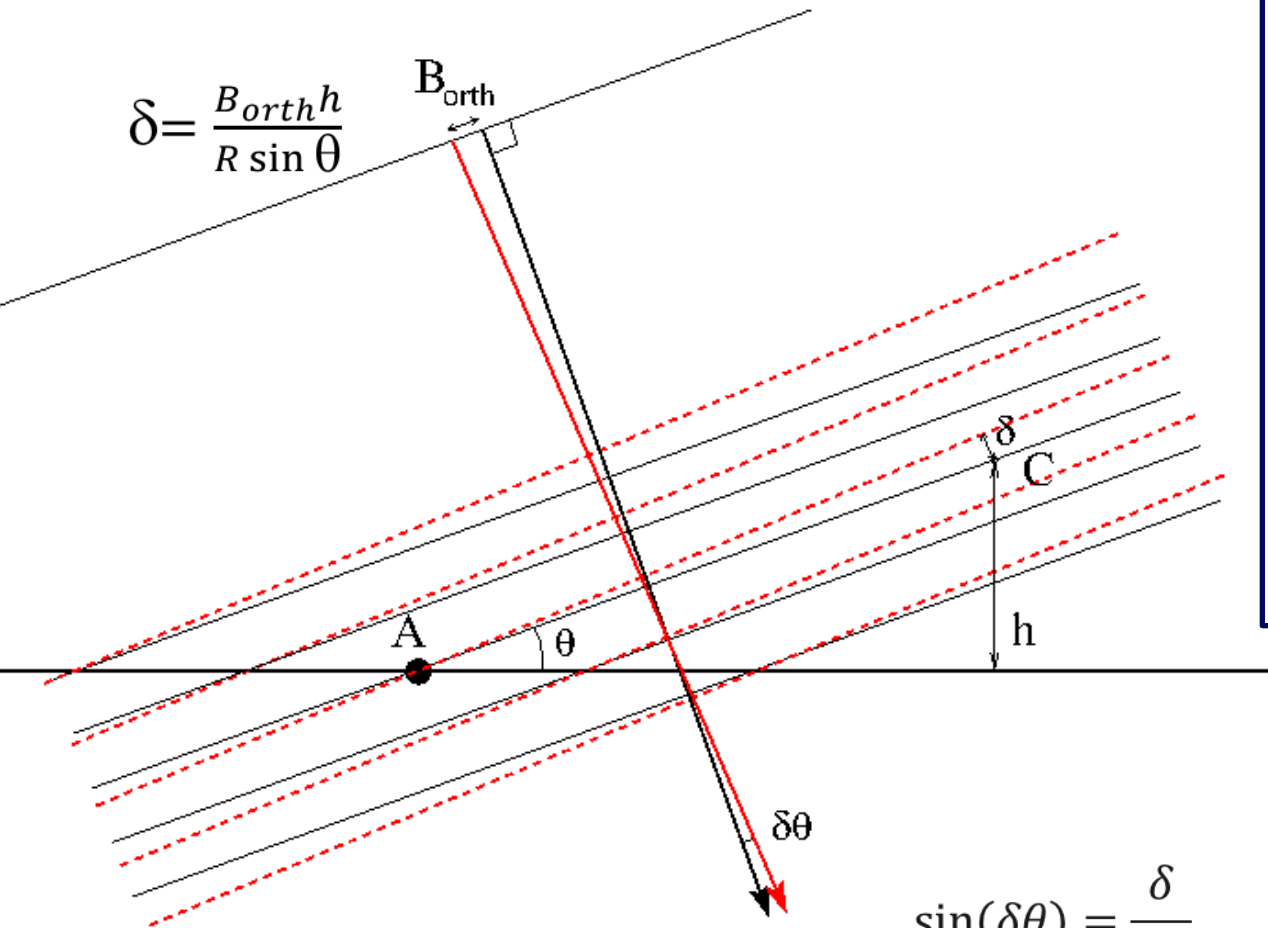


$$\sin \theta = \frac{h}{AC}$$

$$\sin(\delta\theta) = \frac{\delta}{AC}$$

$$\sin(\delta\theta) = \frac{B_{orth} h}{R}$$

Interferometry - principle



$$\phi = \frac{4\pi R}{\lambda} + \phi_{pr}$$

$$\phi_2 - \phi_1 = \frac{4\pi(R_2 - R_1)}{\lambda} = \psi_{1,2}$$

$$R_2 - R_1 = \delta$$

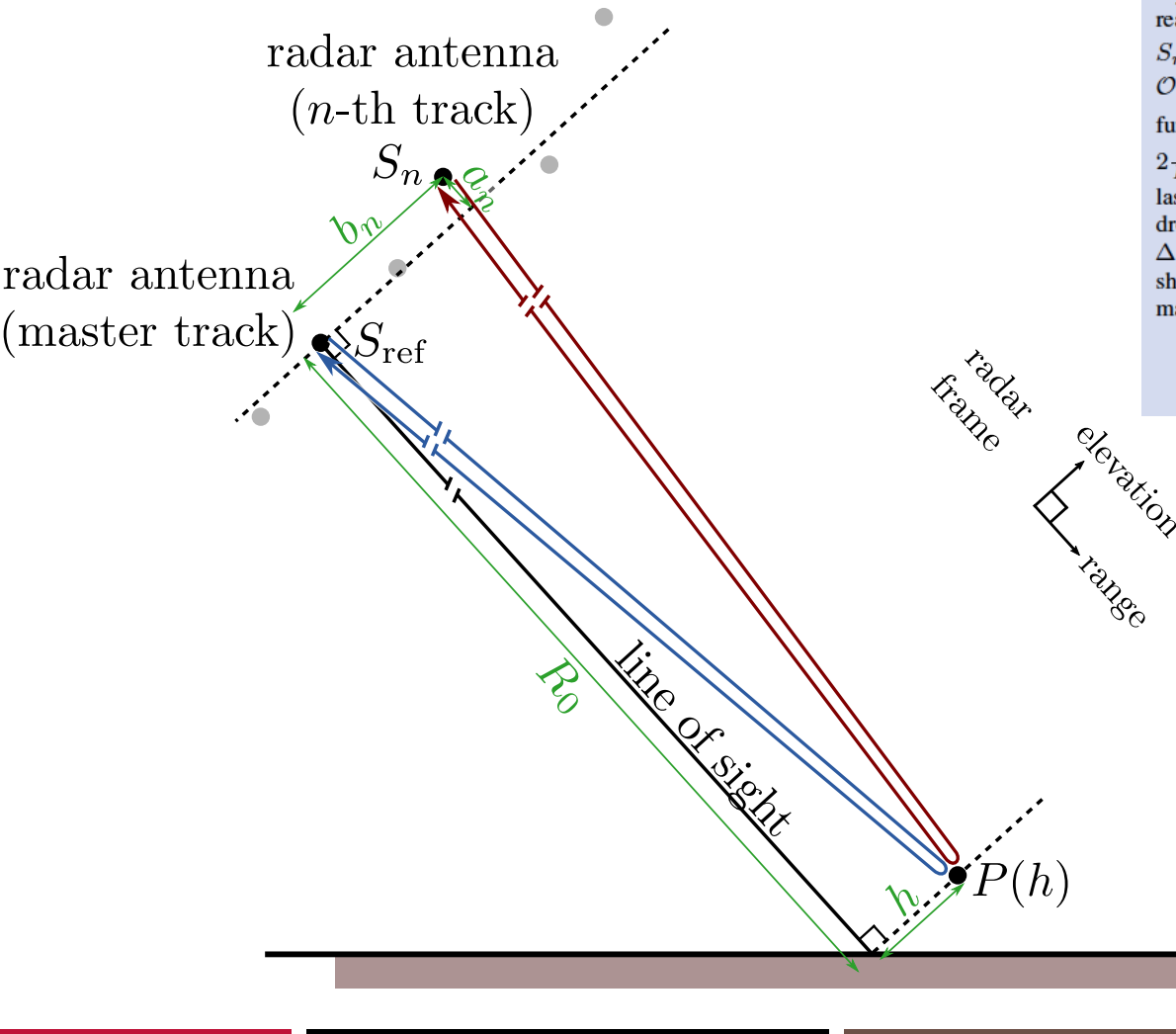
$$\psi_{1,2} = \frac{4\pi B_{\perp 1,2}}{R \sin(\theta) \lambda} h$$

$$\psi_{1,2} = \alpha_{geom 1,2} h$$

$$\sin(\delta\theta) = \frac{\delta}{AC}$$

$$\sin(\delta\theta) = \frac{B_{orth}}{R}$$

Interferometry principles



The path length difference between the round-trip from the master antenna location S_{ref} to point $P(h)$ and the round-trip from the n -th antenna location S_n to point $P(h)$ determines the phase-shift. In the radar frame (orthogonal frame defined by the range and elevation directions, with origin S_{ref}), point $P(h)$ has coordinates $P(h) = [R_0, h]$, the master antenna $S_{ref} = [0, 0]$ and the antenna on the n -th track $S_n = [a_n, b_n]$. The round-trip distance from S_{ref} to point $P(h)$ is equal to $2\sqrt{R_0^2 + h^2}$. Given that $R_0 \gg h$, this distance can be expanded under the form $2R_0 + \frac{h^2}{R_0} + \mathcal{O}\{R_0^{-2}\}$ where $\mathcal{O}\{R_0^{-2}\}$ designates terms that are asymptotically equivalent to R_0^{-2} and may then be neglected. A similar reasoning leads to the following expansion of the round-trip distance from S_n to $P(h)$: $2\sqrt{(R_0 - a_n)^2 + (h - b_n)^2} = 2(R_0 - a_n) + \frac{(h - b_n)^2}{R_0 - a_n} + \mathcal{O}\{(R_0 - a_n)^{-2}\}$. The path difference Δ_p can then be expressed as a function of the elevation h of point $P(h)$: $\Delta_p(h) \approx -2a_n + \frac{b_n^2}{R_0 - a_n} - 2\frac{b_n}{R_0 - a_n}h + \frac{a_n}{R_0(R_0 - a_n)}h^2$. Given that both $a_n \ll R_0$ and $b_n \ll R_0$, the last term can be neglected (it is comparable to the terms in R_0^{-2} previously dropped) and $R_0 - a_n \approx R_0$, which leads to the linear approximation: $\Delta_p(h) \approx \Delta_p(0) - 2\frac{b_n}{R_0}h$, with $\Delta_p(0) = -2a_n + b_n^2/R_0$. The phase shift $\Delta\varphi$ in the interferogram formed between the n -th image and the master image is then, with $\Delta\varphi_0 = (2\pi/\lambda)\Delta_p(0)$:

$$\Delta\varphi = \Delta\varphi_0 - \frac{4\pi b_n}{\lambda R_0}h \pmod{2\pi}. \quad (1)$$

Interferometry - principle

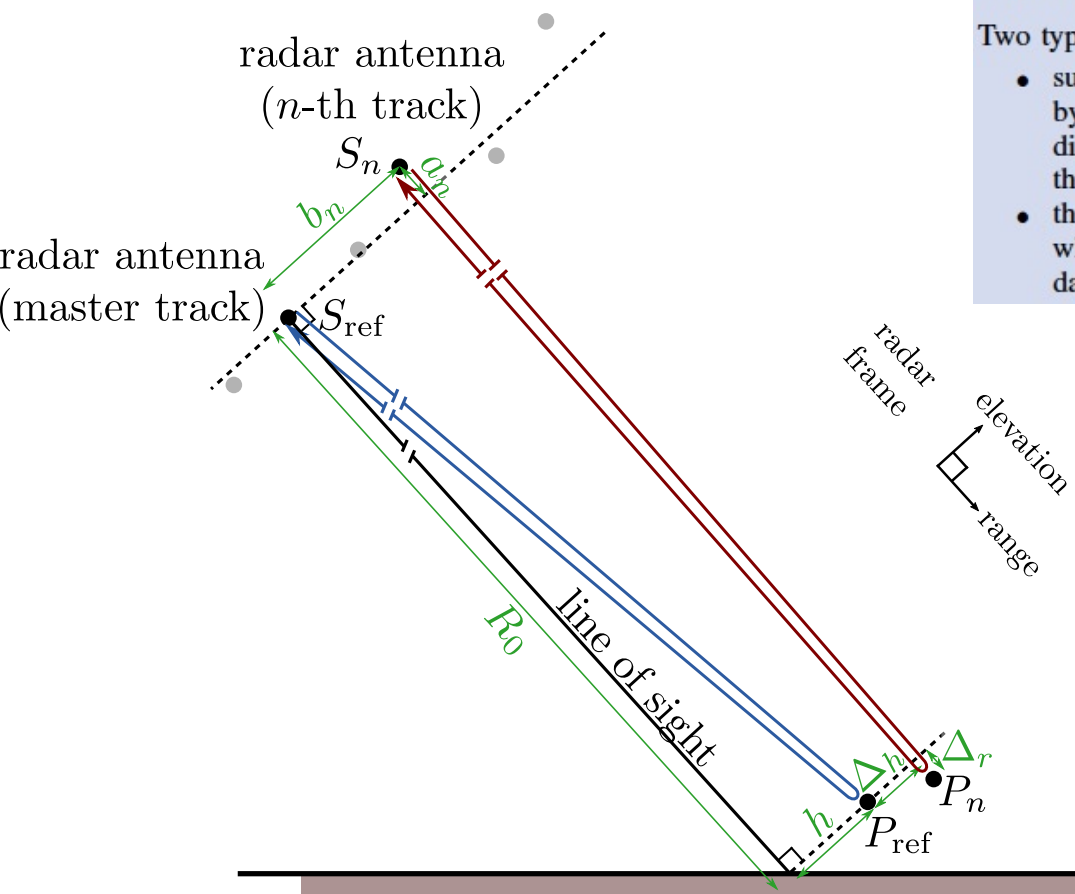
■ Measurement of path length differences :

- When finely registered (same cell sizes), it depends on the point elevation in the radar cell: **topographic fringes**
- Before fine resampling, ground range cells have different size, it implies a phase contribution along the swath (in range): **orbital fringes**

■ Conditions:

- The same scatterers organization should be measured by both sensors (no change of the ground)
- The atmospheric conditions should be the same
- The noise should be limited
- There should be no movement of the ground between the two acquisitions

Elevation and movement



The scatterer, located at $P_{ref} = [R_0, h]$ in the master image, moved between the acquisitions and is located at $P_n = [R_0 + \Delta_r, h + \Delta_h]$ when the n -th image is acquired. The path length for the master image has not changed. For the n -th image, the new path length is equal to $2\sqrt{(R_0 + \Delta_r - a_n)^2 + (h + \Delta_h - b_n)^2}$. The same approximations as in the previous paragraph lead to:

$$\Delta\varphi = \Delta\varphi_0 - \frac{4\pi b_n}{\lambda R_0} h + \frac{4\pi}{\lambda} \Delta_r + \frac{4\pi(b_n + h)}{\lambda R_0} \Delta_h \pmod{2\pi}. \quad (2)$$

Since $R_0 \gg b_n + h$ and $h \gg \Delta_h$, the last term is negligible compared to the others: only the motion in the direction of the line-of-sight Δ_r can be recovered.

Two types of motion are generally modeled:

- subsidence at a constant velocity: displacement on image n is given by $\Delta_r = \mu_{defo} \cdot t_n$, where μ_{defo} is the velocity in the line-of-sight direction and t_n is the time difference between the n -th image and the reference image,
- thermal dilation: displacement on image n is given by $\Delta_r = k_{th} \cdot T_n$, where k_{th} is a thermal coefficient and T_n is the temperature at the date of the n -th image.



Interferometry – processing chain

■ Interferometric processing chain

- Acquisition of 2 SAR images in interferometric configuration
- Fine registration of the 2 images
- Computation of the phase difference
- Phase unwrapping

Interferometry – processing chain

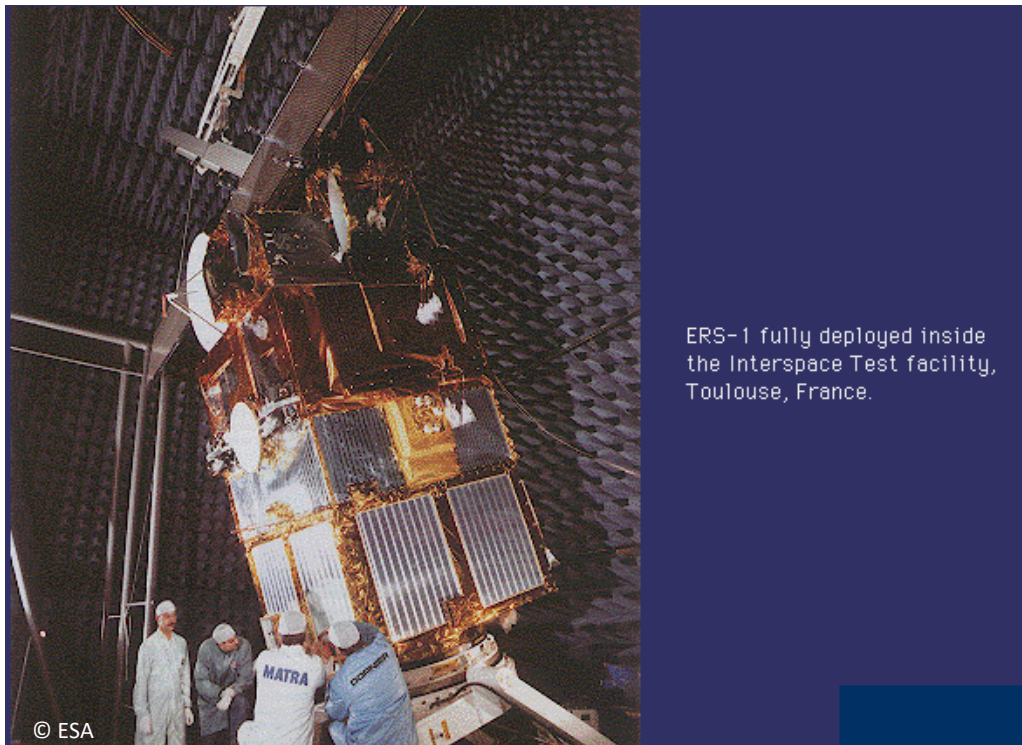
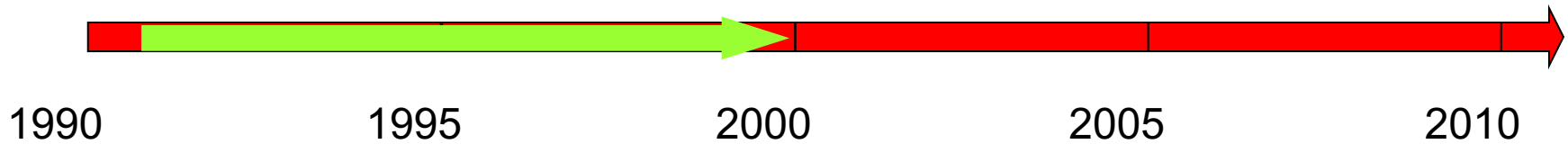
■ Interferometric processing chain

- Acquisition of 2 SAR images in interferometric configuration
- Fine registration of the 2 images
- Computation of the phase difference
- Phase unwrapping

Interferometry – Main steps

- **Acquisition of 2 SAR images in interferometric configuration**
- **Conditions**
 - Slight difference of incidence angle
 - No change of scatterers
 - Same atmospheric conditions
- **Repeat pass interferometry**
 - Same orbit, same incidence angle
 - Revisit time
- **Single pass interferometry (simultaneous acquisitions)**
 - SRTM (Shuttle Radar Topographic Mission)
 - Airborne acquisitions
 - TanDEM-X / TerraSAR-X

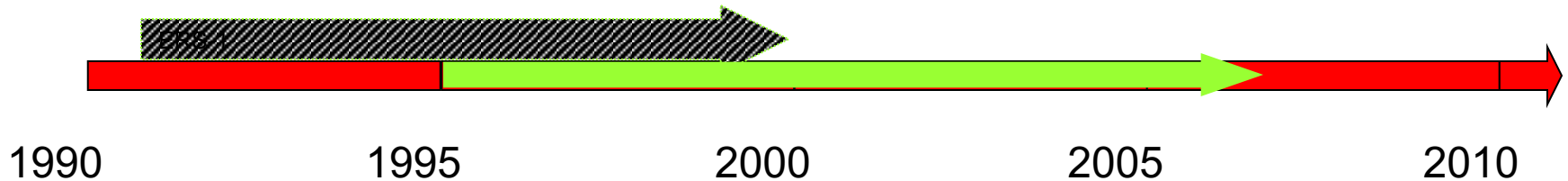
Satellites for SAR Interferometry: ERS-1



<http://earth.esa.int/ers/satconc/satconc.html>

- Operated by ESA
- Launched 1991 (†2000)
- C-Band (5.6 cm)
- 15.5 MHz bandwidth
- 35 day repeat polar orbit,
- Highly successful mission
- Initiated cross track and along track SAR interferometry

Satellites for SAR Interferometry: ERS-2



http://earth.esa.int/rootcollection/eeo/_foto21b.gif

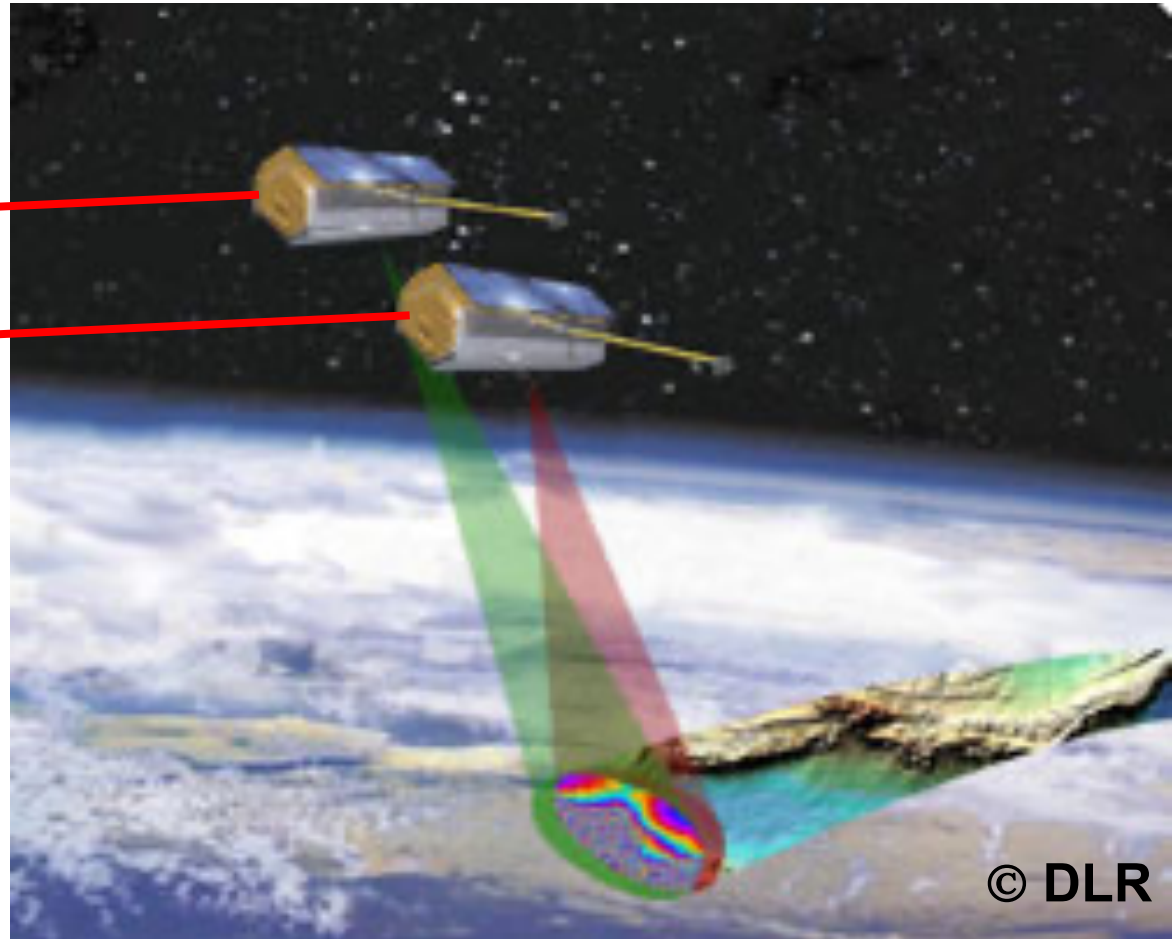
- Operated by ESA
- Launched 1995
- SAR instrument and orbit identical to ERS-1
 - 1 day time delay
- ERS-1/2 tandem operation 1995-1998
 - controlled baseline
- 1 day time lag → low decorrelation → DEM generation

Acquisition - SAR multi-pass (Terrasar-X)

Day J

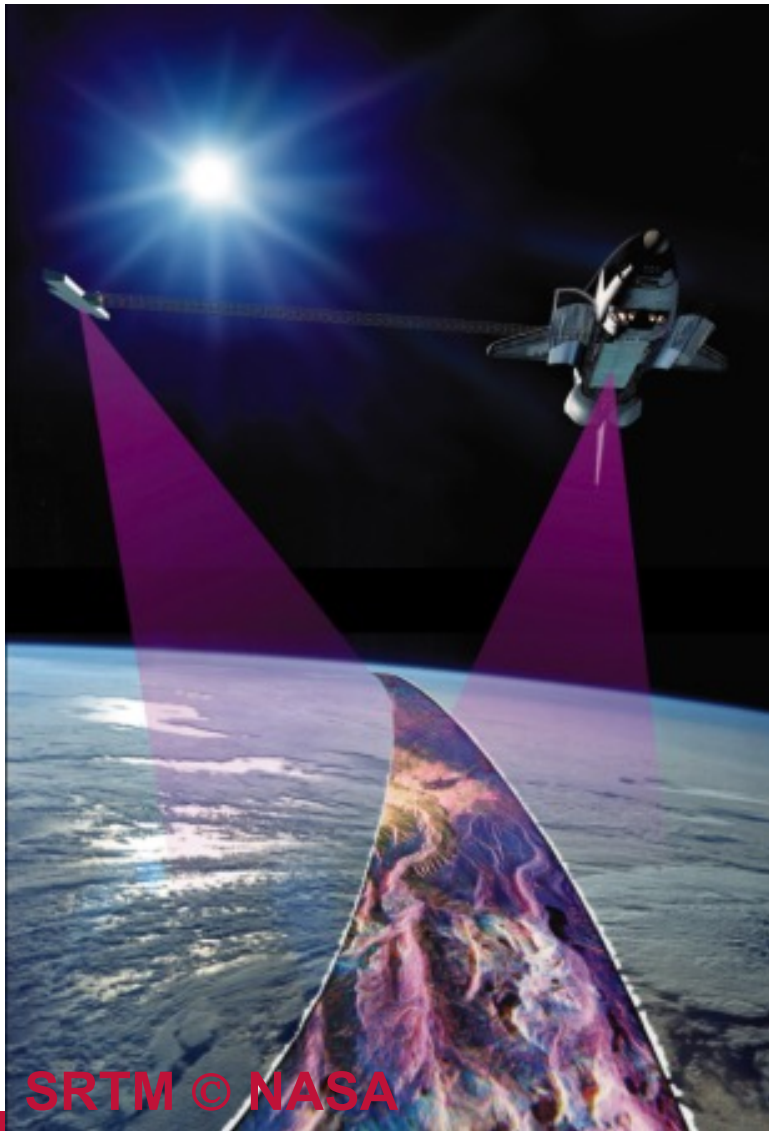
Day J + 11

Exploitation of the revisit of the sensor on the same orbit



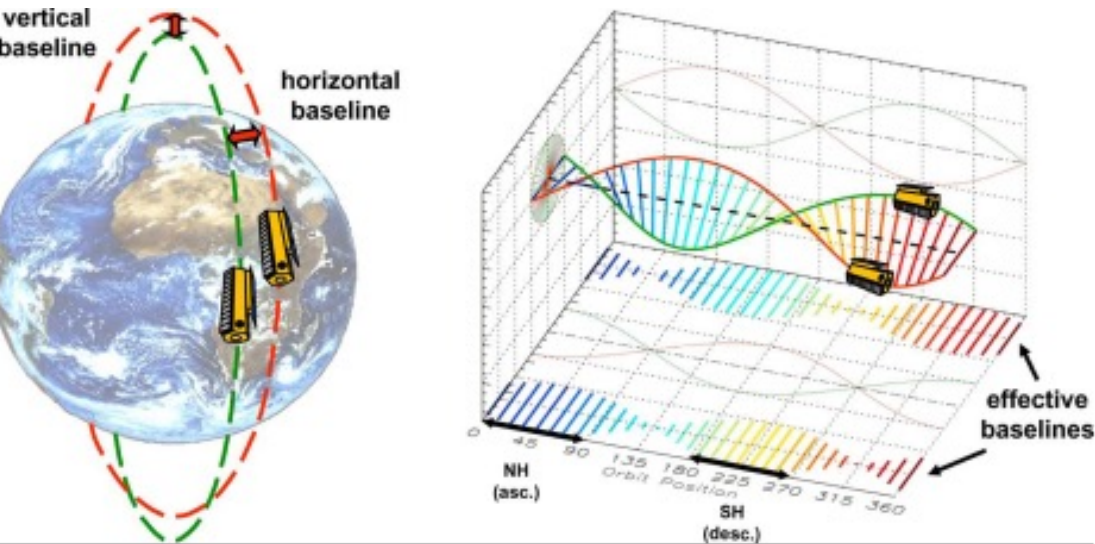
© DLR

Acquisition - SAR mono-pass



Acquisition - SAR mono-pass

TerraSAR-X: 2007
TanDEM-X: 2011



TanDEM-X © DLR

HELIX satellite formation for TanDEM-X

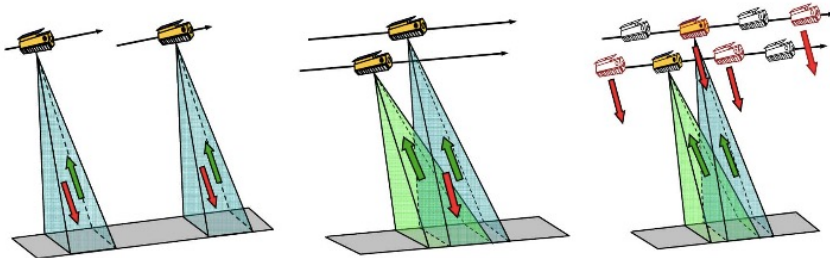


Fig. 1. Examples of data acquisition modes for TanDEM-X. (Left) Pursuit monostatic mode, (middle) bistatic mode, and (right) alternating bistatic mode.



Interferometry – Main steps

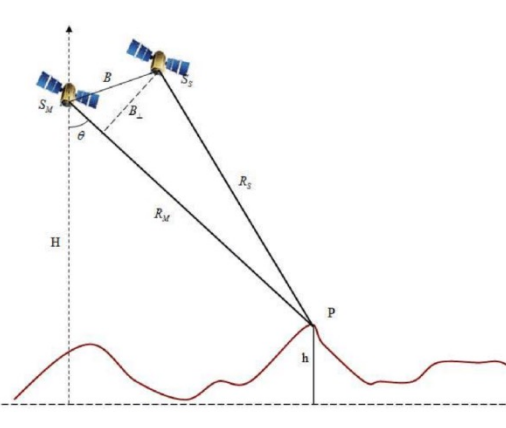
■ Processing chain

- Acquisition of 2 SAR images in interferometric configuration
- Fine registration of the 2 images
- Computation of the phase difference
- Phase unwrapping

Registration

■ Repeat pass interferometry :

- Same orbital track, same incidence angle, same mode, same polarization
- Different times, different positions (baseline)
- Parallel baseline: relative image shift
- Orthogonal baseline: range cell size variation along flat earth



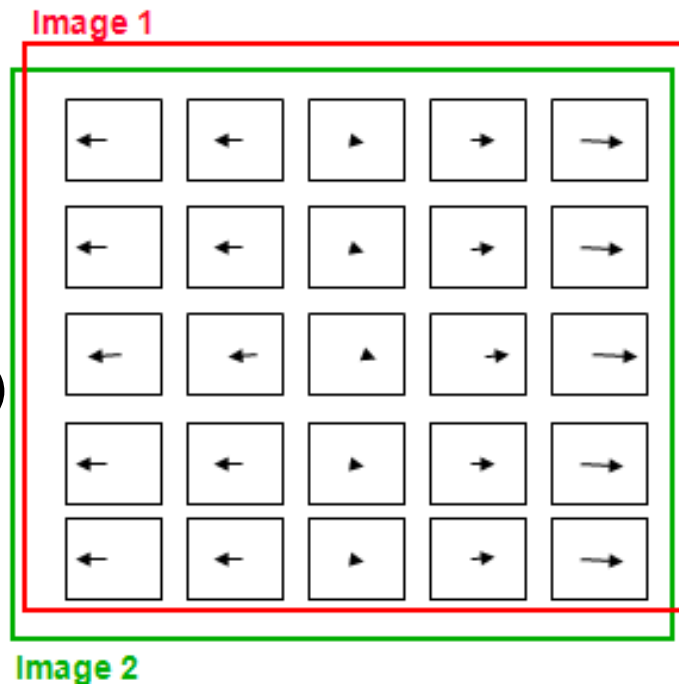
Registration in practice – different approaches

■ Accurate knowledge of sensor parameters: geometric registration

- Orbit, speed, clocks, times
- Resampling of one image (« slave ») in the « master » image geometry

■ Image processing driven re-sampling

- Over-sampling with a factor of 100 (range)
- Complex cross-correlation maximization
- Computation of an affine transform



Registration in practice – coarse registration

Image processing registration

- Search for a global translation between the two amplitude images
- Minimization of the MSE between the master image and the translated slave image

$$MSE(k, l) = \sum_{(i, j)} (A_1(i, j) - A_2(i + k, j + l))^2$$

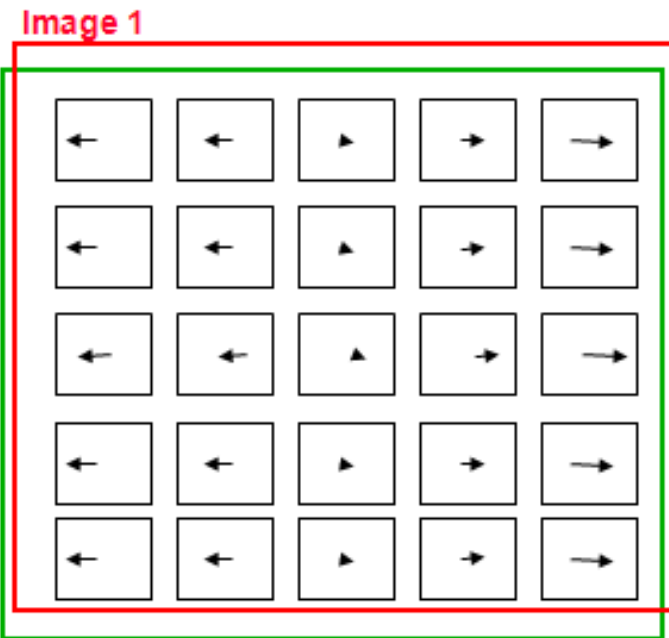
- Maximization of the correlation = convolution between the inverse of the translated master image and the slave image

$$Corr(k, l) = \sum_{(i, j)} A_1(i, j) A_2(i + k, j + l) = \tilde{A}_1 * A_2(k, l) \quad (\text{See practical work session})$$

$$Corr(k, l) = TF^{-1}(TF(A_1)^* . TF(A_2))$$

$$z_1 = A_1 e^{j\phi_1}$$

$$z_2 = A_2 e^{j\phi_2}$$



Registration in practice – coarse registration

Image processing registration

$$z_1 = A_1 e^{j\phi_1}$$

$$z_2 = A_2 e^{j\phi_2}$$

- The correlation peak gives the translation values between the master and the slave image
- Sub-pixelic registration: to be perfectly aligned the phase shift due to the difference of pixel size should be taken into account
- Two strategies:
 - Resampling of the slave image
 - Phase ramp correction= orbital fringe correction

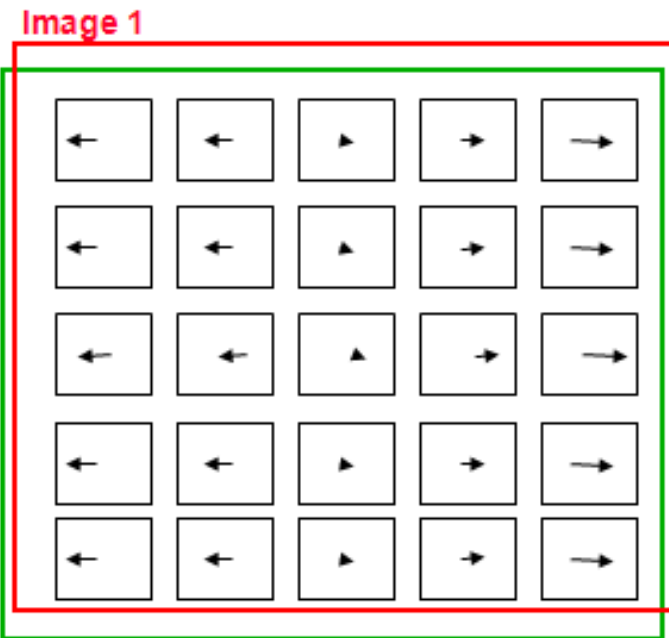
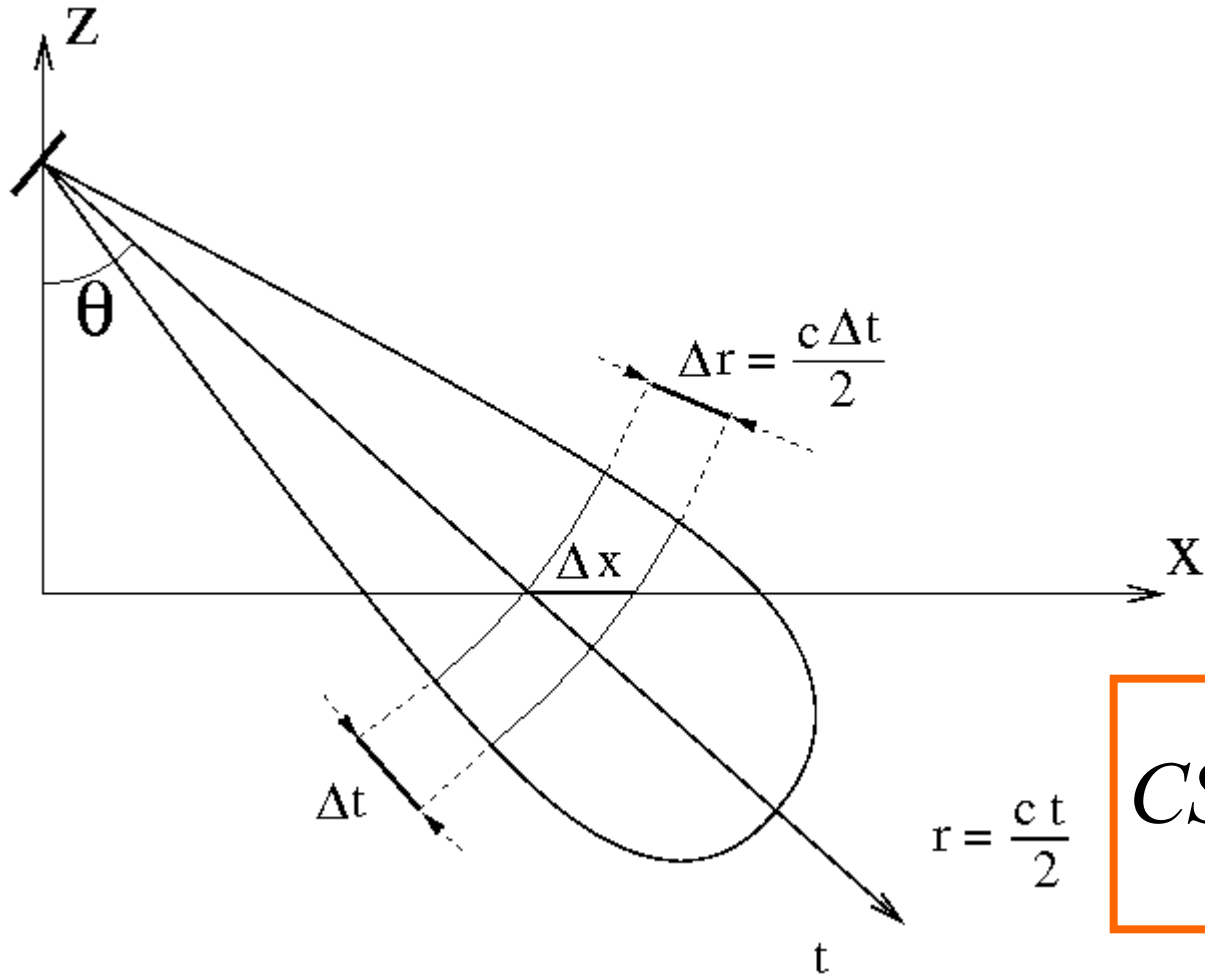


Image 2

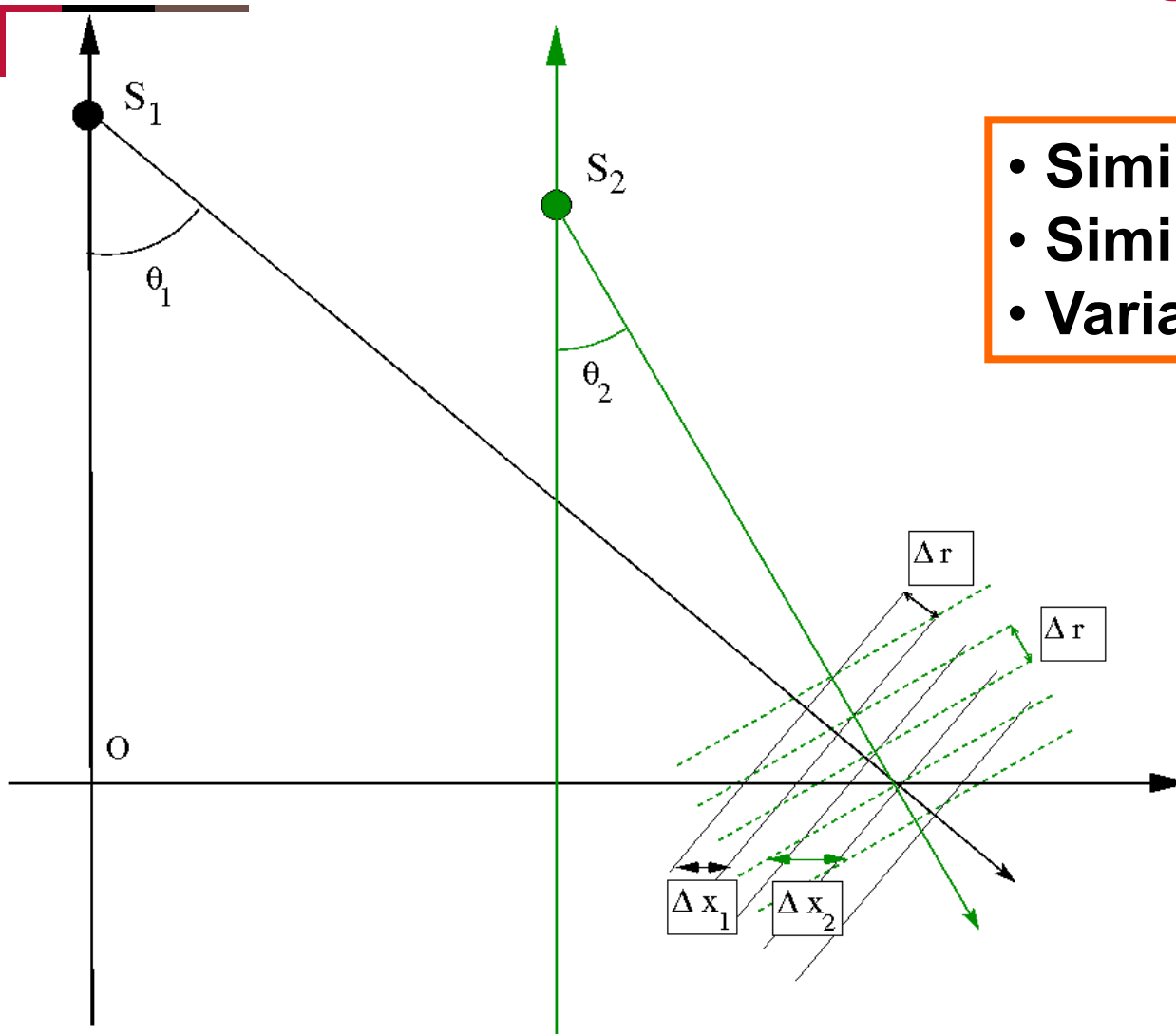
(See practical work session)

Registration in practice – fine registration



$$CS = \Delta x = \frac{\Delta r}{\sin(\theta)}$$

Flat earth: two incidence angles

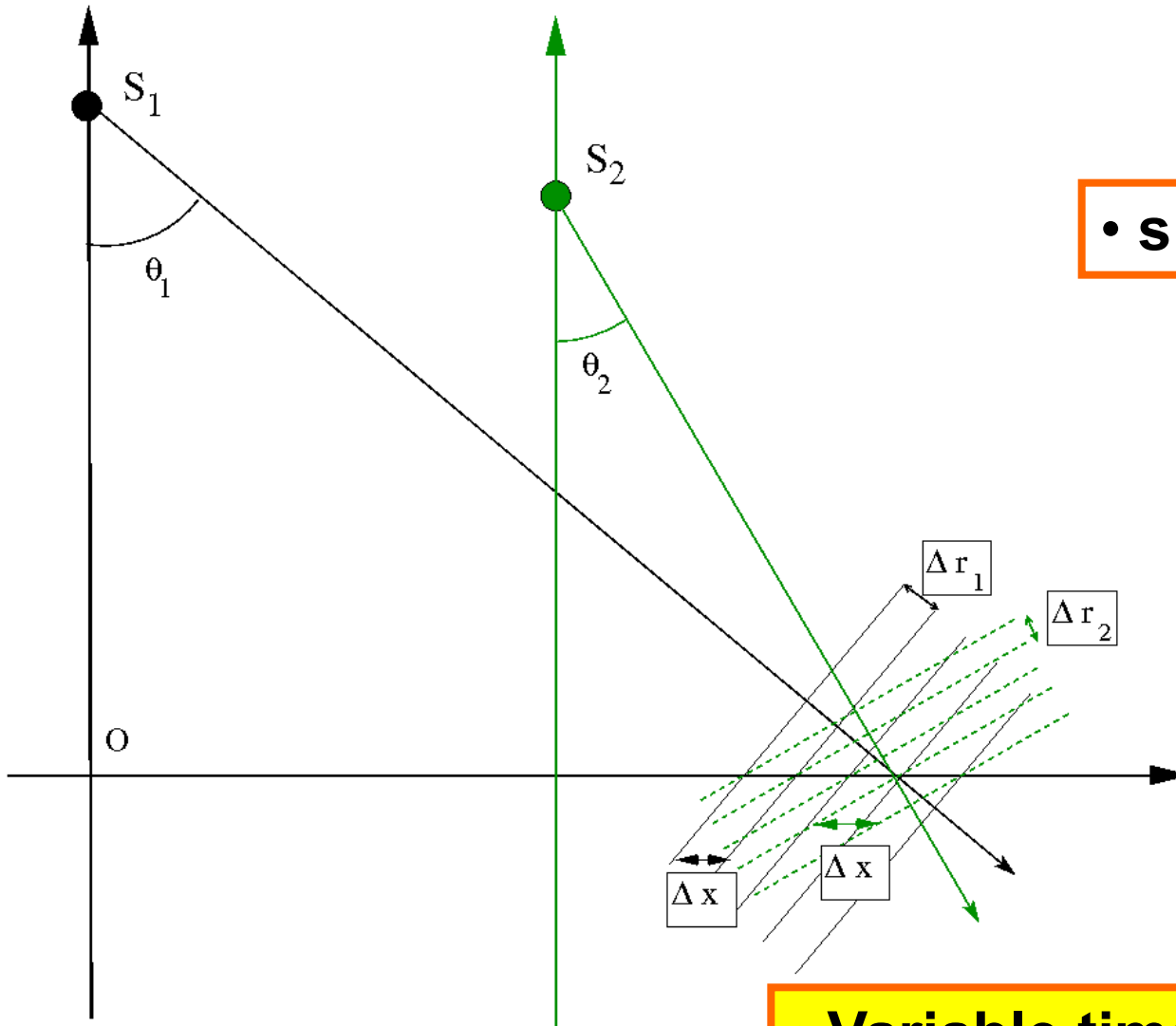


- Similar time cell
- Similar range cell
- Variable ground cells

$$\Delta x_1 = \frac{\Delta r}{\sin \theta_1}$$
$$\Delta x_2 = \frac{\Delta r}{\sin \theta_2}$$

- Re-sampling in time of one of the image to have similar ground cells

After re-sampling



• similar ground cells

$$\Delta r_1 = \Delta x \sin \theta_1$$
$$\Delta r_2 = \Delta x \sin \theta_2$$

• Variable time cells

Phase shift for one pixel

- Phase contribution of flat earth

$$\Delta r = \frac{c\Delta t}{2} \quad \Delta x = \frac{\Delta r}{\sin \theta} = \frac{c}{2 F_e \sin \theta}$$

- Pixel size for master and slave images:

$$\Delta x_M = \frac{c}{2 F_e \sin \theta} \quad \Delta x_S = \frac{c}{2 F_e \sin (\theta + \delta \theta)}$$

- Pixel size difference

$$\Delta x_M - \Delta x_S = \frac{c}{2 F_e} \left(\frac{1}{\sin \theta} - \frac{1}{\sin (\theta + \delta \theta)} \right)$$

Phase shift for one pixel

■ Pixel size difference and induced phase shift

$$\Delta x_M - \Delta x_S = \frac{c}{2F_e} \left(\frac{1}{\sin \theta} - \frac{1}{\sin(\theta + \delta\theta)} \right)$$

$$\sin(\theta + \delta\theta) = \sin \theta \cos \delta\theta + \sin \delta\theta \cos \theta$$

$$\Delta x_M - \Delta x_S \approx \frac{c}{2F_e \sin \theta} \frac{\sin \delta\theta \cos \theta}{\sin \theta}$$

$$\sin \delta\theta = \frac{B_{\perp}}{R}$$

$$\Delta_{CS} = \Delta x_M - \Delta x_S \approx \Delta x \frac{B_{\perp} \cos \theta}{R \sin \theta}$$

$$\Delta_R = \Delta_{CS} \sin \theta \approx \Delta x \frac{B_{\perp}}{R} \cos \theta$$

$$\Delta\phi_{orb} = \frac{4\pi \Delta_R}{\lambda} = \frac{4\pi B_{\perp}}{\lambda R} \cos \theta \Delta x$$

Phase shift for one pixel

- Phase contribution due to uncorrected pixel size difference between the two sensors (flat earth)

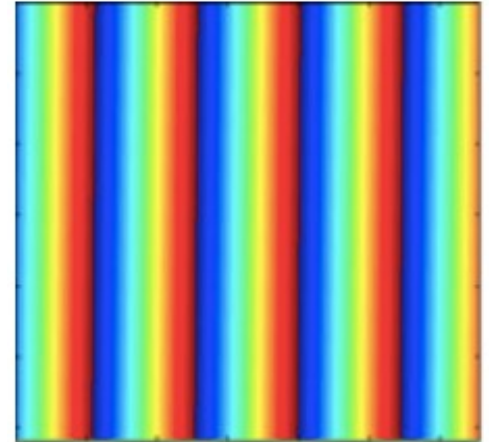
$$\Delta\phi_{orb} = \frac{4\pi\Delta R}{\lambda} = \frac{4\pi B_{\perp}}{\lambda R} \cos\theta \Delta x$$

- Can be computed using the sensor parameters
- Create fringes in the range direction = orbital fringes are parallel to the track
- To correct the orbital fringes:
 - compute the phase ramp

$$z_{orb}(n) = e^{jn\Delta\phi_{orb}}$$

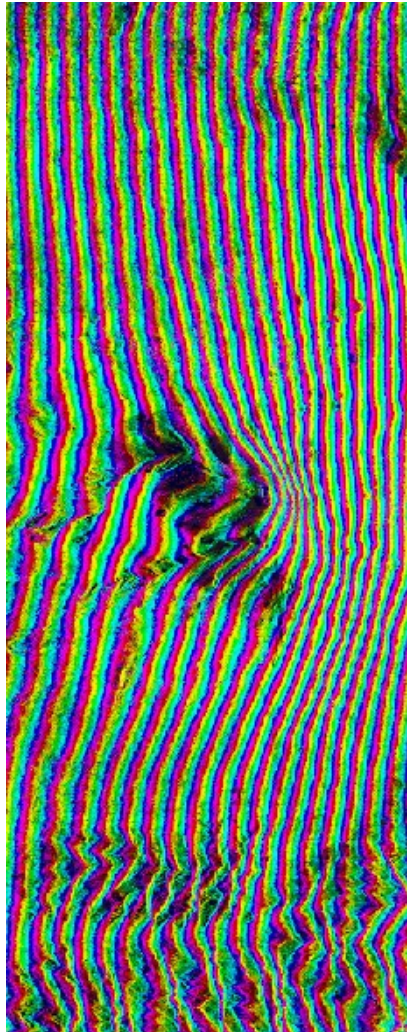
- Correct the phase shift

$$z_s^c(n) = z_s(n)e^{jn\Delta\phi_{orb}}$$

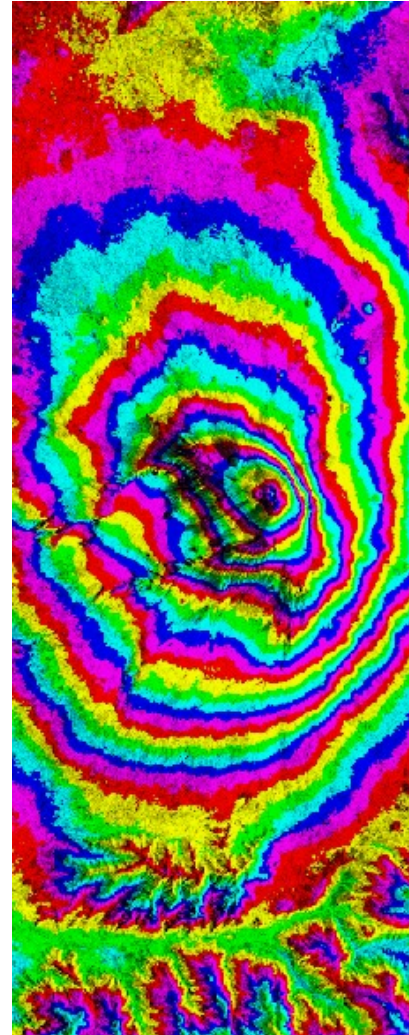


Example of orbital fringes

$$z_m z_s^*$$



$$z_m z_s^{C*}$$





Interferometry – Main steps

■ Processing chain

- Acquisition of 2 SAR images in interferometric configuration
- Fine registration of the 2 images
- Computation of the phase difference
- Phase unwrapping

Computation of phase difference

- Two finely registered complex images:

$$z_1(m, n) = A_1(m, n)e^{i\phi_1(m, n)}$$

$$z_2(m, n) = A_2(m, n)e^{i\phi_2(m, n)}$$

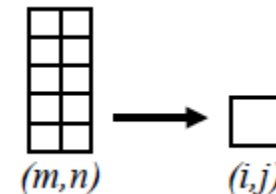
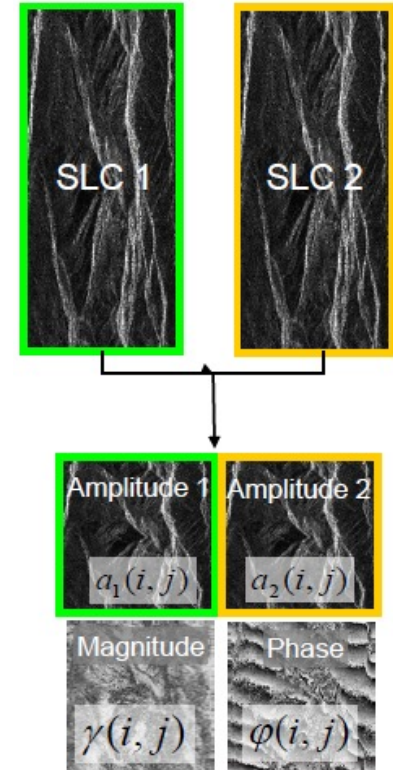
- Hermitian product

$$z_1(m, n)z_2^*(m, n) = A_1(m, n)A_2(m, n) \exp(\phi_1(m, n) - \phi_2(m, n))$$

- Interferometric product (multi-look)

$$\gamma(i, j)e^{i\phi(i, j)} = \frac{\sum_{(m, n)} z_1(m, n)z_2^*(m, n)}{\sqrt{\sum_{(m, n)} |z_1(m, n)|^2} \sqrt{\sum_{(m, n)} |z_2(m, n)|^2}}$$

- Assume local stationarity



Interferometric product

■ Interferometric phase

- Less noisy when large window but loss of resolution

■ Interferometric coherence

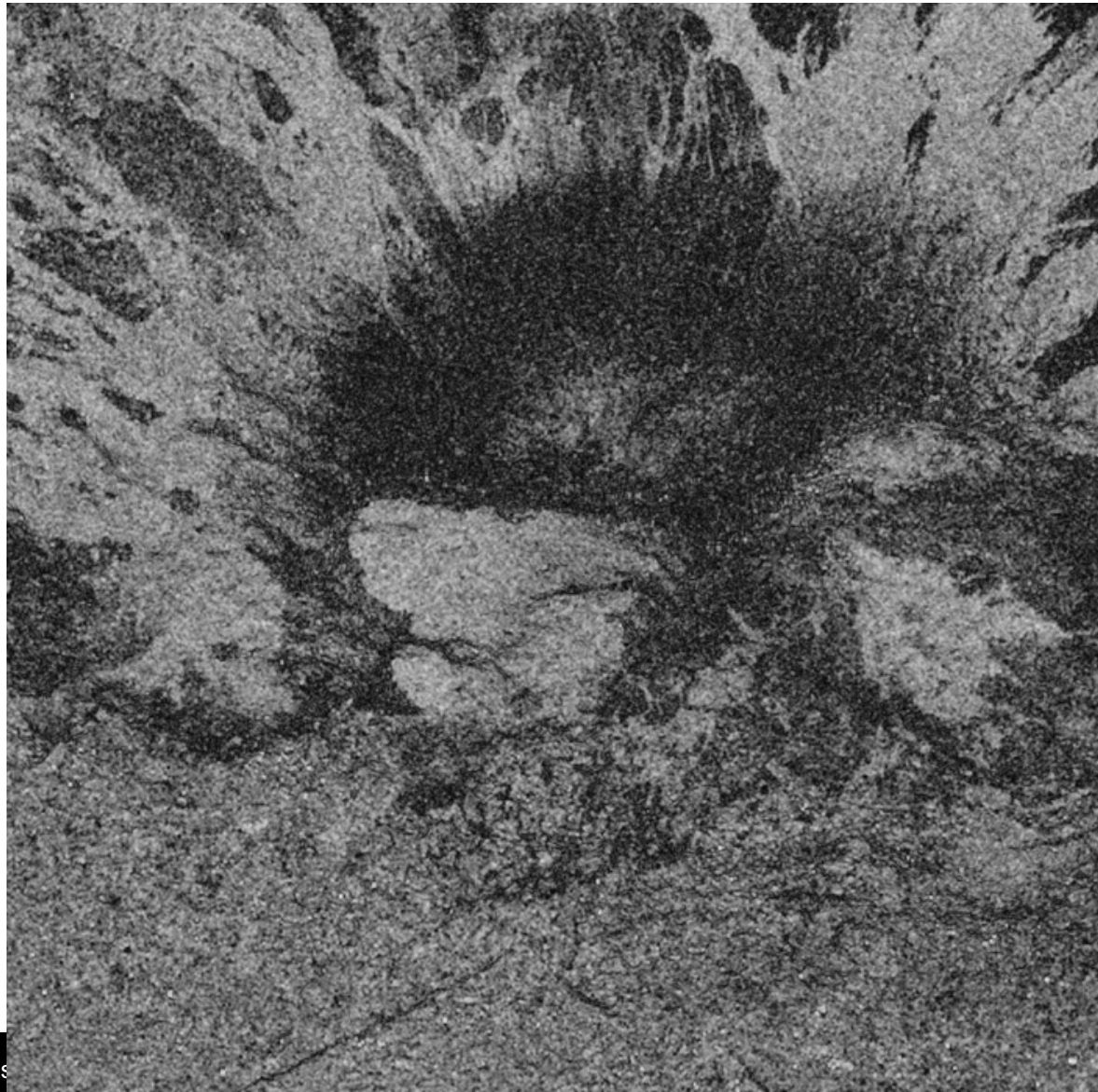
- In $[0,1]$
- High coherence: similar complex values = reliable interferometric phase information
- Low coherence: variable complex values (temporal changes, no signal – shadow / smooth areas, high difference of incidence angles, atmospheric conditions, ...)

■ Interferometric filtering

- Replace the square window averaging by sample selection

Example of interferometric coherence

Mount ETNA
ERS1/2 Tandem
Mission



Some parameters

■ Altitude of ambiguity

- Wrapped phase :

$$\psi_{1,2} = \frac{4\pi B_{\perp 1,2}}{R \sin(\theta) \lambda} h$$

$$\psi_{1,2} = \alpha_{geom 1,2} h$$

- Elevation causing one topographic fringe

$$\psi_{1,2} = 2\pi$$

$$h_{amb} = \frac{\lambda R \sin \theta}{2B_{\perp 1,2}}$$

- Increase of the baseline : decrease of the altitude of ambiguity :

- increase the topographic sensitivity
- More difficult to unwrapp !

$$\sigma_h = \sigma_\psi \frac{h_{amb}}{2\pi}$$

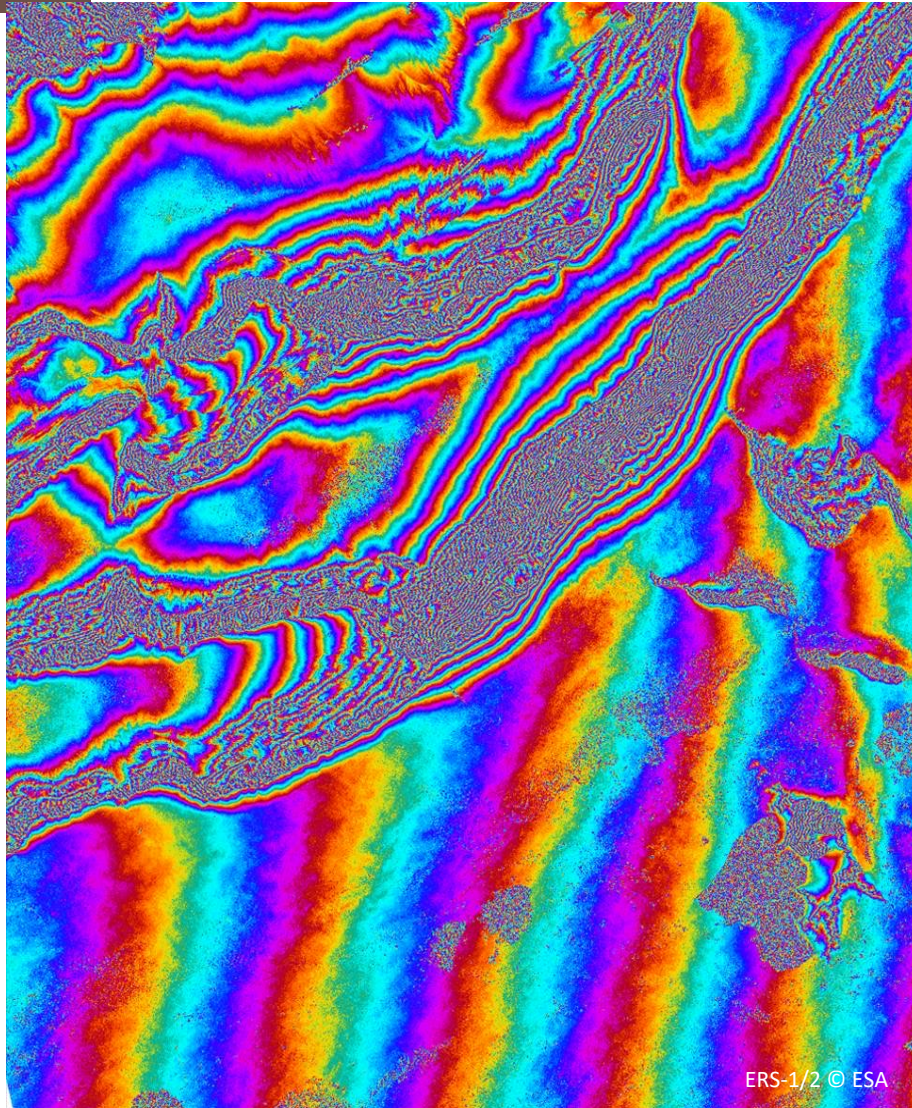
ERS SAR Image



Bachu, China

approx. 100 km × 80 km

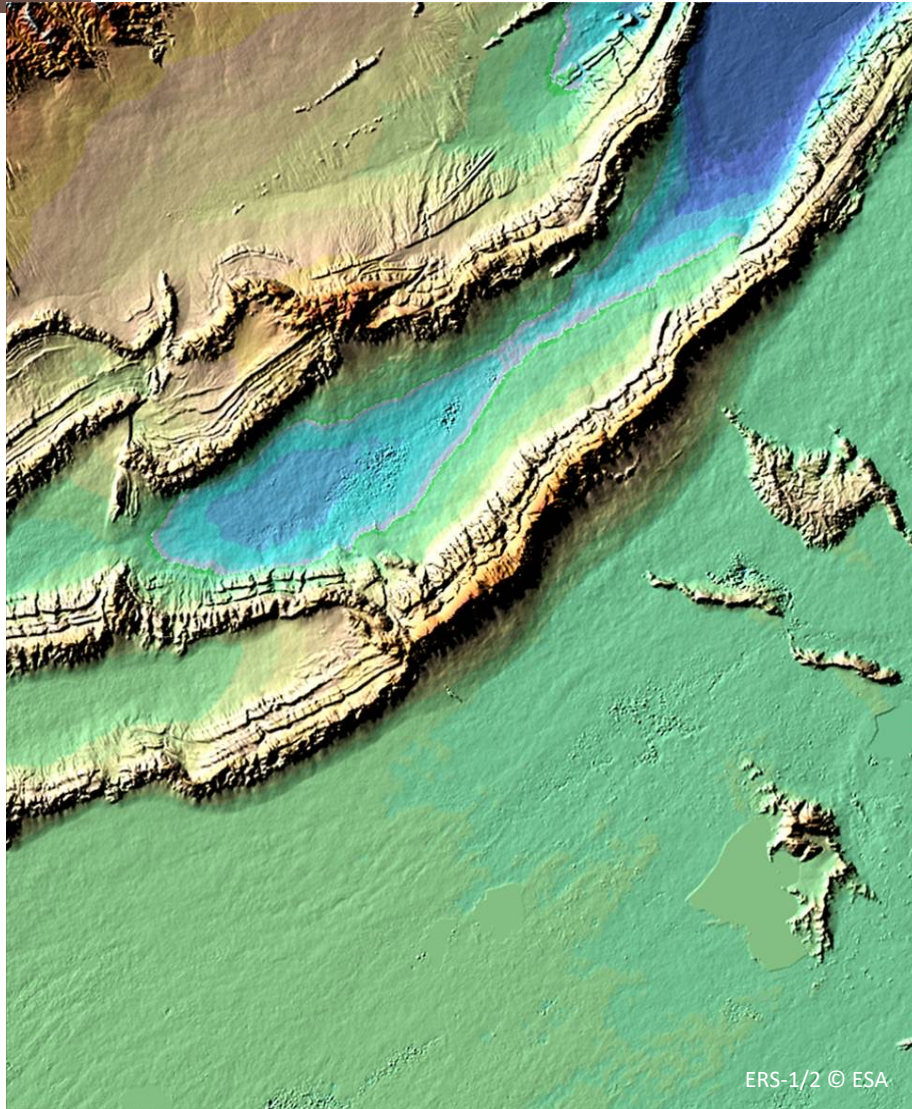
Interferometric Phase



Bachu, China

approx. 100 km × 80 km

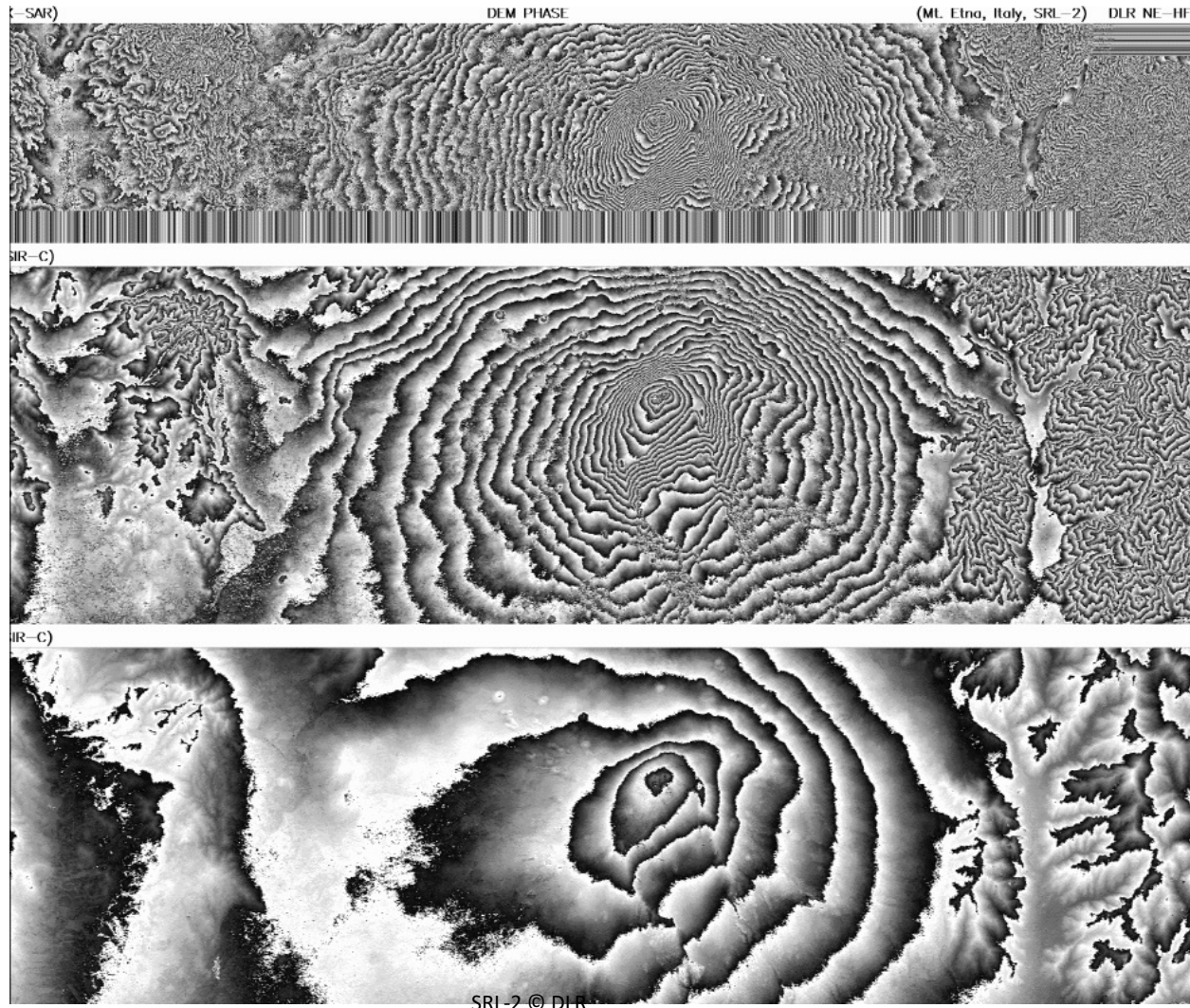
InSAR DEM (ERS-1/2)



Bachu, China

approx. 100 km × 80 km

Interferometric Sensitivity as a Function of Wavelength



$$h_{amb} = \frac{R \sin(\theta) \lambda}{2B_{\perp 1,2}}$$

X-band

C-band

L-band

Fig.: Mt. Etna
data: SRL-2 (© DLR)

Some parameters

■ Altitude of ambiguity

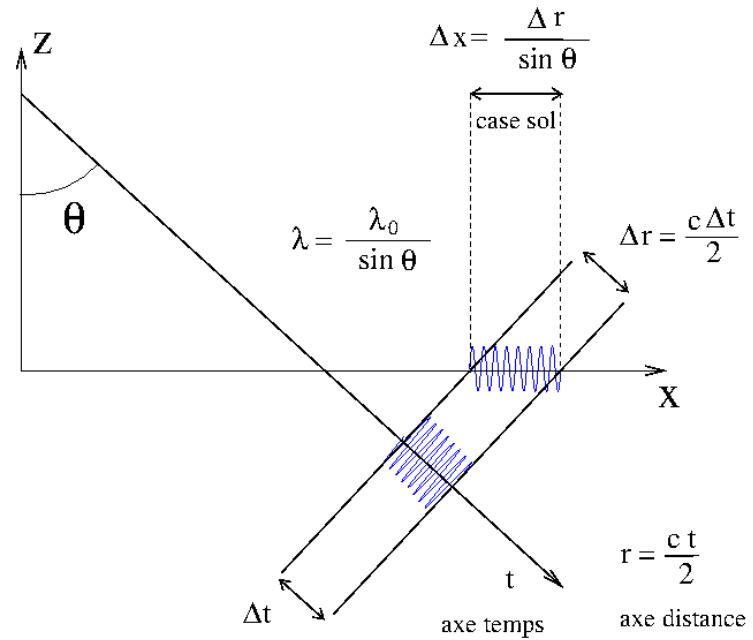
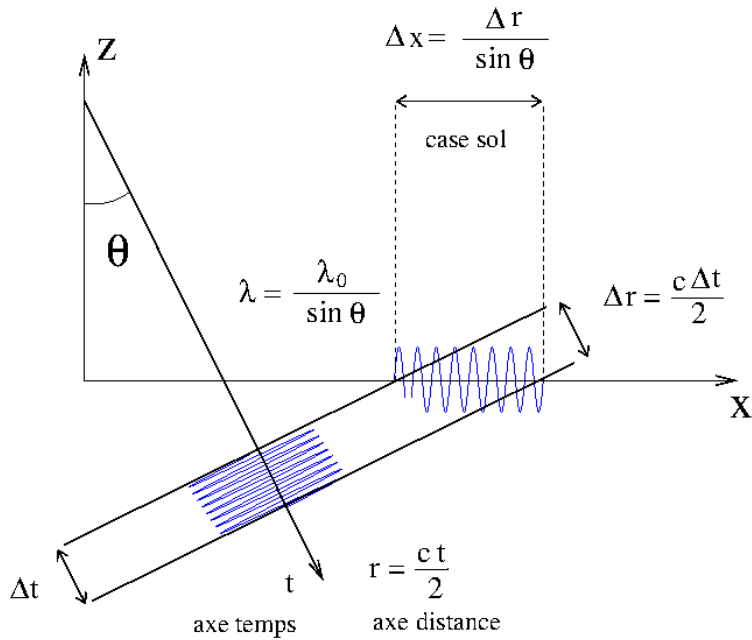
- The largest the baseline : the best the sensitivity

$$\sigma_h = \sigma_\psi \frac{h_{amb}}{2\pi}$$

■ Critical orthogonal baseline

- The largest the baseline : the noisiest the phase
- Difference of incidence angles: geometric decorrelation (the scatterers are seen with different viewing angles)

Critical baseline :



- Same backscattering of the pixels
- \Rightarrow angle difference should be limited

$$\Delta\phi_{orb} = 2\pi \iff \frac{4\pi B_{\perp}}{\lambda R} \cos\theta \Delta x = 2\pi$$

$$B_{\perp}^{crit} = \frac{\lambda R}{2 \cos\theta \Delta x} = \frac{\lambda R \tan\theta}{2\Delta r}$$

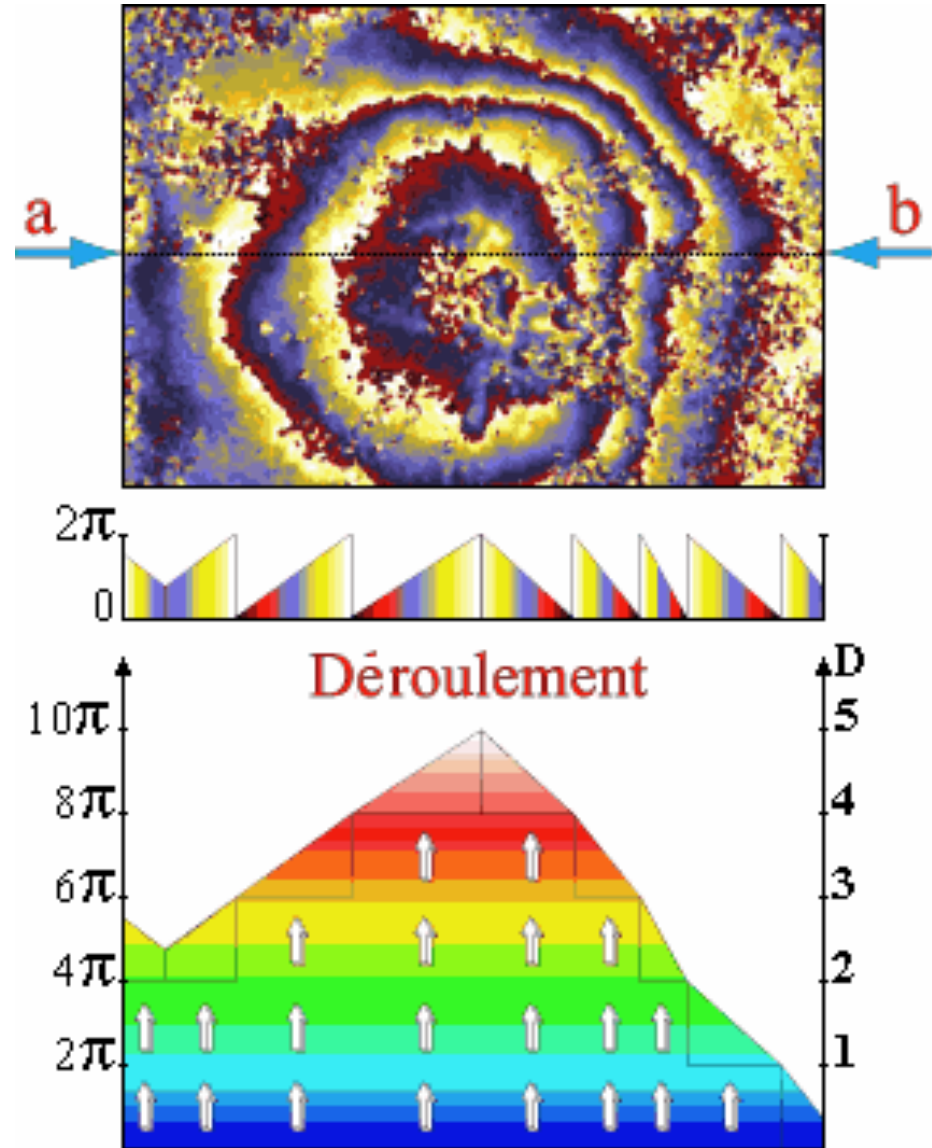
Interferometry – Main steps

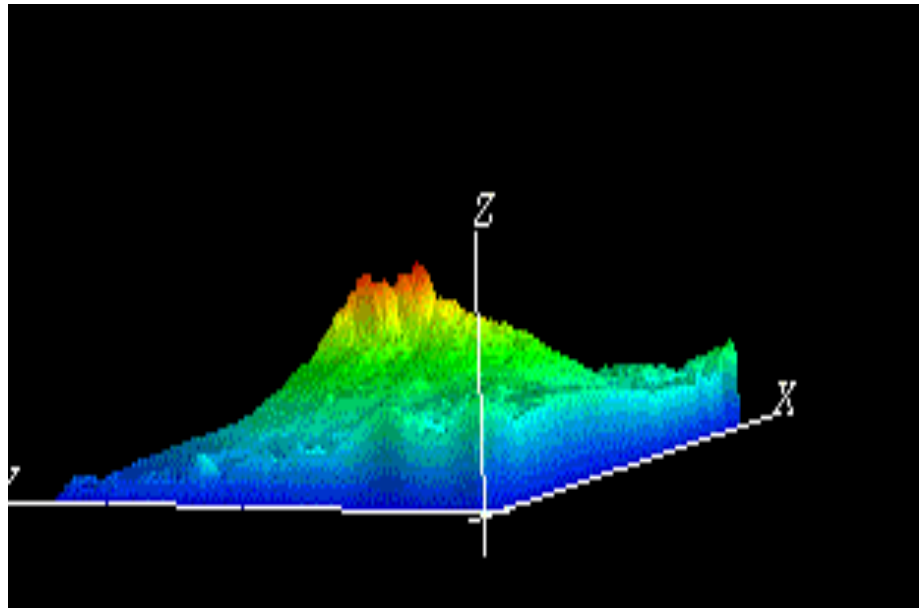
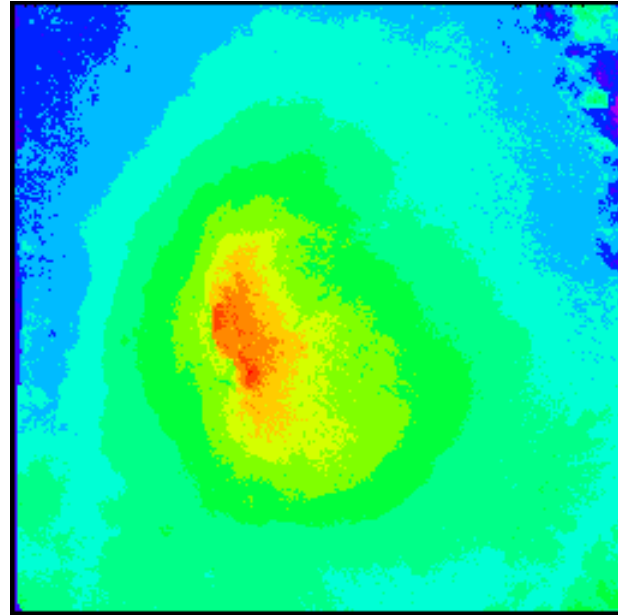
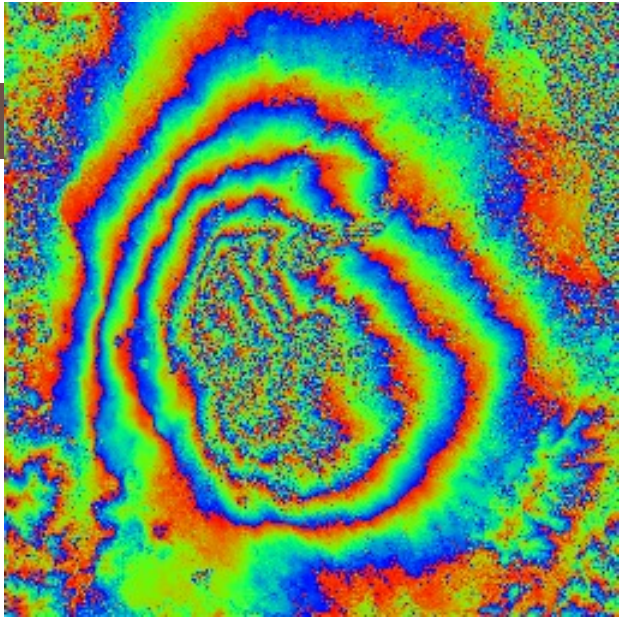
■ Processing chain

- Acquisition of 2 SAR images in interferometric configuration
- Fine registration of the 2 images
- Computation of the phase difference
- Phase unwrapping

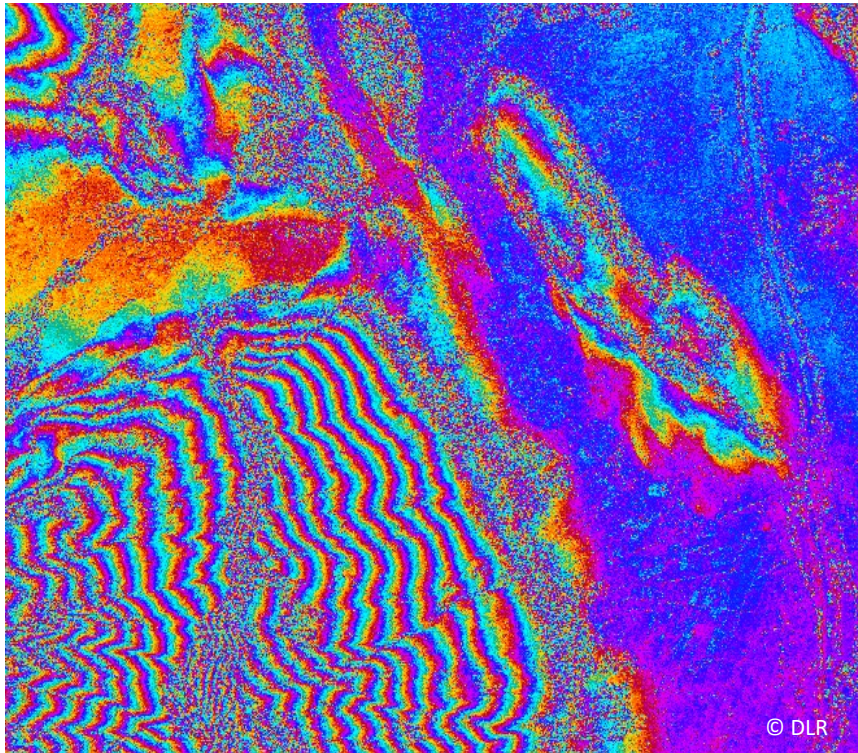
Phase unwrapping

$$\Phi(P) = \phi(P) + 2k\pi$$



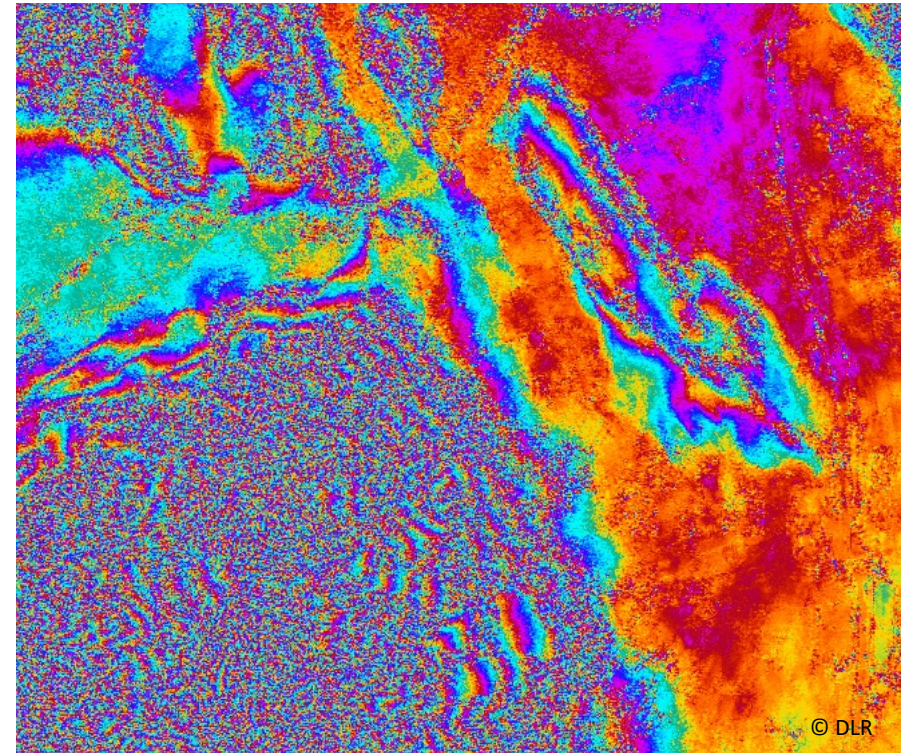


Interferometric Phase is Ambiguous



good fringe quality

ERS-1/2, 13/14 Jan. 1996



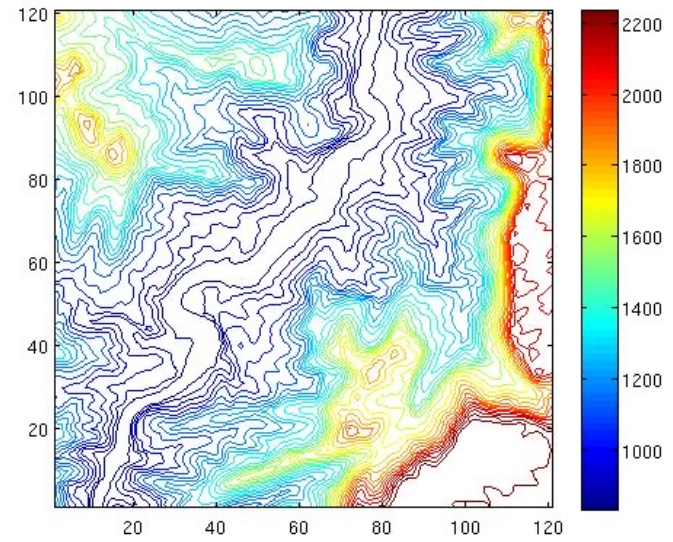
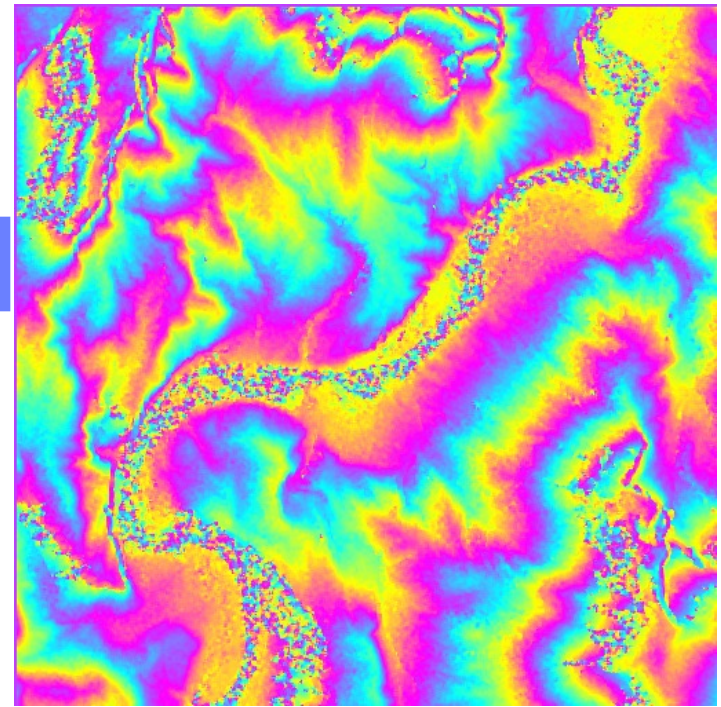
bad fringe quality

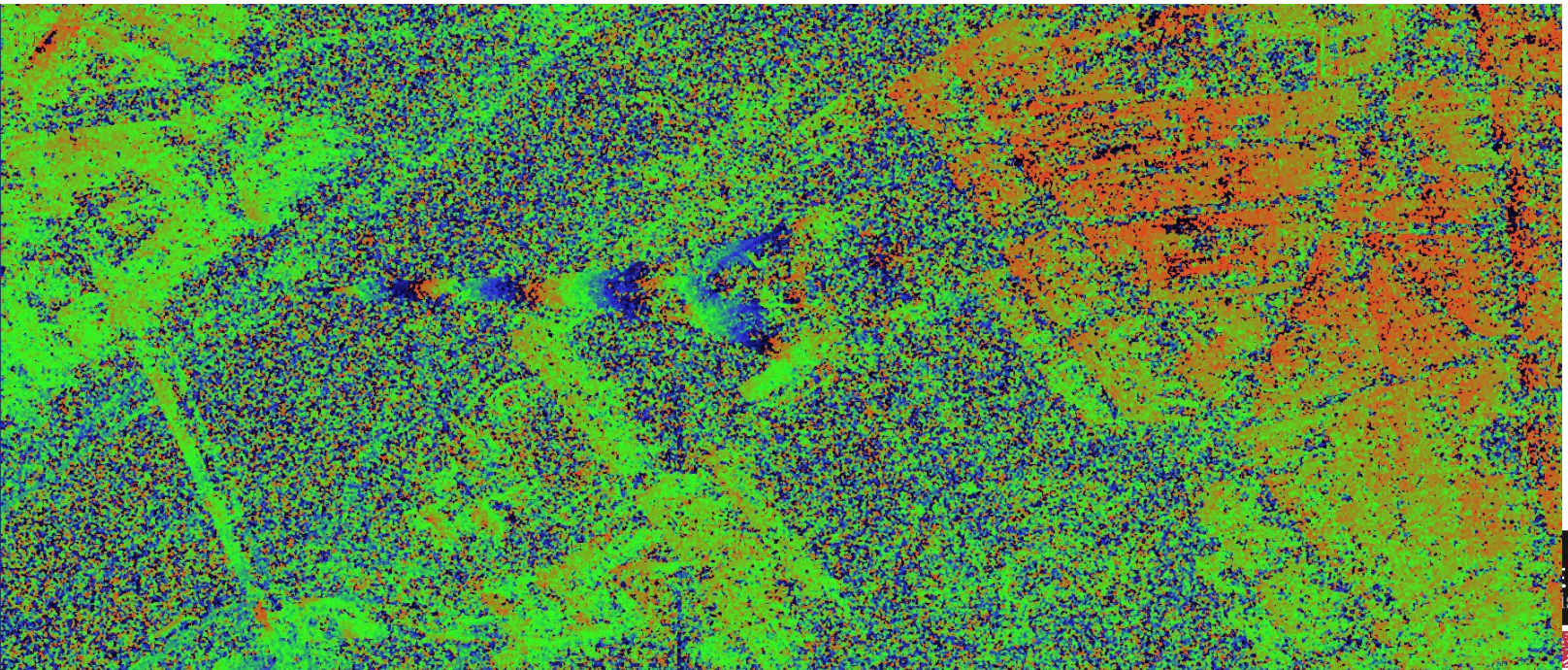
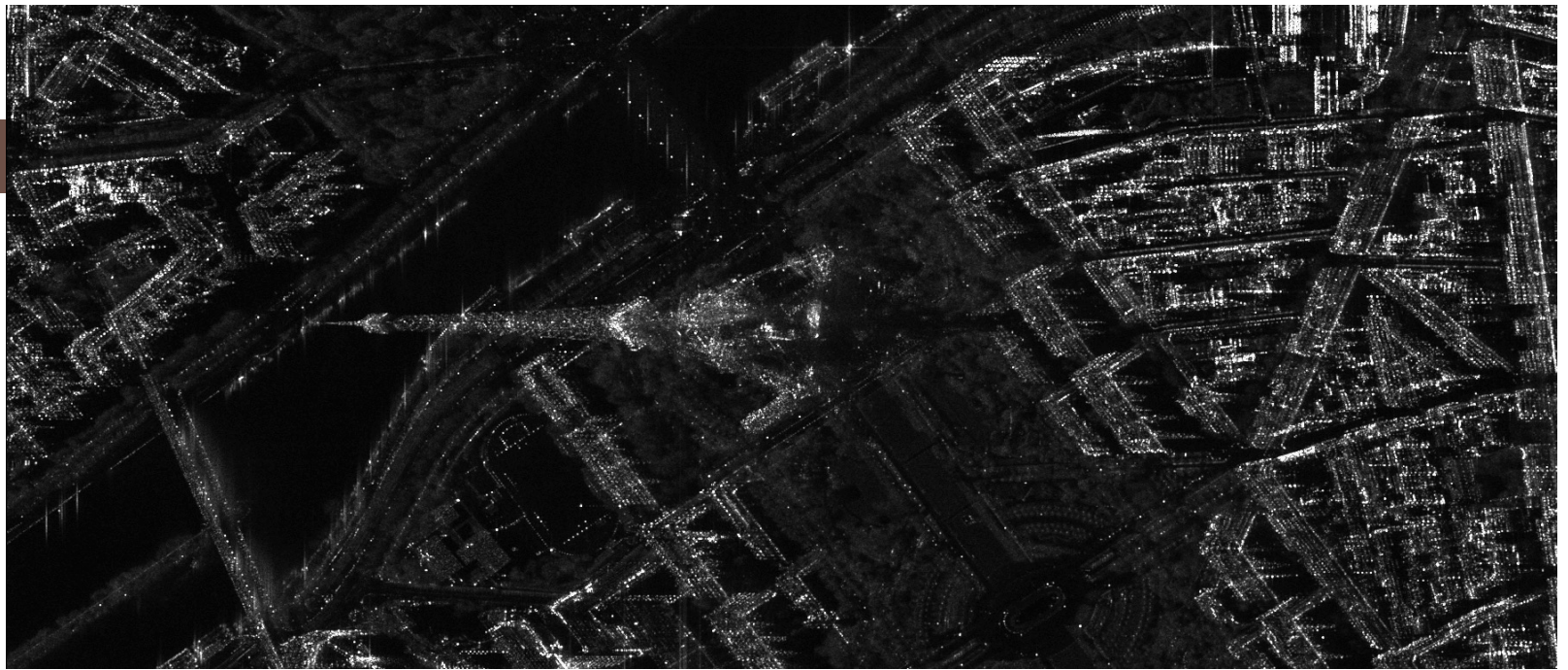
ERS-1/2, 23/24 March 1996

Interferometry Grand Canyon

Jour J

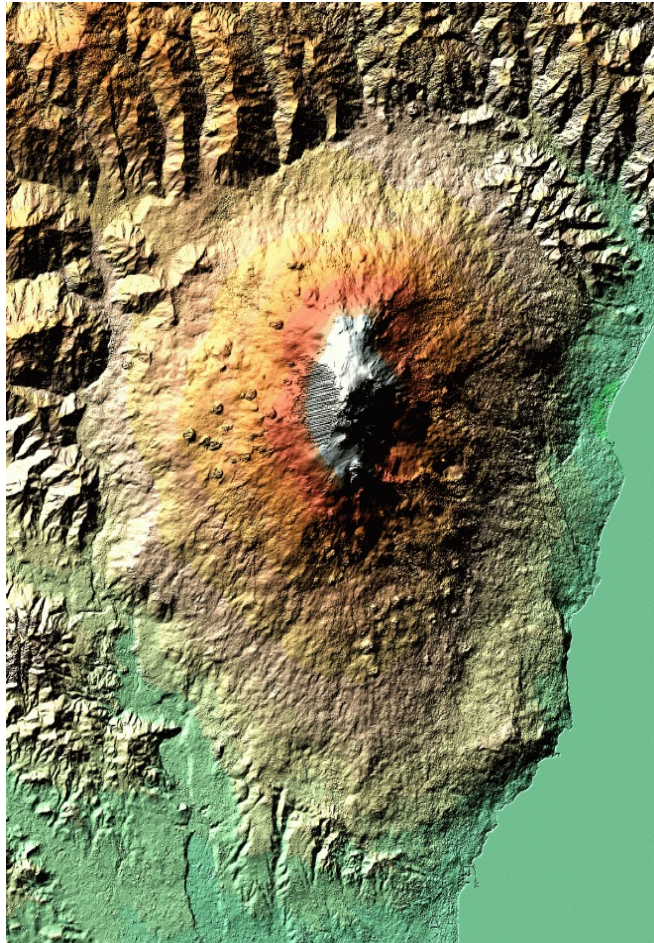
Jour J+cycle



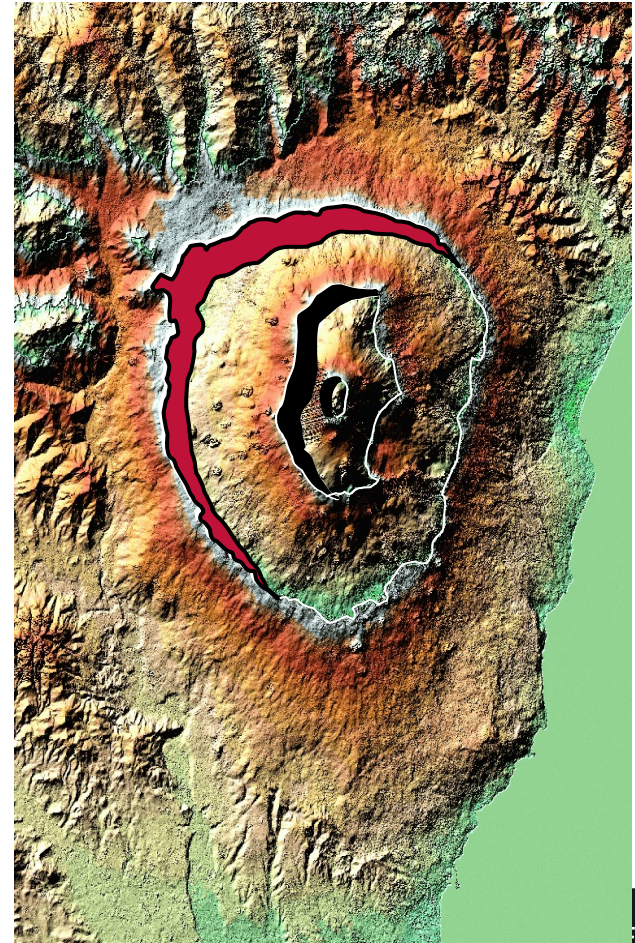


Find the “Most Likely” Solution

this is much more likely ...



... than this



Unwrapping approaches

■ Local approaches

- Local unwrapping by adding the $2k\pi$ values
- Problem : uncoherencies when unwrapping condition not fulfilled

■ Global approaches

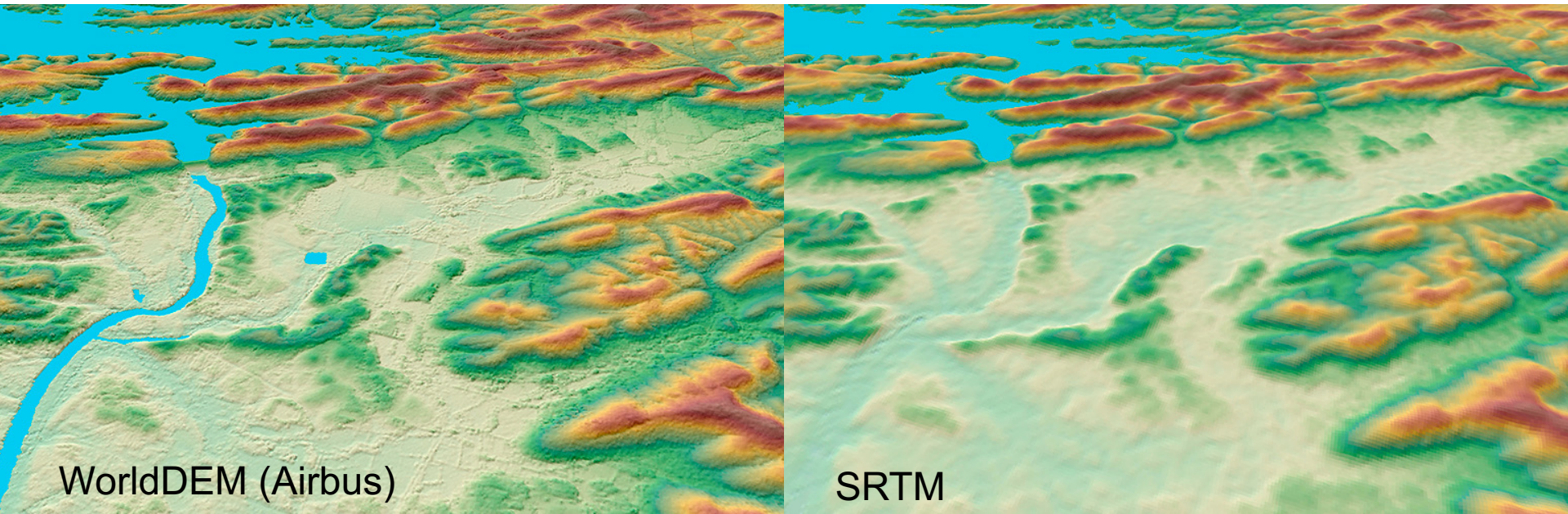
- Global optimization of a functional (likelihood given by wrapped phase values + prior smoothness constraint)

■ Multi-channel / multi-frequency approaches

- Phase becomes non - ambiguous

InSAR - DEM

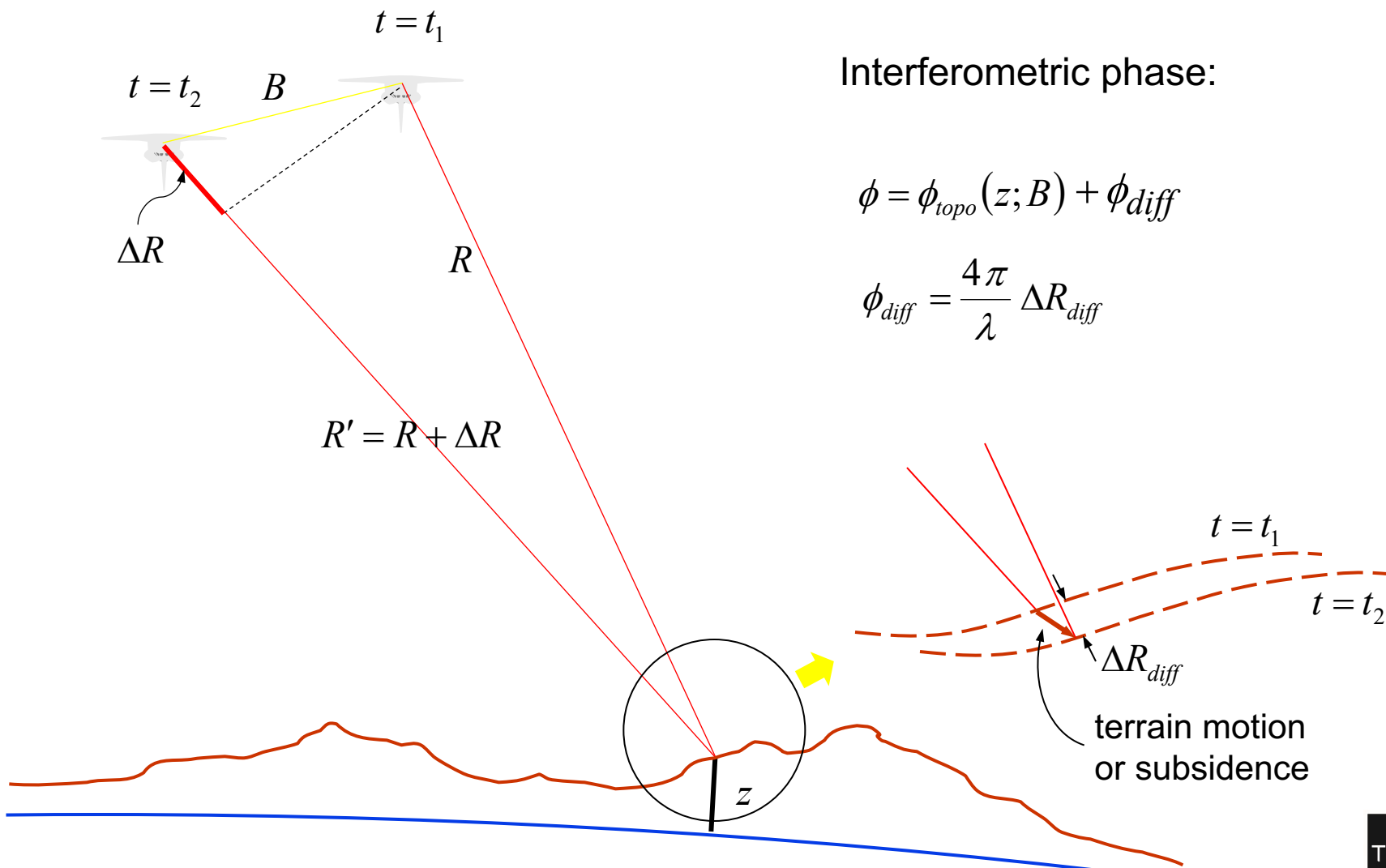
Mission	mode	Planimetric accuracy	Altimetric accuracy
SRTM (2000)	Bande X Mono-pass interferometry	60m (30m)	16m abs. 10m rel.
TanDEM-X WorldDEM (2011)	Mono & multi pass interferometry	12m	4m abs. 2m rel.



WorldDEM (Airbus)

SRTM

Differential Interferometry



Interferometric phase:

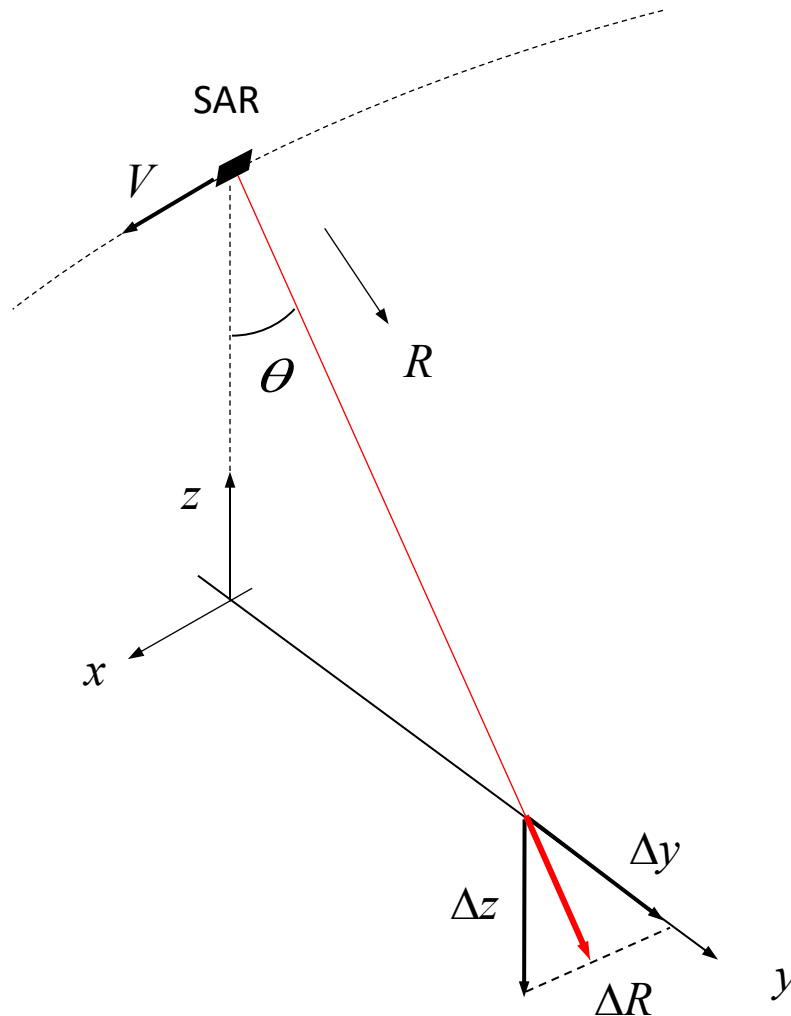
$$\phi = \phi_{topo}(z; B) + \phi_{diff}$$

$$\phi_{diff} = \frac{4\pi}{\lambda} \Delta R_{diff}$$

$$R' = R + \Delta R$$

terrain motion
or subsidence

Sensitivity for Displacement



$$\psi_{t,t'} = \frac{4\pi\delta R}{\lambda}$$

$$\Delta R = \Delta y \sin \theta - \Delta z \cos \theta$$

$$\psi_{t,t'} = 2\pi \iff \delta R = \frac{\lambda}{2}$$

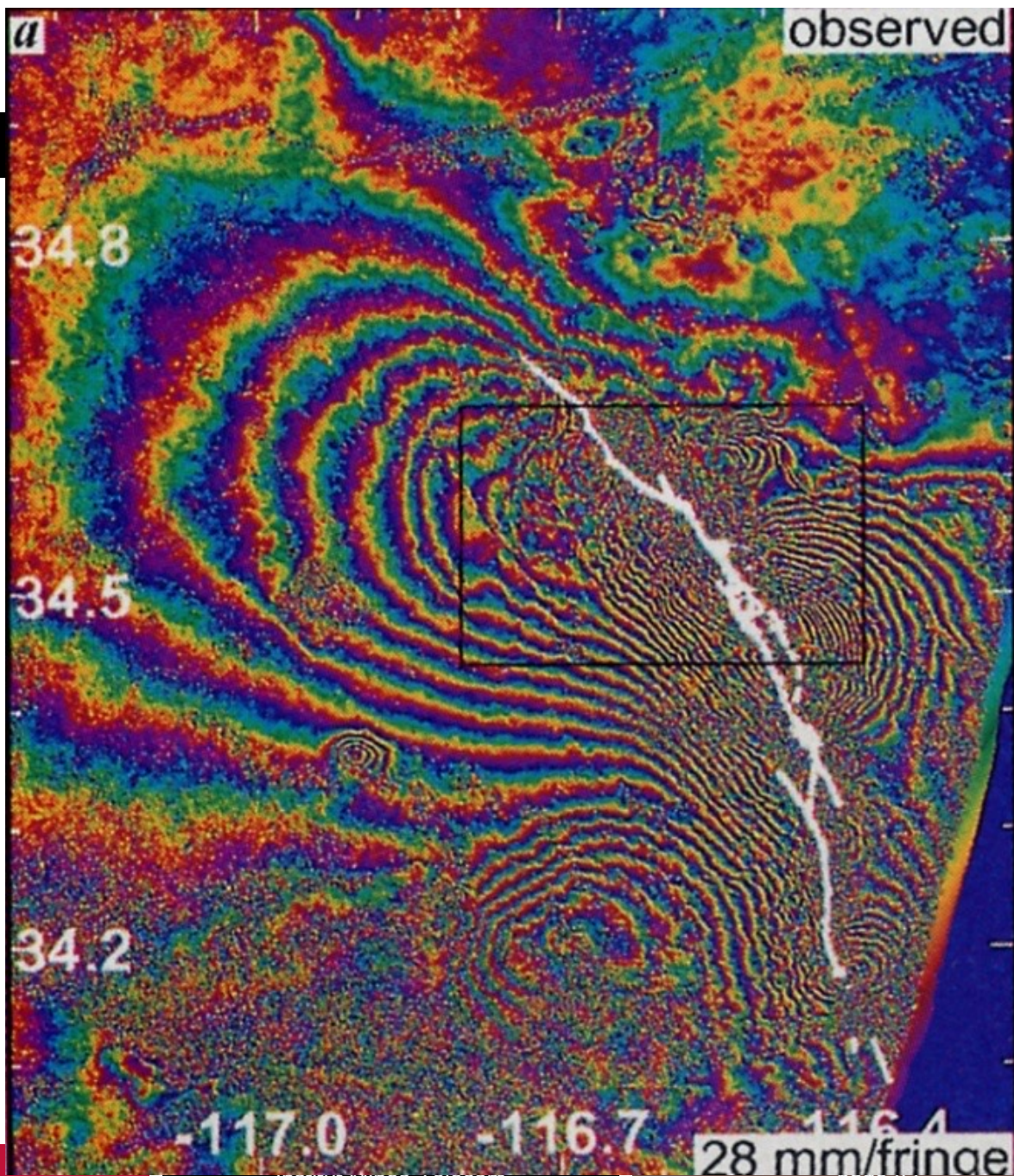
for ERS:

1 fringe (2π) corresponds to

2.8 cm in R

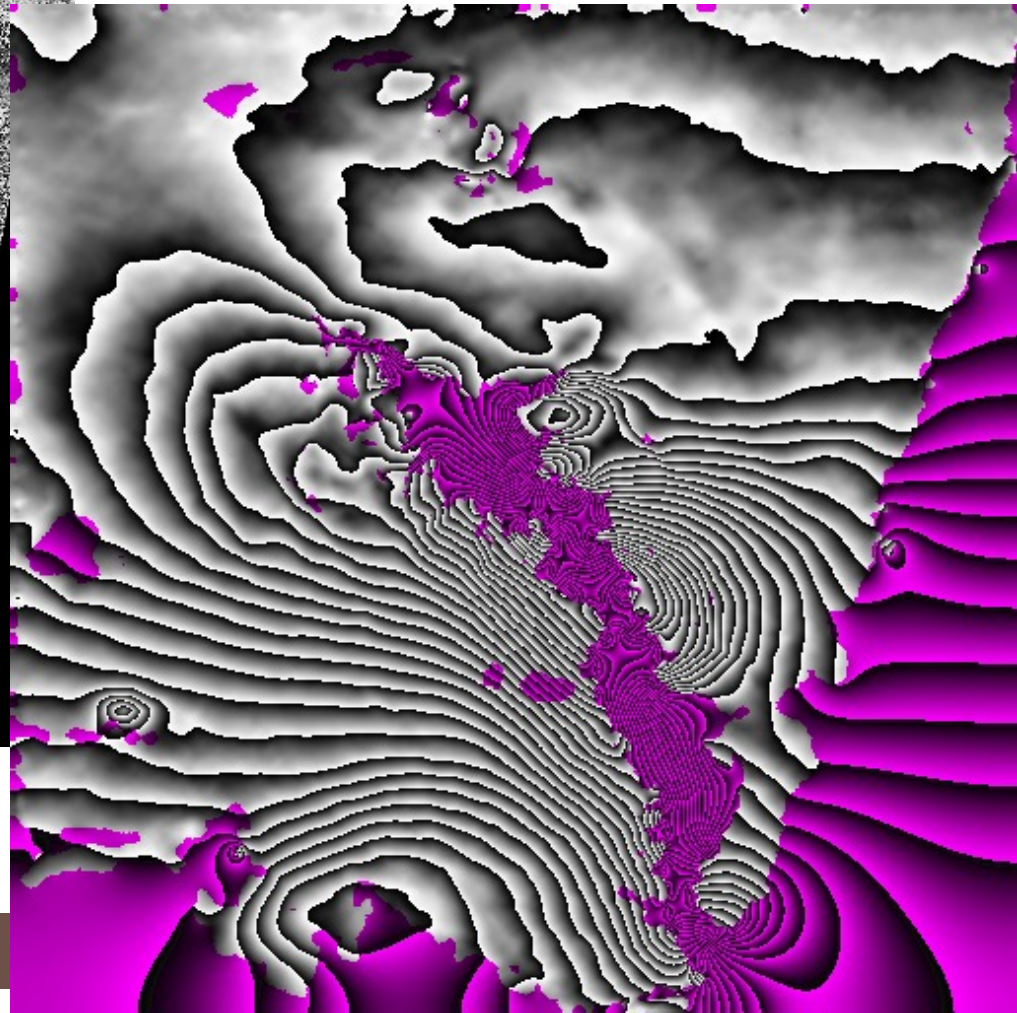
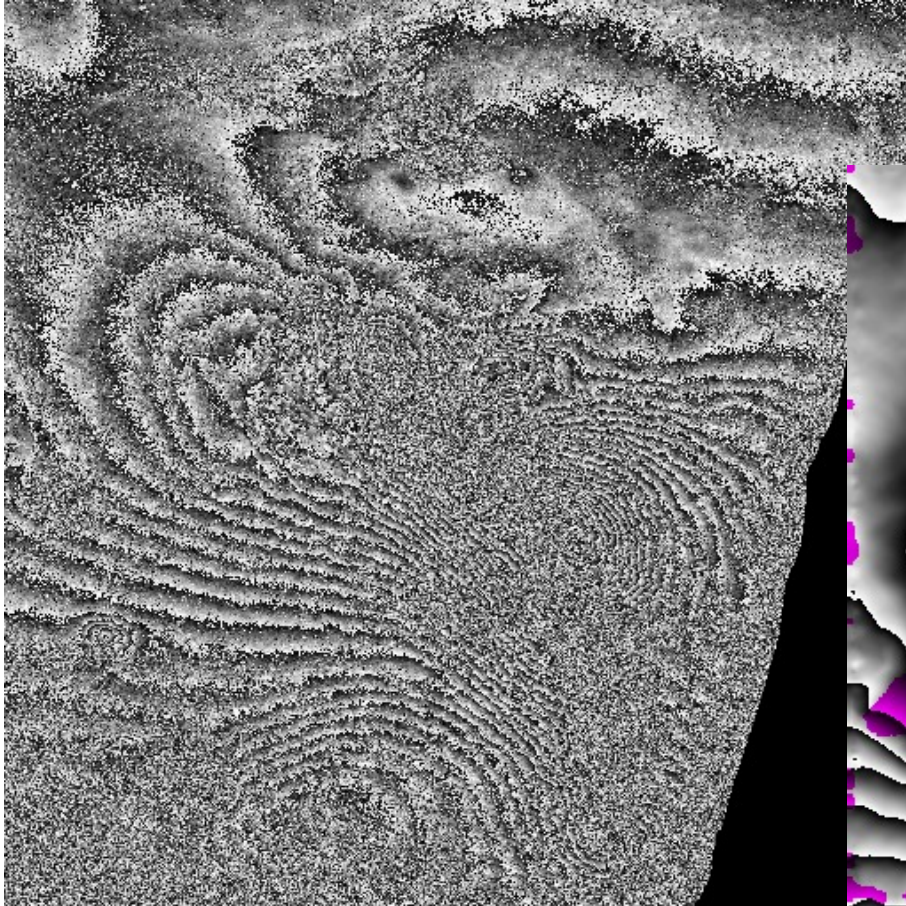
3.0 cm in z (e.g. subsidence)

7.2 cm in y (motion)

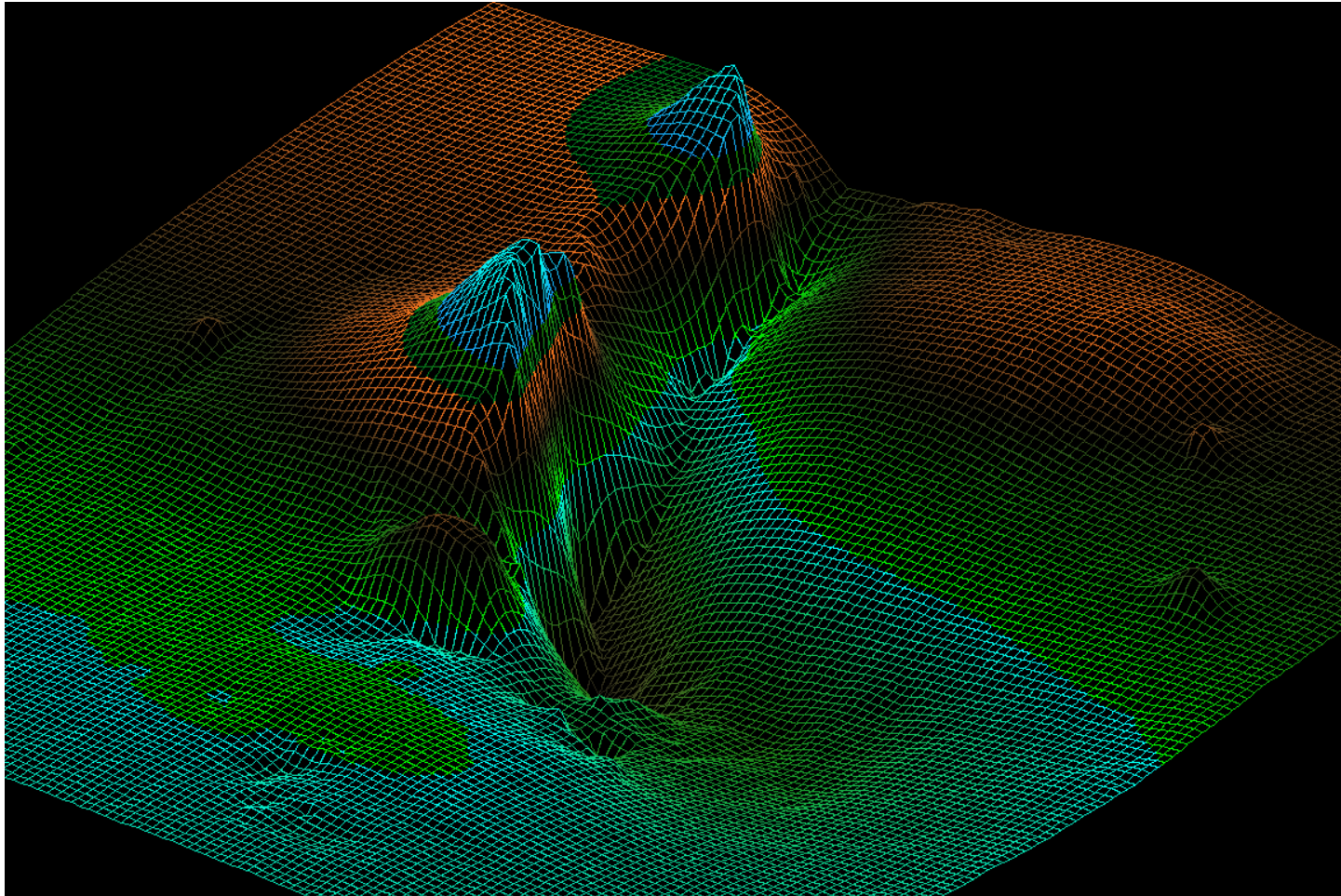


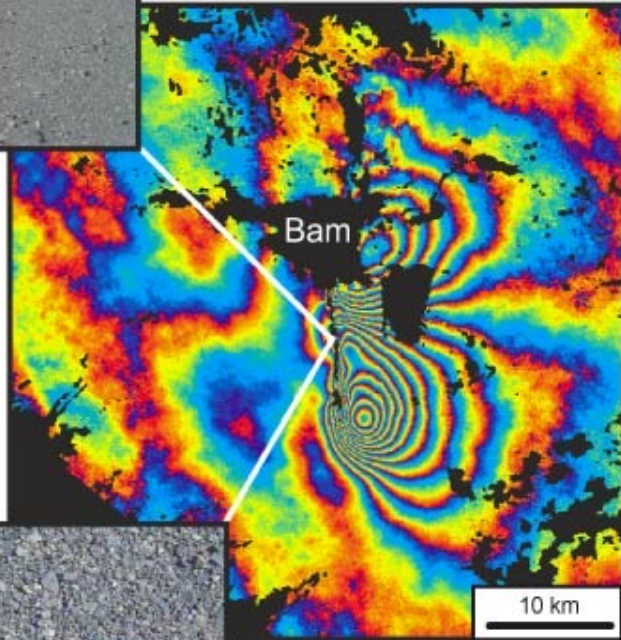
Massonnet et al., The displacement field of the Landers earthquake mapped by radar interferometry, Nature 364, 1993.

Differential interferometry



Differential interferometry





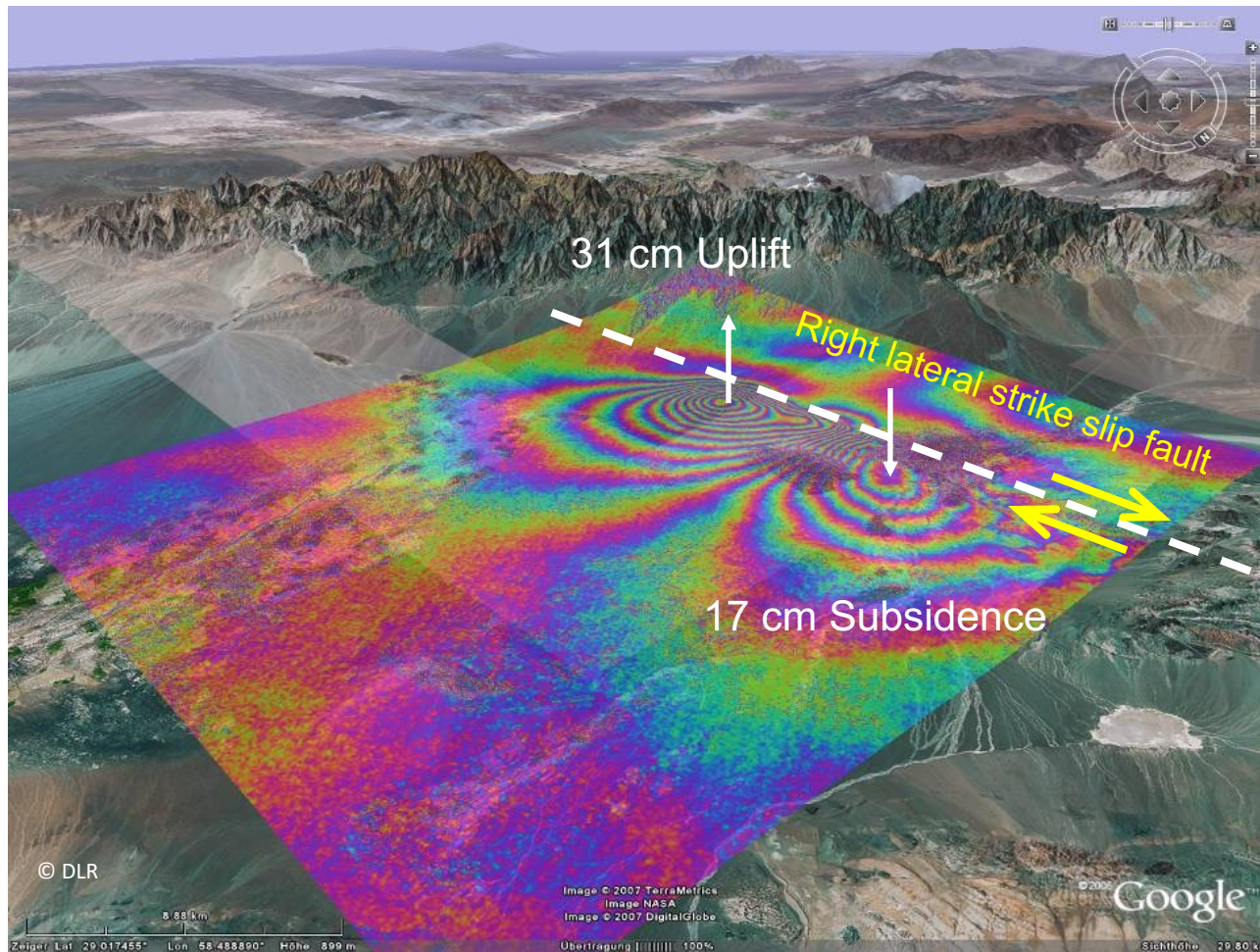
©<http://www.comet.nerc.ac.uk>

- **Baseline = 0.5 m !!**
- **1 frange \leftrightarrow 5 cm**

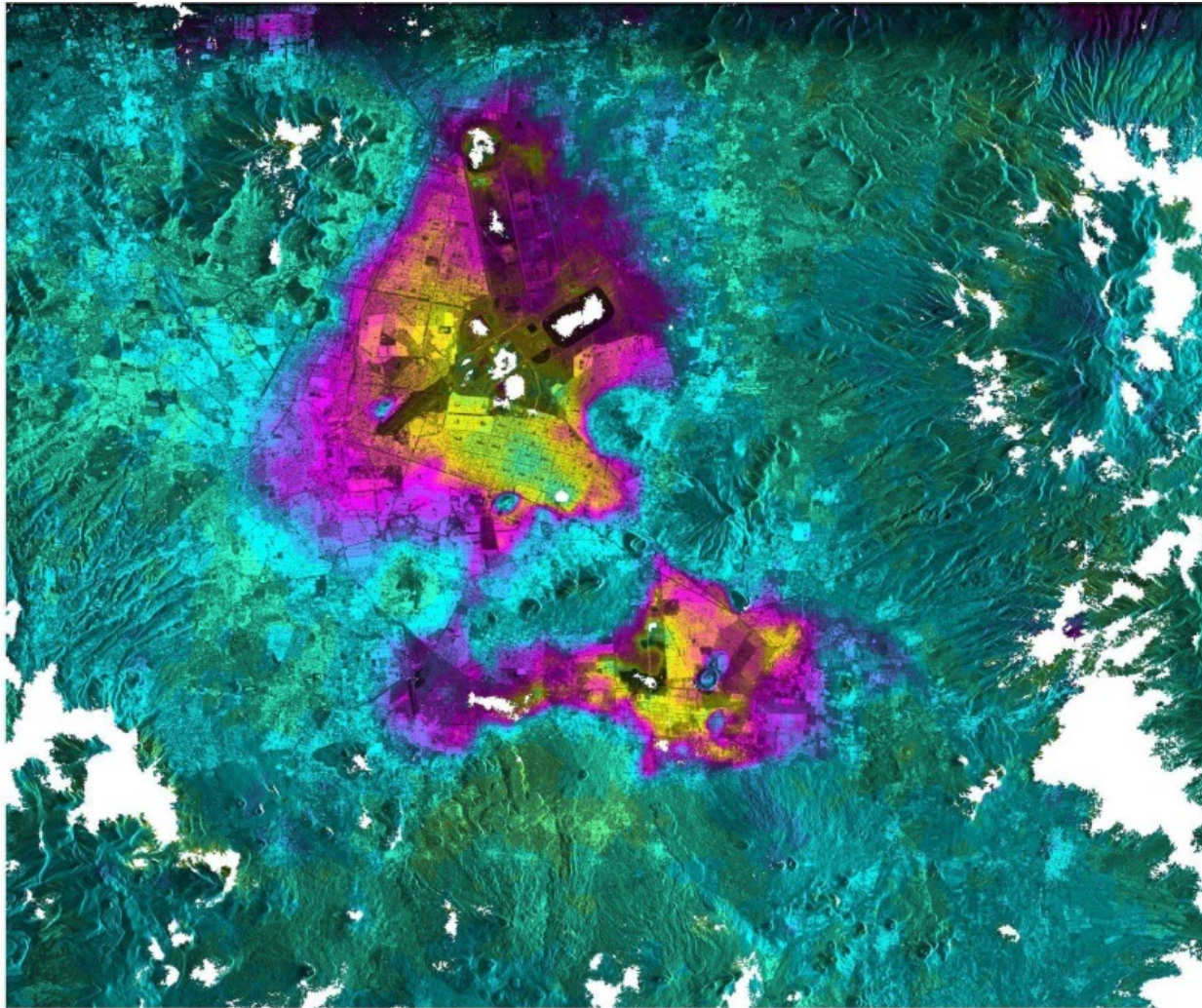
ENVISAT



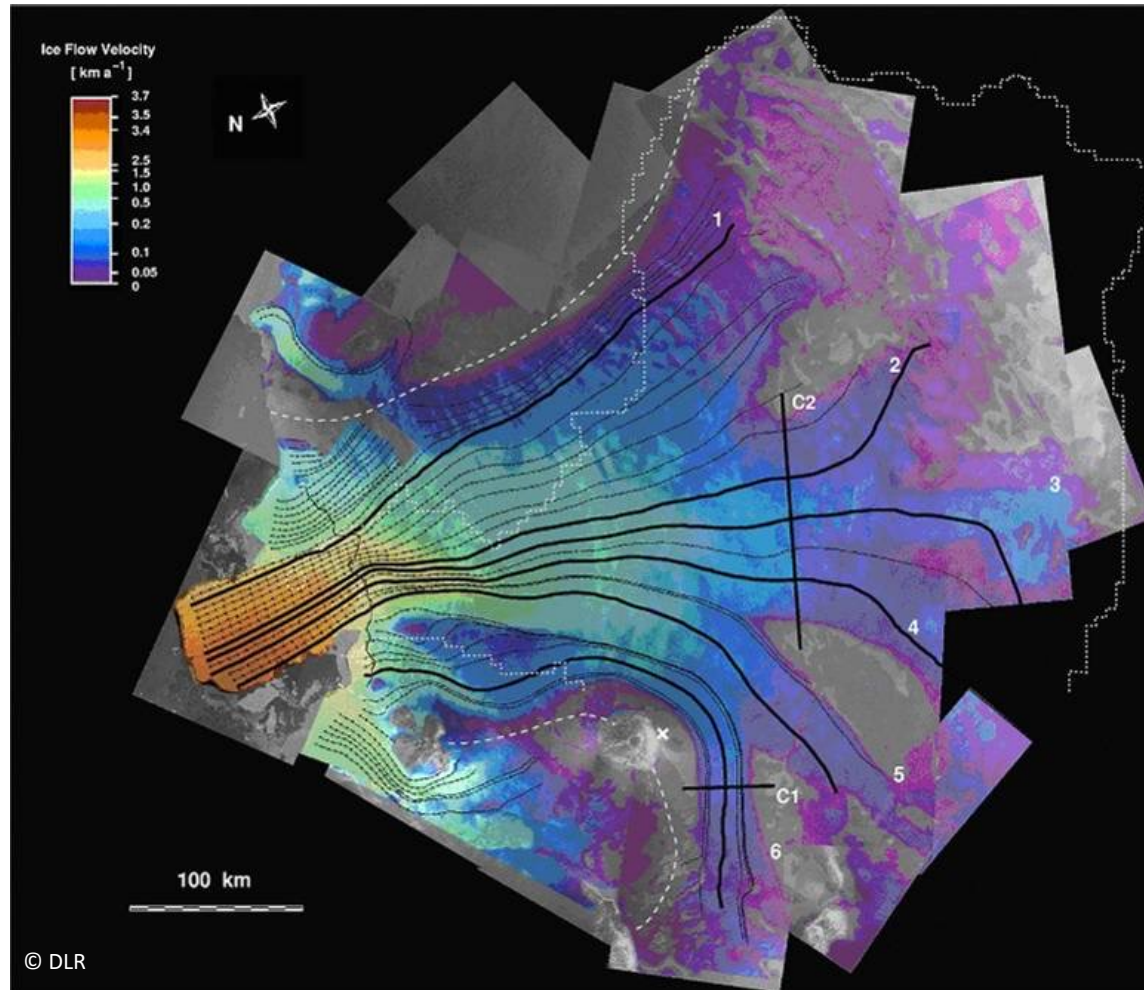
Coseismic Deformation of Bam Earthquake 26 Dec 2003



Differential interferometry



Glacier Flow Field Derived from D-InSAR

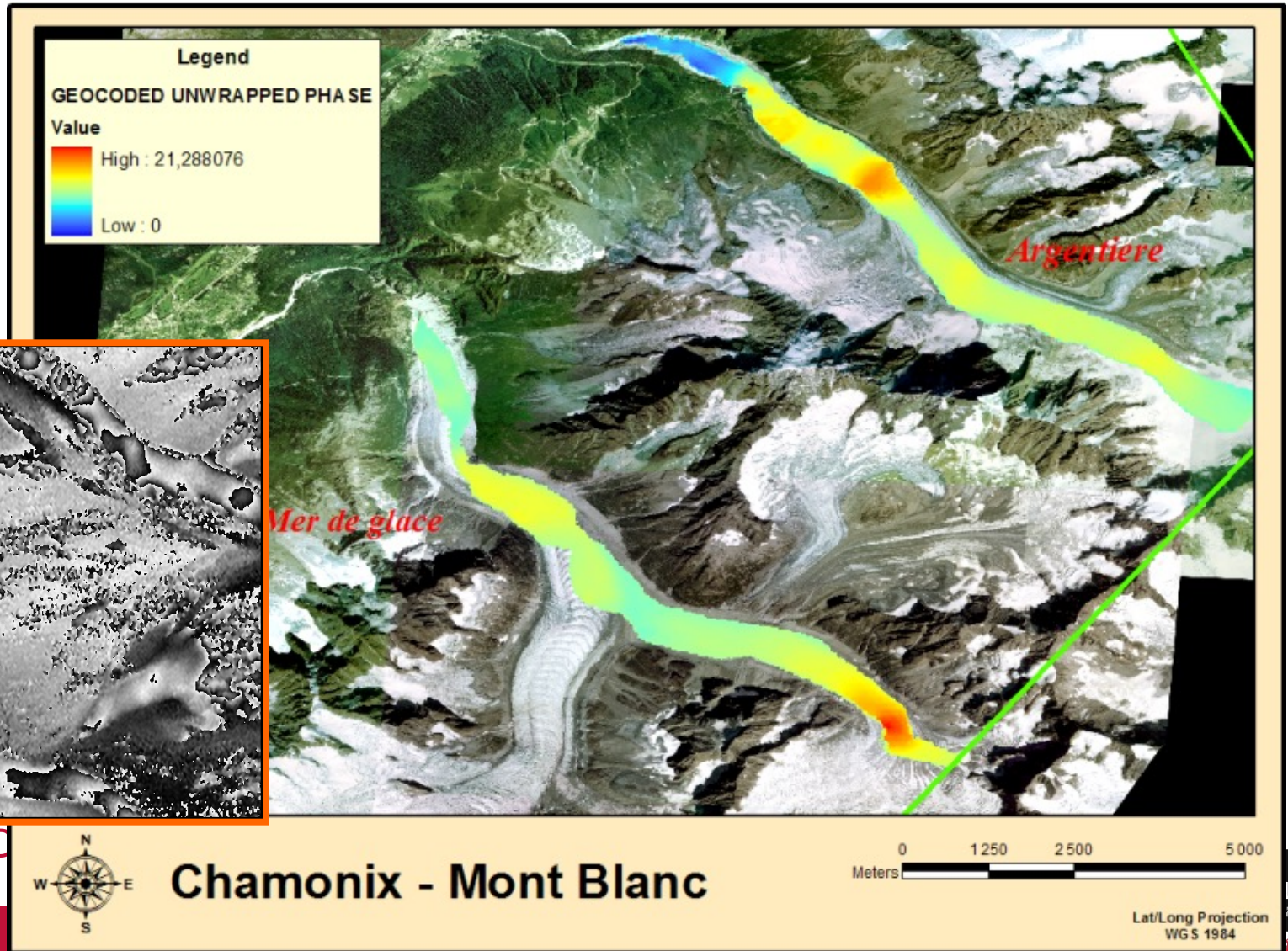


Antarctic
Thwaites
glacier
Data: ERS-1/2,
©ESA

approx.
500 km x 500 km

(Lang et al., 2004)

Differential interferometry + radargramm.



Multi-temporal SAR interferometric data

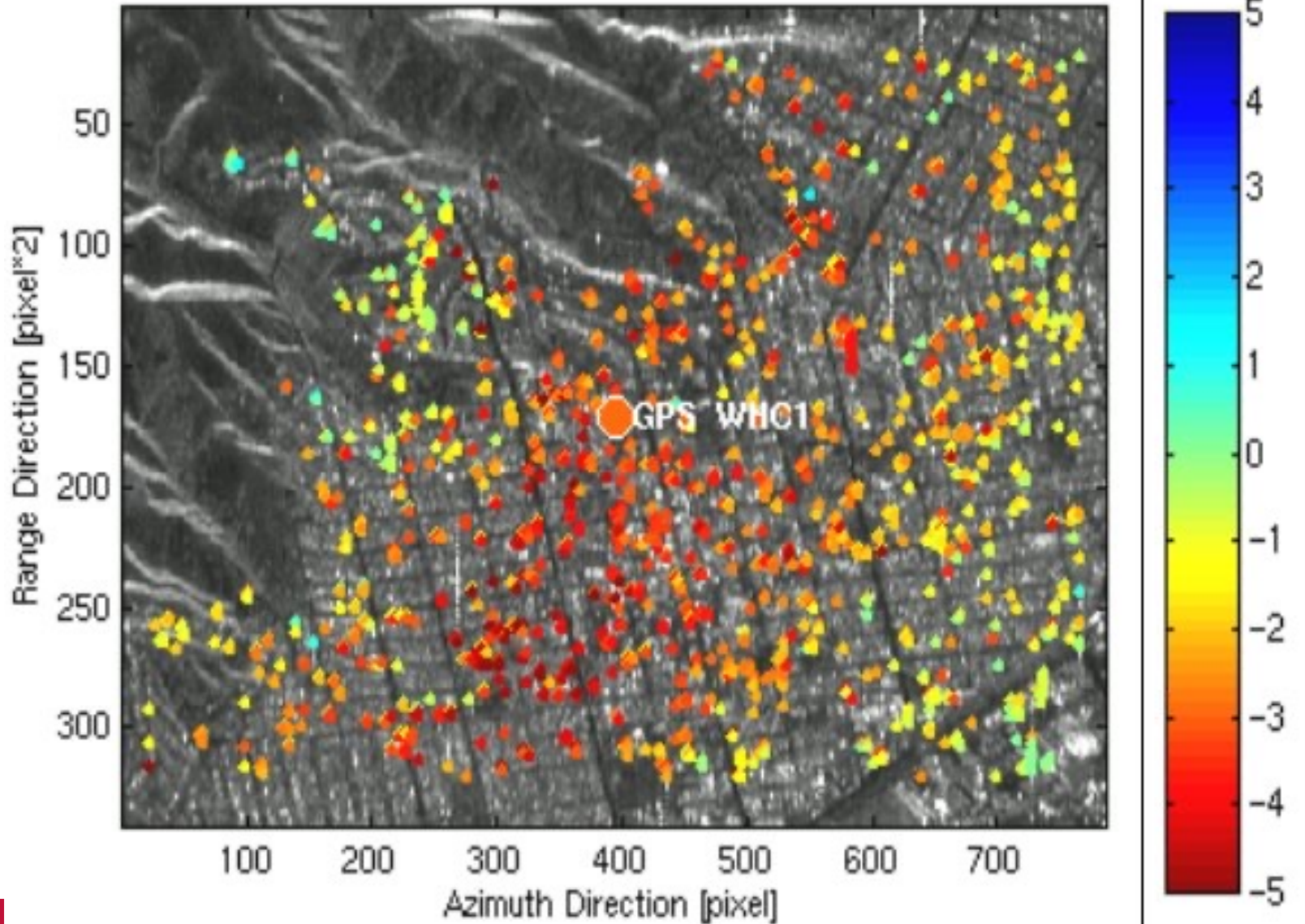
■ Point target analysis

- Exploitation of highly stable points
limited temporal and geometric decorrelation
(corners –man-made structures-, rocks,...)
- Permanent scatterers (PS) approaches
 - Exploitation of the whole set of interferograms
 - Inversion constrained by a deformation model



■ Distributed targets

- Small Baseline (SBAS approaches)
 - Selection of interferograms with sufficient correlation
(limited temporal and geometric decorrelation)
 - Temporal inversion



Permanent Scatterers for subsidence



Subsidence of Pomona: animation of Politecnico di Milano

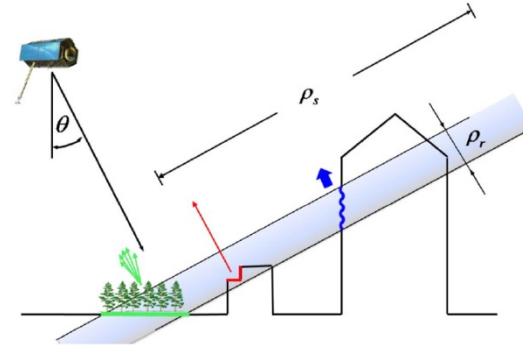
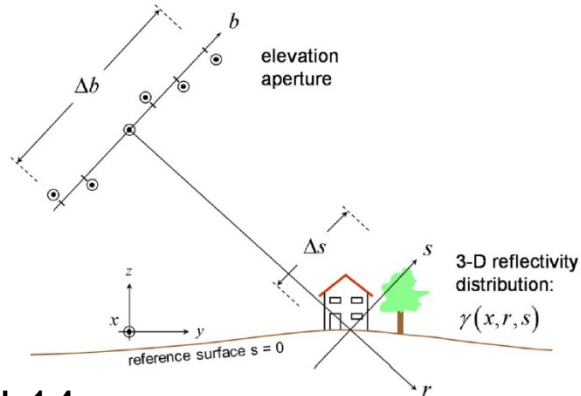
Summary: SAR Interferometry ...

... combines two or more complex-valued SAR images to derive geometric information about the imaged objects (compared to using a single image) by exploiting **phase differences**.

⇒ Images must differ in at least one aspect (= “baseline”)

baseline type	known as ...	applications: measurement of ...
$\Delta\theta$	across-track	topography, DEMs
$\Delta t = \text{ms to s}$	along-track	ocean currents, moving object detection, MTI
$\Delta t = \text{days}$	differential	glacier/ice fields/lava flows, Snow Water Equivalent (SWE), hydrology
$\Delta t = \text{days to years}$	differential	subsidence, seismic events volcanic activities, crustal displacements
$\Delta t = \text{ms to years}$	coherence estimator	sea surface decorrelation times land cover classification

SAR tomography



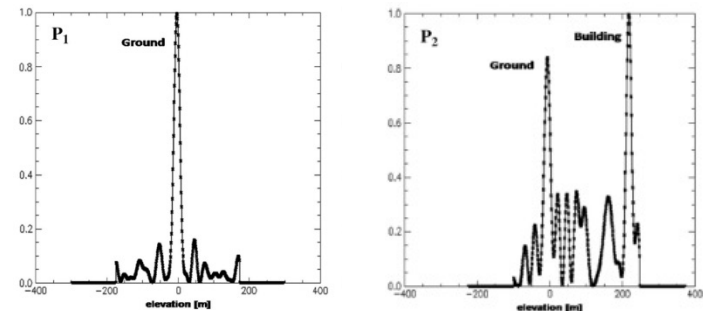
Zhu et al.14

$$g_n = \int_{\Delta s} \gamma(s) \exp(-j2\pi\xi_n s) ds, \quad n = 1, \dots, N$$

$$\mathbf{g} = \mathbf{R}\boldsymbol{\gamma}$$

Inversion :

- Spectral analysis methods
- Parse methods



SAR tomography

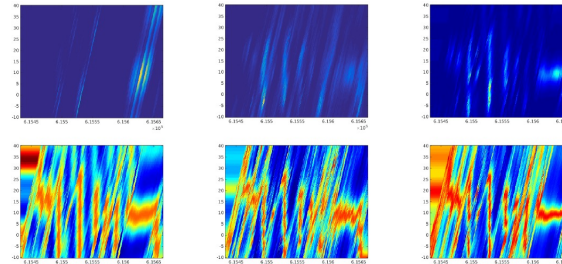
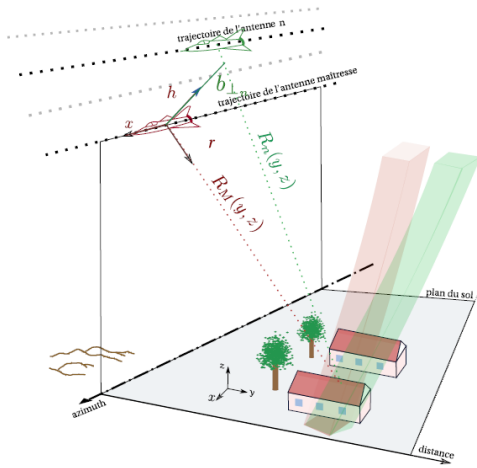
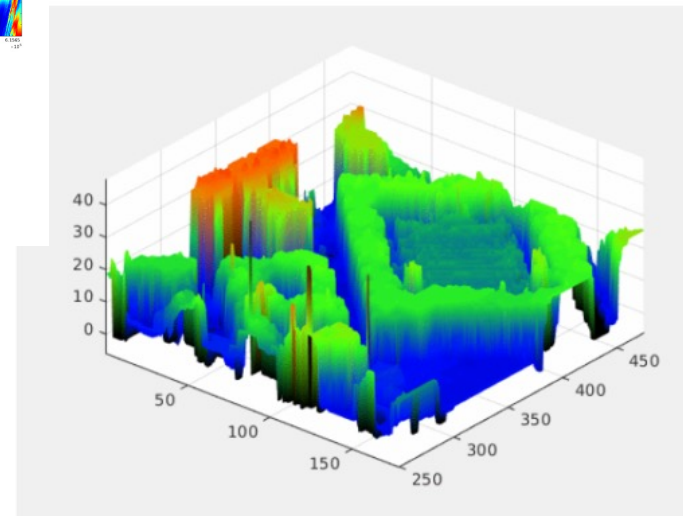
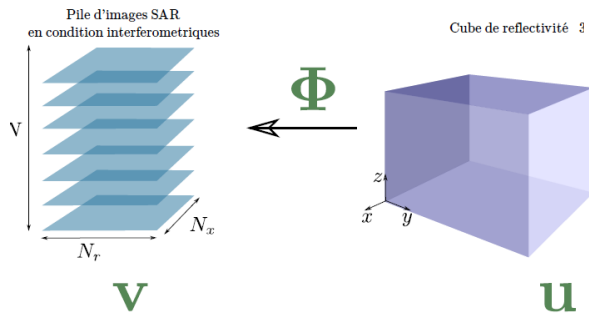
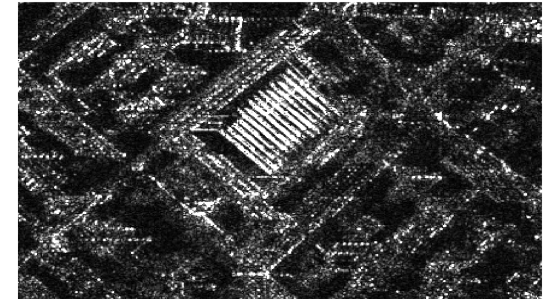
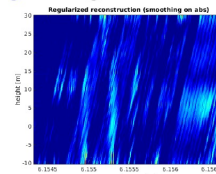
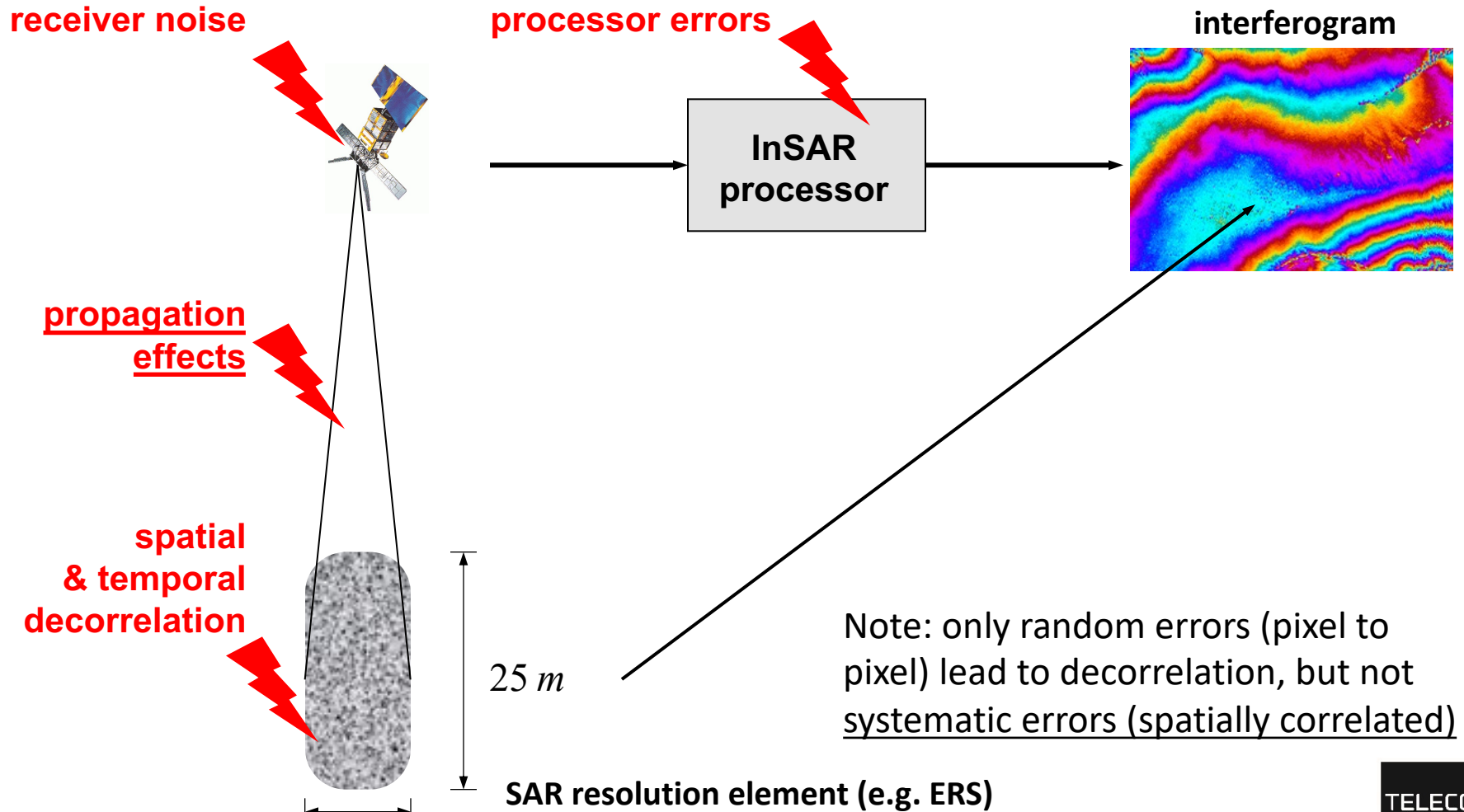


Figure: Regularized inversion



Interferometric Phase Error Sources



InSAR limits

$$\phi = \phi_{orb} + \phi_{topo} + \phi_{mvt} + \phi_{atm} + \phi_{noise}$$

■ Many error sources:

- Atmospheric decorrelation
- Temporal decorrelation
- Baseline (geometric) decorrelation + lay-over and shadows
- Phase noise

■ Corrections :

- Mono-pass systems
- Atmospheric corrections
- Phase filtering
- Multi-sensors combination